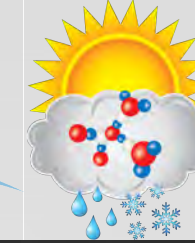




Integrated Cloud,
Land-Surface, &
Aerosol System Study
ICLASS



ASR
Atmospheric
System Research



CACTI Facilitated Science: Past, Present, and Future

Adam Varble

Pacific Northwest National Laboratory

**with vital contributions
from many others**

(who I will do my best to highlight in this talk)

2023 ARM/ASR Joint User Facility and PI Meeting

August 7, 2023



PNNL is operated by Battelle for the U.S. Department of Energy

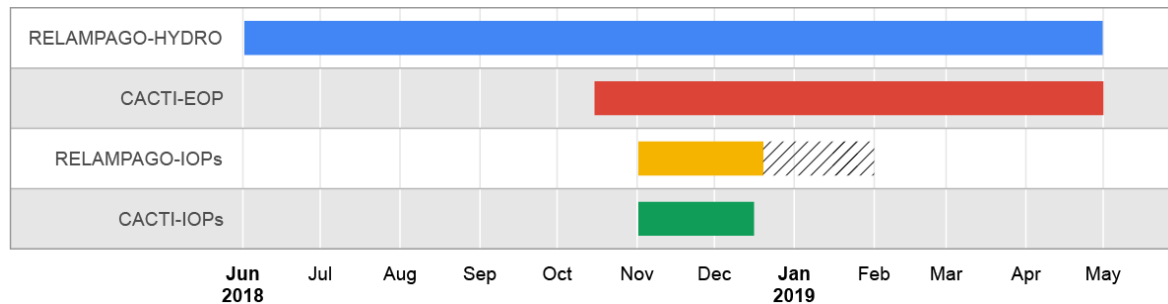


Early stages of the 25 January 2019 storm that reached nearly 21 km ASL.
Photo courtesy of Ramón Alberto Acuña (SMN).

Cloud, Aerosol, and Complex Terrain Interactions (CACTI) Background

First deployment of CSAPR2 with AMF1 instruments between Oct 2018 and Apr 2019 in the Sierras de Córdoba range of central Argentina.

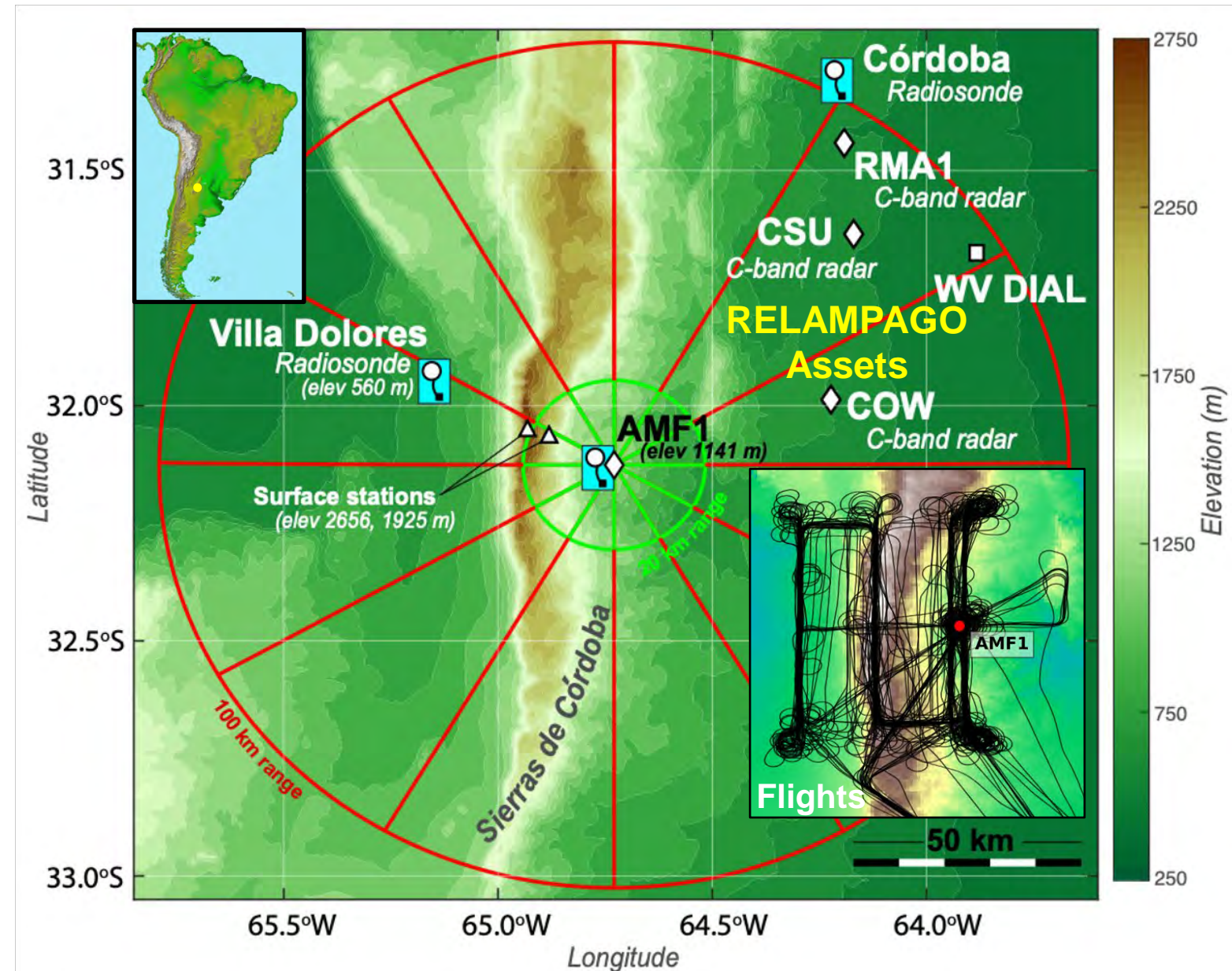
IOP (Nov-Dec 2018) with 22 G-1 flights (8 Deep CI, 8 Cu, 3 μ -physics, 3 clear air), coincident with the NSF-led RELAMPAGO field campaign.



Amongst the most (> 250) datastreams/products produced of any AMF campaign.

<https://www.arm.gov/research/campaigns/amf2018cacti>

Varble, A. C., et al., 2021: Utilizing a Storm-Generating Hotspot to Study Convective Cloud Transitions: The CACTI Experiment. *BAMS*, doi:10.1175/BAMS-D-20-0030.1.



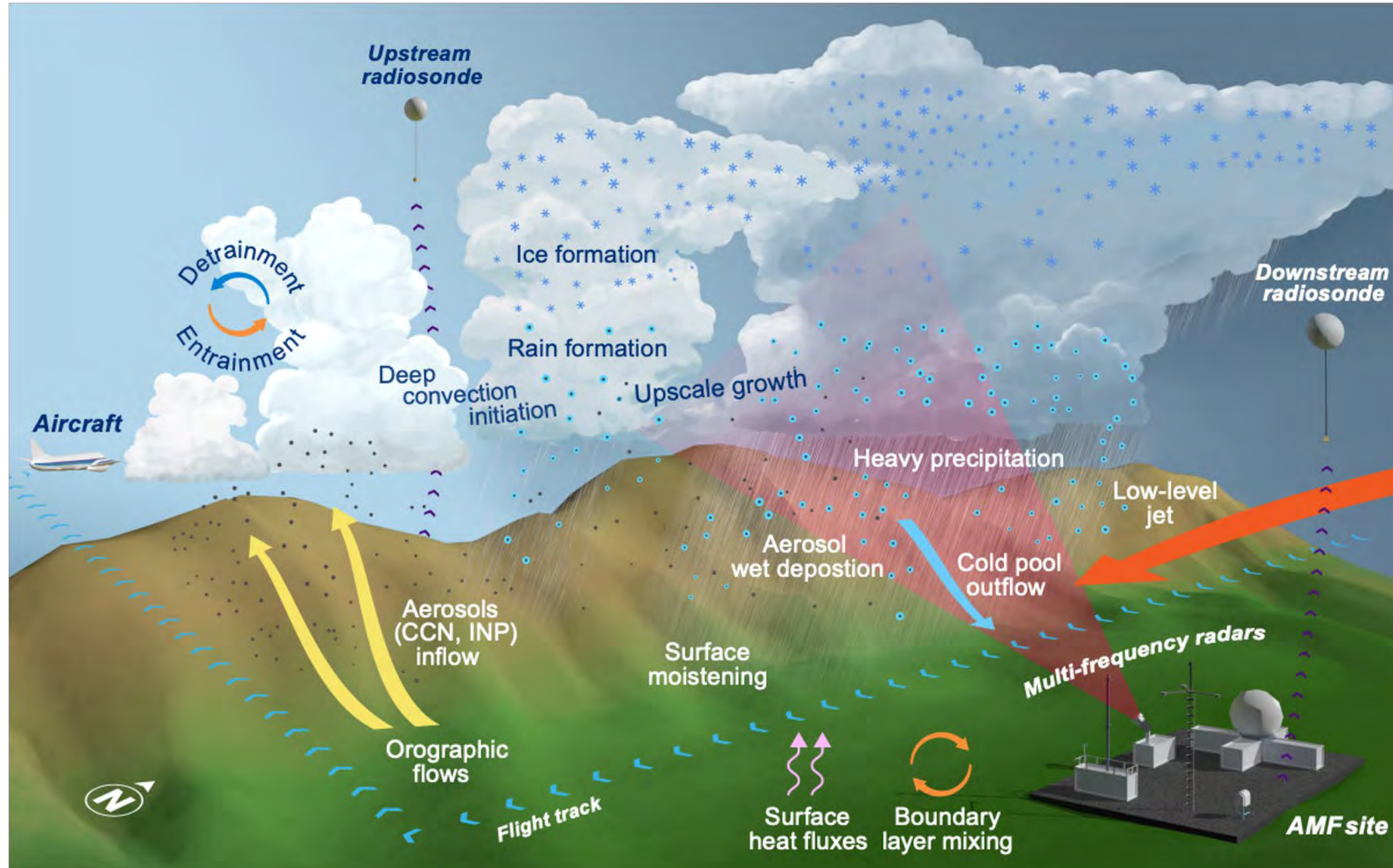
Nesbitt S. W., et al., 2021: A Storm Safari in Subtropical South America: Proyecto RELAMPAGO. *BAMS*, doi:10.1175/BAMS-D-20-0029.1.

CACTI Objectives

Varble, A. C., et al., 2021: Utilizing a Storm-Generating Hotspot to Study Convective Cloud Transitions: The CACTI Experiment. *BAMS*, doi:10.1175/BAMS-D-20-0030.1.

Nesbitt S. W., et al., 2021: A Storm Safari in Subtropical South America: Proyecto RELAMPAGO. *BAMS*, doi:10.1175/BAMS-D-20-0029.1.

AMS special collection: <https://journals.ametsoc.org/collection/RELAMPAGO-CACTI>



Proposing Science Team

Principal Investigator

Adam Varble, Pacific Northwest National Laboratory

Co-Investigators

Stephen Nesbitt, University of Illinois

Edward Zipser, University of Utah

Greg McFarquhar, University of Illinois

Sonia Kreidenweis, Colorado State University

Kristen Rasmussen, Colorado State University

Pavlos Kollias, McGill University

David Romps, Lawrence Berkeley National Laboratory

Eldo Avila, Universidad Nacional de Córdoba

Paloma Borque, University of Illinois

Paola Salio, Universidad de Buenos Aires

Susan van den Heever, Colorado State University

Paul DeMott, Colorado State University

Robert Houze, Jr., University of Washington

Michael Jensen, Brookhaven National Laboratory

Ruby Leung, Pacific Northwest National Laboratory

David Gochis, National Center for Atmospheric Research

Christopher Williams, University of Colorado-Boulder/NOAA

With critical support from ARM infrastructure and management, INVAP (in country management), local landowners and government officials, NOAA (providing us GOES-16 rapid scan data), and NASA Langley (performing satellite retrievals).

Thank you to all the researchers that have worked with CACTI datasets since the campaign.

Management, Infrastructure, Support

Critical In Country Support

INVAP, Servicio Meteorológico Nacional (SMN), Forecasting Team (Lynn McMurdie, SMN and students), local government officials in Villa Yacanto and Rio Cuarto, Universidad de Córdoba, Fuerza Aérea Argentina (Air Force), Aeropuertos Argentina 2000 (AA2000), Empresa Argentina de Navegación Aérea (EANA), and Gobierno de la Provincia de Córdoba

ARM Ground Facilities

Heath Powers, Tim Goering, Peter Argay: *AMF1 Operations Management*

Kim Nitschke: *Former AMF1 Manager*

Vagner Castro, Juarez Viegas, Tercio Silva, Bruno Cunha: *Site Technicians*

Nitin Bharadwaj, Joseph Hardin, Andrei Lindenmaier, Brad Isom, Pete Argay, and Todd Houchens: *Radar Engineering*

Stephen Springston, Art Sedlacek: *Aerosol Systems Engineering*

Many others: *Instrument Operations, Engineering, Data Mentorship*

ARM Aircraft Facility

Beat Schmid: *Facility Manager*

Jason Tomlinson: *Engineering Manager*

Mike Hubbell: *Flight Operations Manager/Pilot*

Clayton Eveland, Jon Ray, and Jen Armstrong: *Pilots*

Alyssa Matthews, Mikhail Pekour, Lexie Goldberger, Fan Mei, Matt Newburn, Kaitlyn Suski, Alla Zelenyuk-Imre, Mike Crocker, Luke Marx, Pete Carroll, Albert Mendoza, Dan Nelson, and Tom Hill: *Engineering, Operations, and Data Mentors*

ARM Infrastructure

Jim Mather, Nicki Hickmon, Jennifer Comstock, Sally McFarlane: *ARM Management*

Hanna Goss, Ryan Risenmay, Michael Wasseem, Rolanda Jundt, Eric Francavilla, Robert Stafford, Cory Ireland: *Communications*

Giri Prakash, Cory Stuart, Maggie Davis, Rob Records, David Swank: *Data Flow and Storage*

Adam Theisen, Ken Kehoe, Austin King, Sherman Beus: *Data Quality*

And so many others who contributed to engineering, import/export, installation, operations, communications, mentoring of instruments, and data quality/flow/storage without which CACTI would not exist!

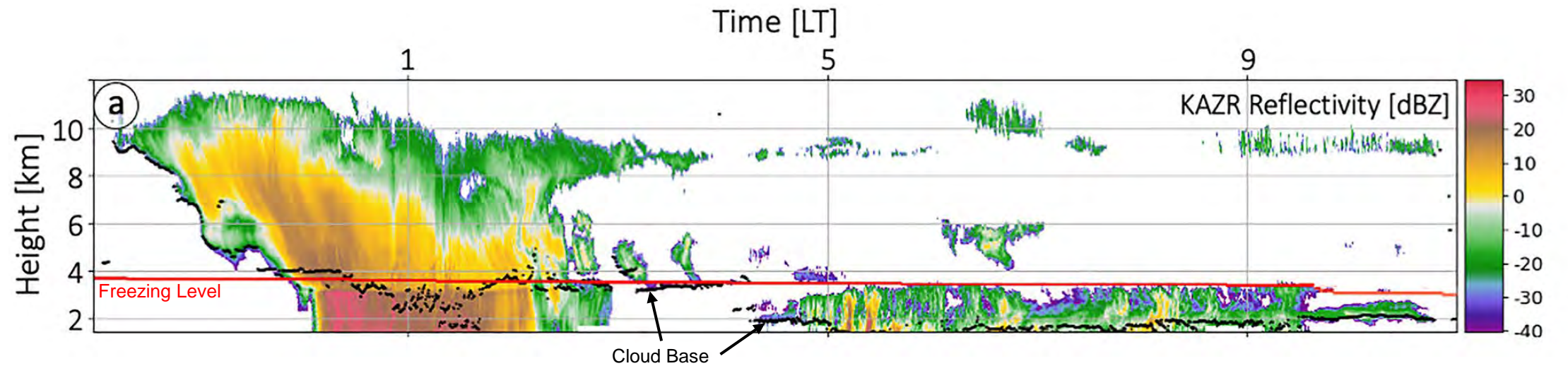
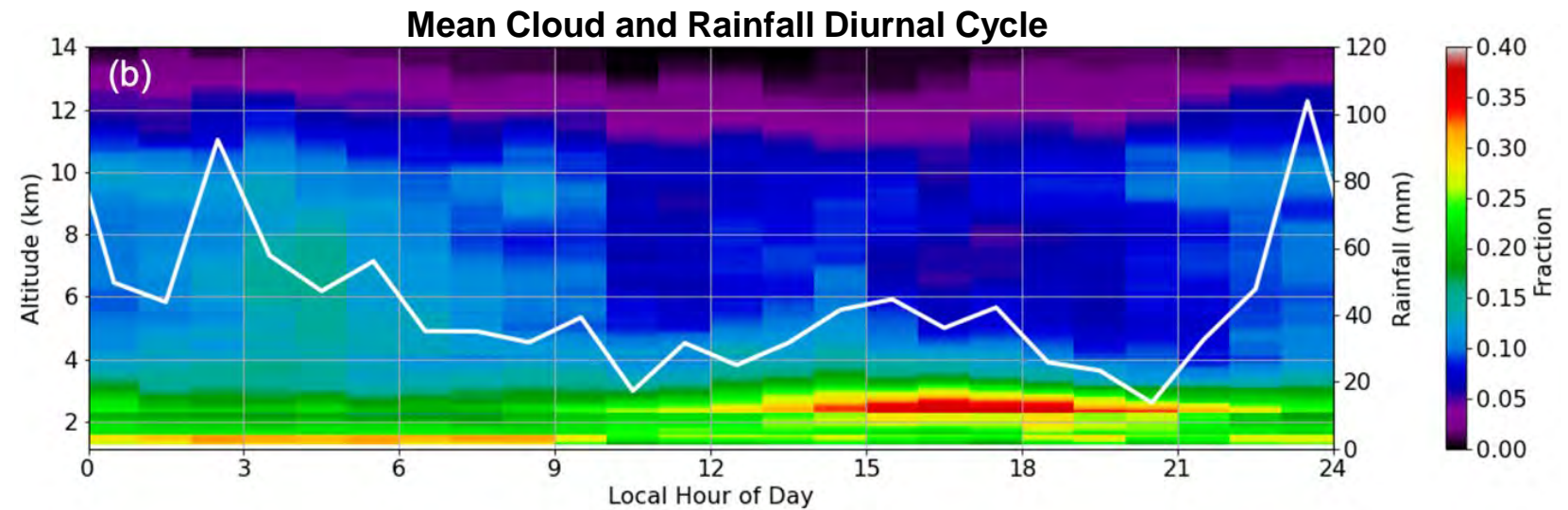
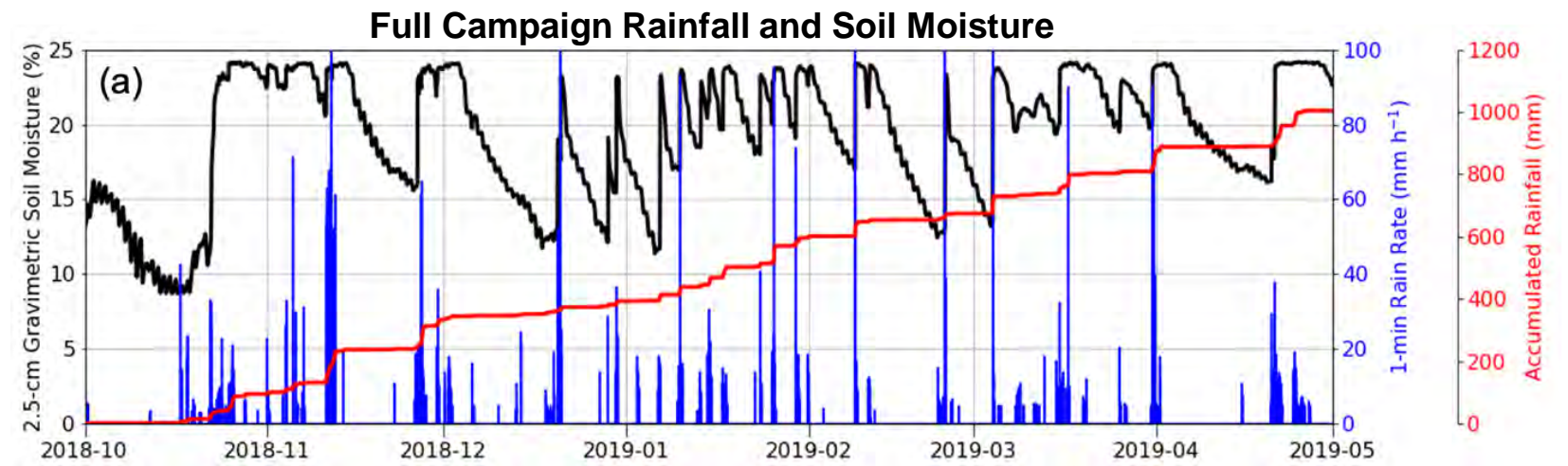
Cloud and Precipitation Conditions

Shallow clouds were observed directly overhead on 191 of 212 days, 165 of which had liquid clouds lasting 30 minutes or longer, many of which produced drizzle.

About 160 deep convective systems passed directly over the site on 83 separate days with a wide range of depth and organization.

Varble, A. C., et al., 2021, *BAMS*, doi:10.1175/BAMS-D-20-0030.1.

Borque, P., et al., 2022: Peak rain rate sensitivity to observed cloud condensation nuclei and turbulence in continental warm shallow clouds during CACTI. *JGR Atmos.*, doi:10.1029/2022JD036864.

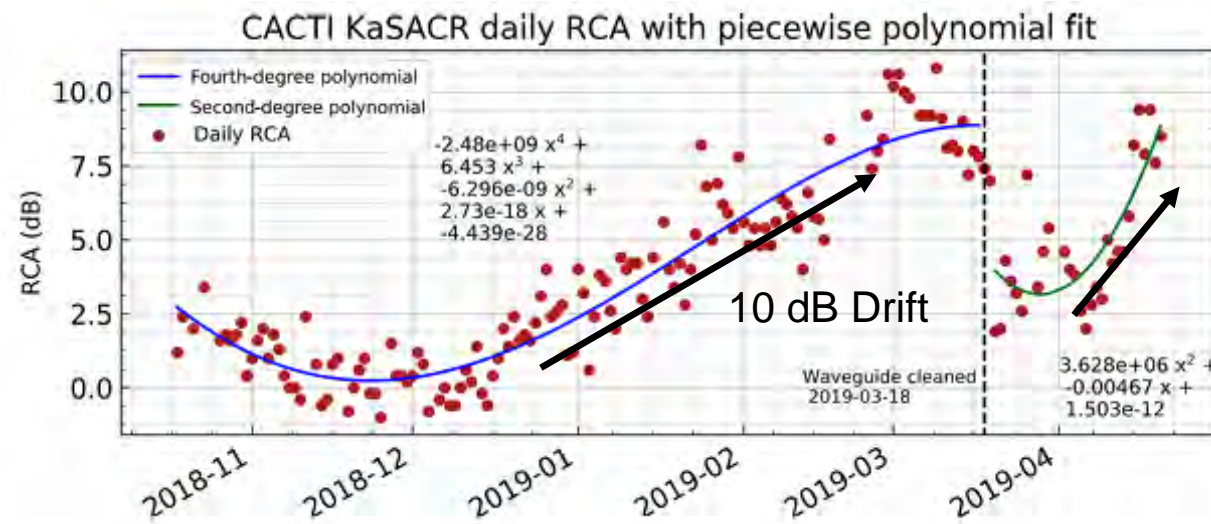


Radar calibration using ground clutter

Alexis Hunzinger, Joe Hardin (PNNL)

Hardin, J. C., et al., 2020: CACTI Radar b1 Processing: Corrections, Calibrations, and Processes Report, DOE/SC-ARM-TR-244.

Hunzinger, A., et al., 2020: An extended radar relative calibration adjustment (eRCA) technique for higher-frequency radar and range-height indicator (RHI) scans, *AMT*, doi:10.5194/amt-13-3147-2020.

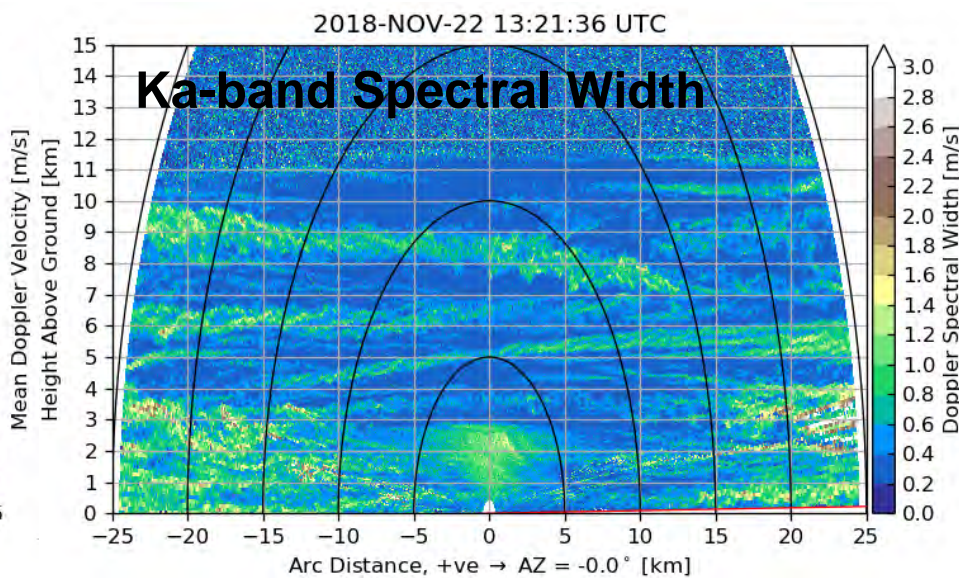
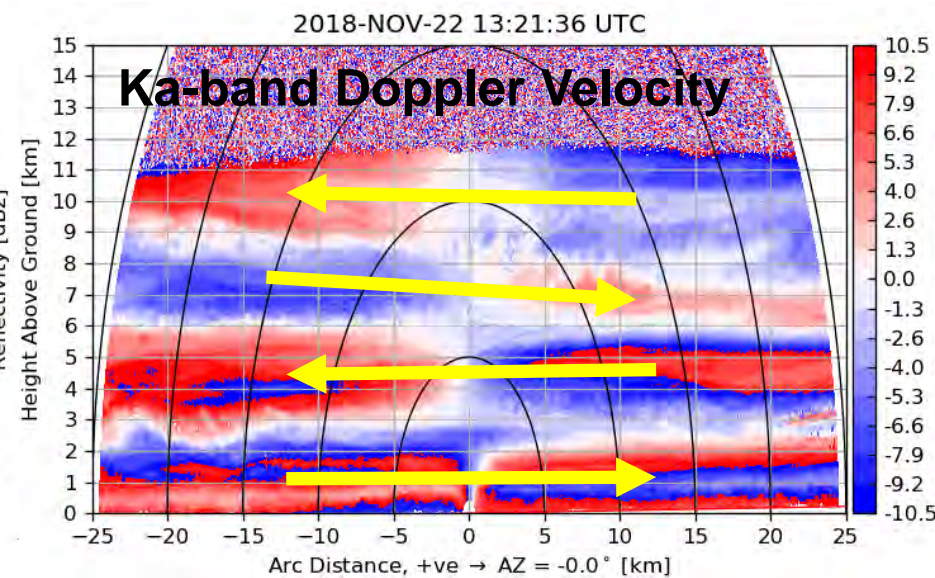
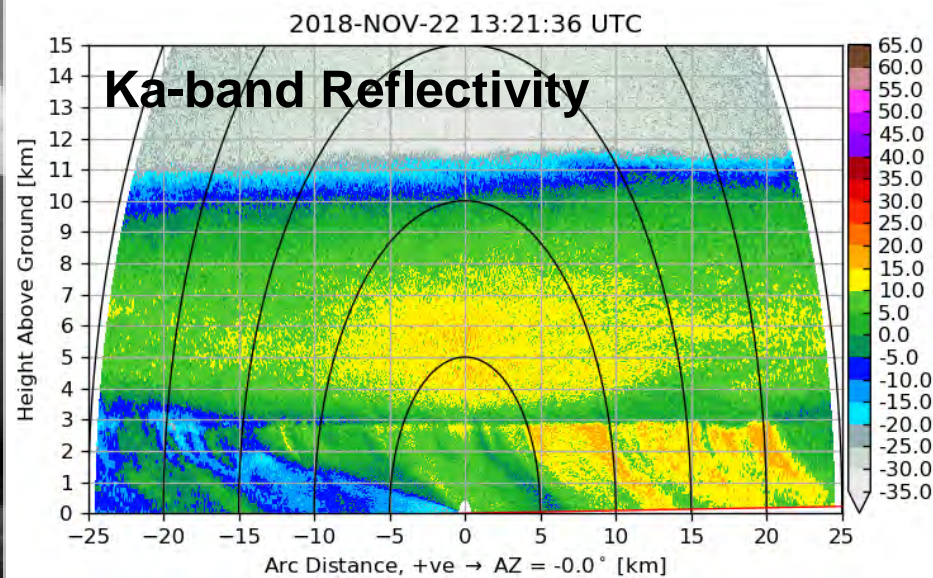


First extension of relative calibration via ground clutter to frequencies higher than C-band and RHI scans

Ka-, X-, and C-bands cross-calibrated using C-band absolute calibration

A one of a kind, 6.5-month Ka/X-SACR dataset that has been gridded, co-located with KAZR and C-SAPR2

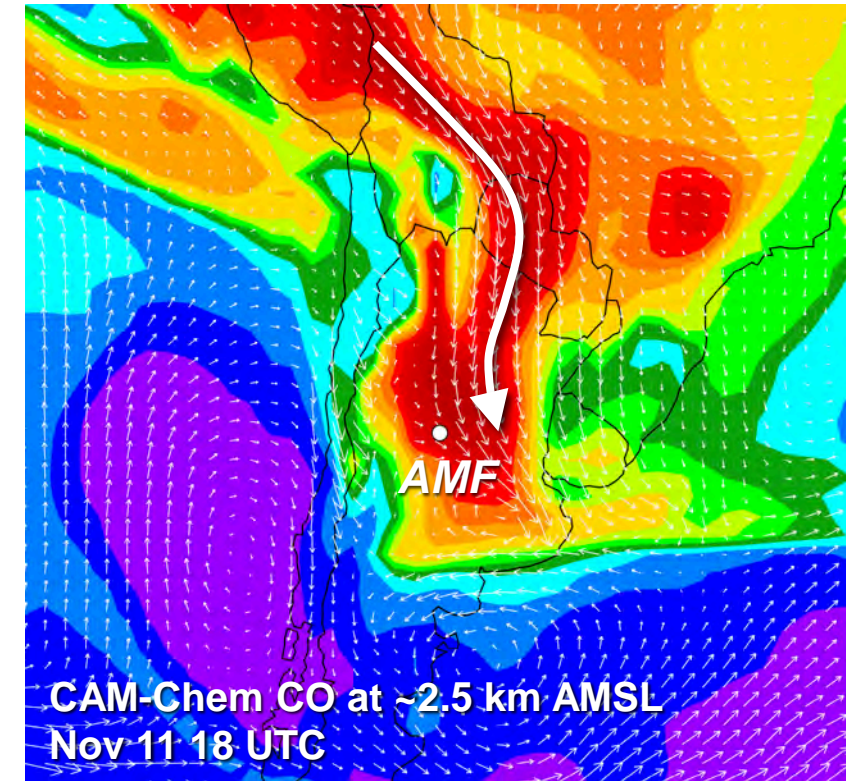
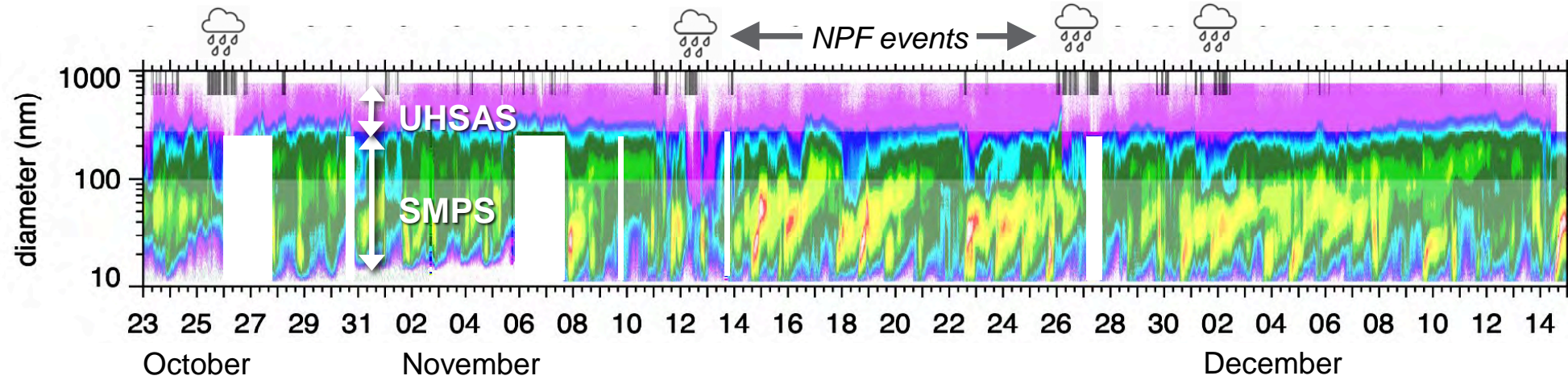
Many shallow (including fog) and medium depth precipitating clouds, often with good low-level clear air signals



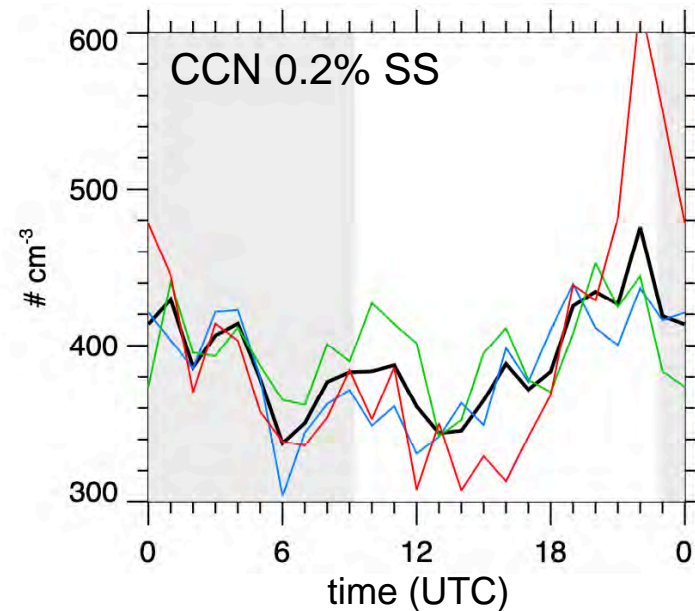
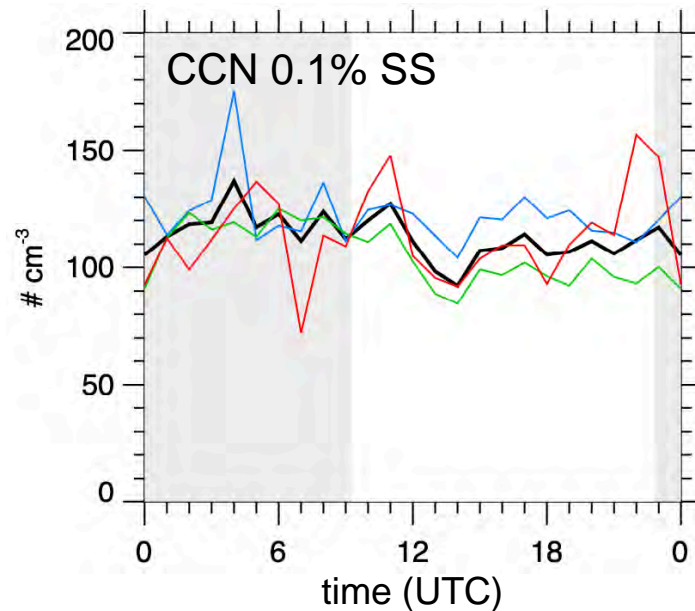
Imagery from Nitin Bharadwaj and Joseph Hardin

Ongoing Work: Spatiotemporal variability of aerosols

Jerome Fast (PNNL); See session 2 poster 24

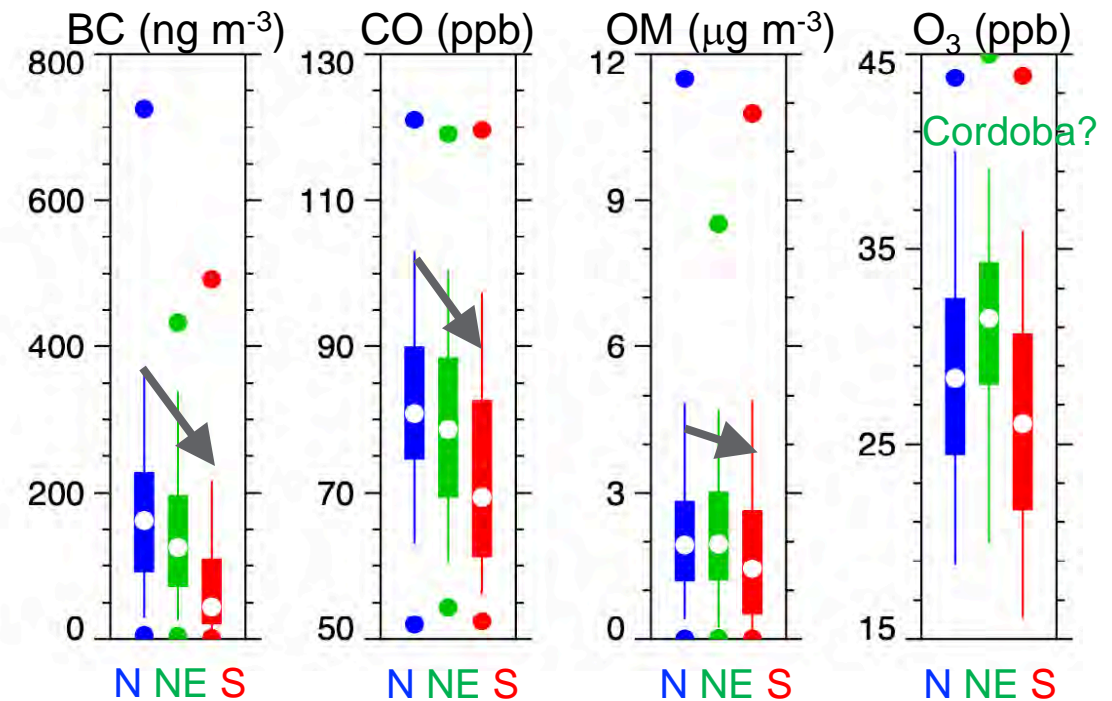


Mean Diurnal Variation



All days (Oct 23 – Dec 15)
19 days with # always < 4000 cm⁻³

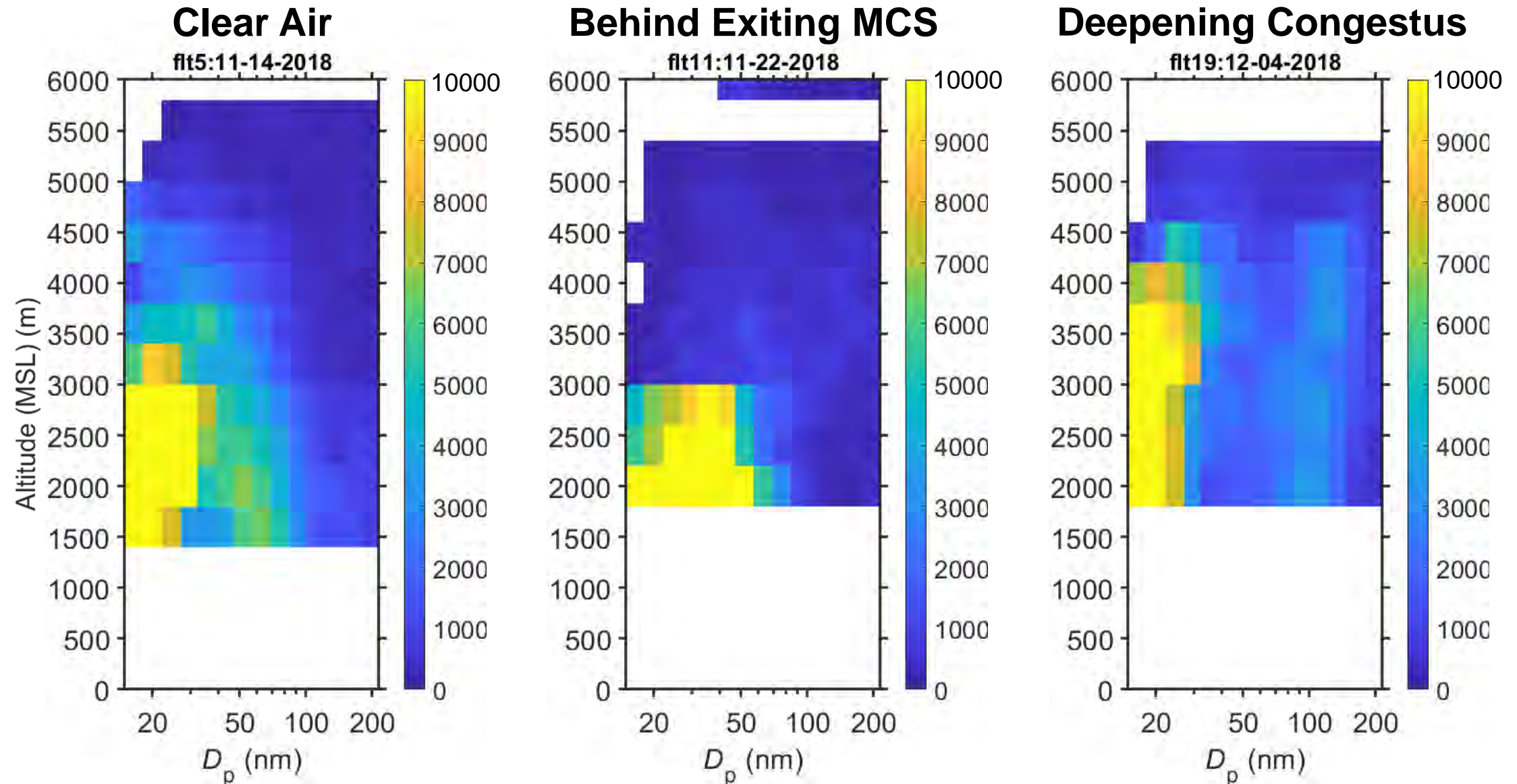
11 days with # > 8000 cm⁻³ for 1 hour or more
24 remaining days



Ongoing Work: Interactions between NPF and convective clouds

Yang Wang, Marcus Batista Oliveira (U. Miami)

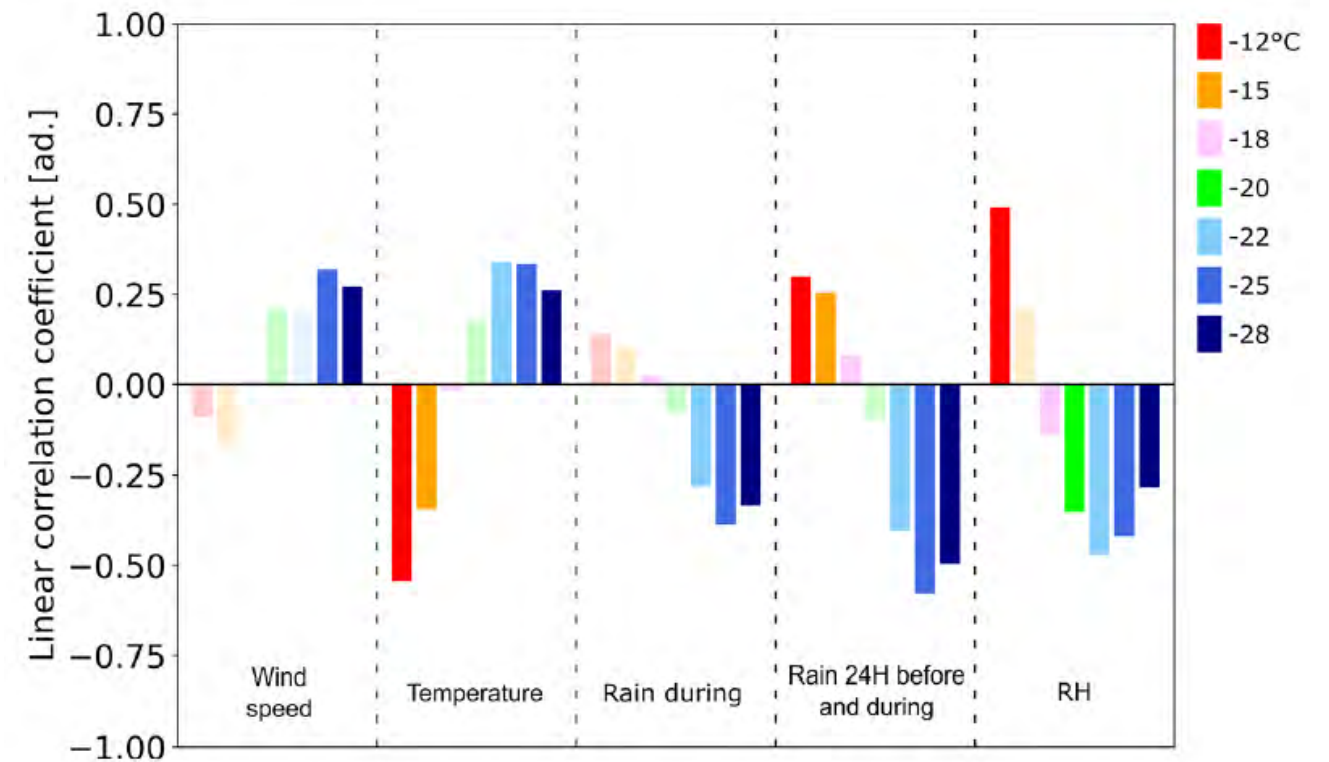
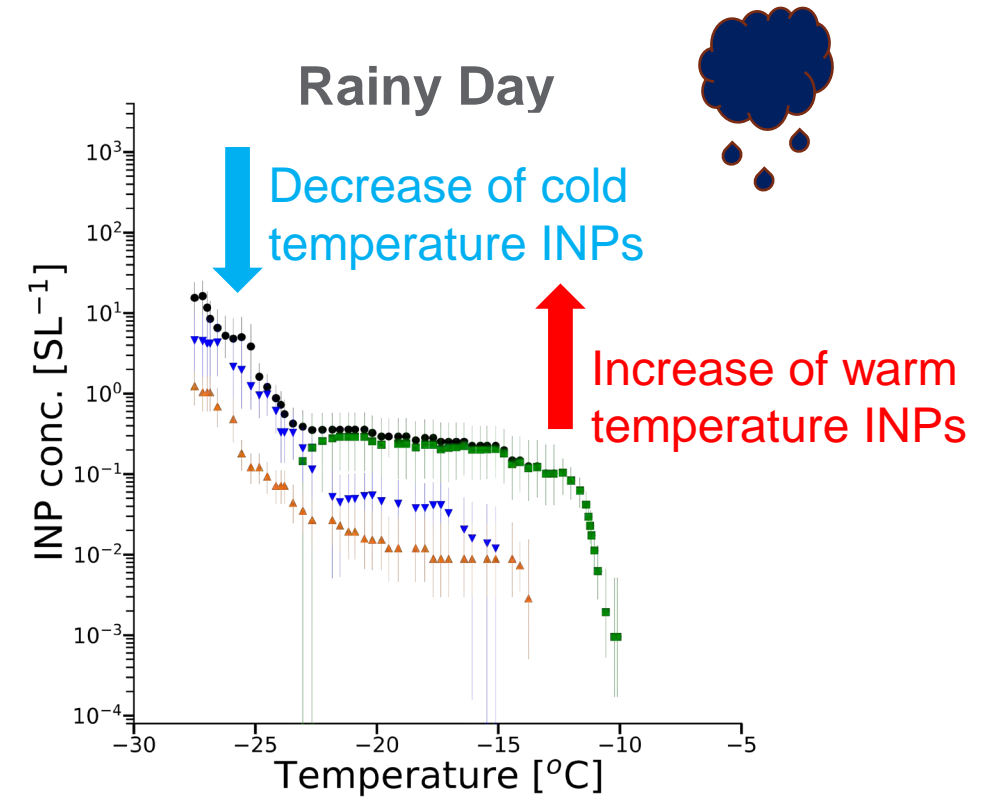
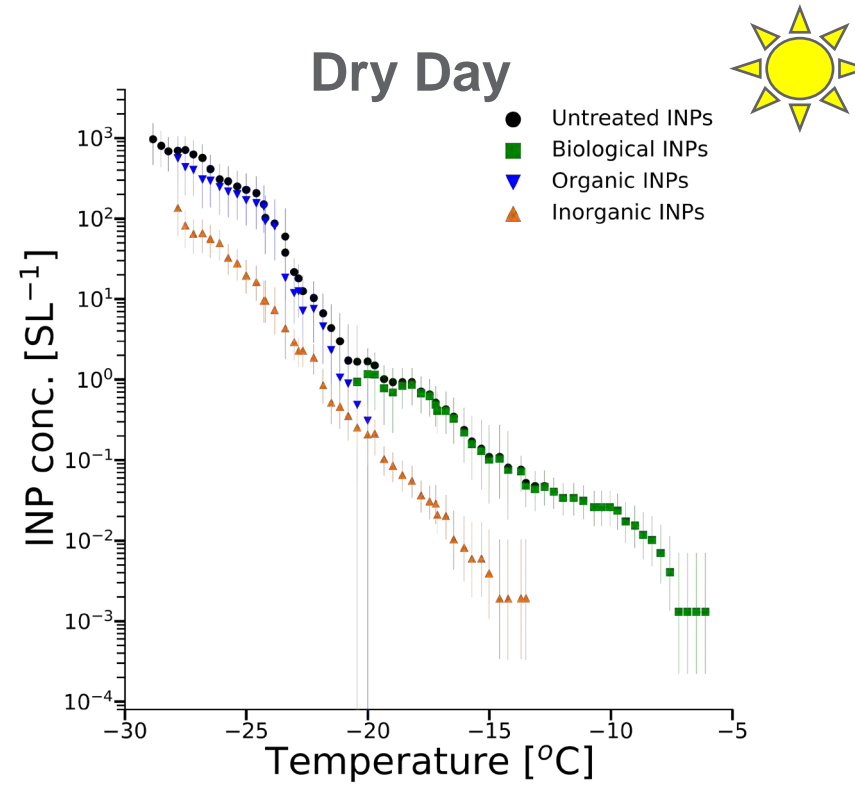
- New particle formation events identified in G-1 data
- Examining how these relate to and interact with convective clouds



Processes controlling INP variability

Baptiste Testa (U. Lyon), Paul DeMott (CSU), and colleagues

Testa, B., et al., 2021: Ice nucleating particle connections to regional Argentinian land surface emissions and weather during the Cloud, Aerosol, and Complex Terrain Interactions experiment, *JGR Atmos.*, doi:10.1029/2021JD035186.

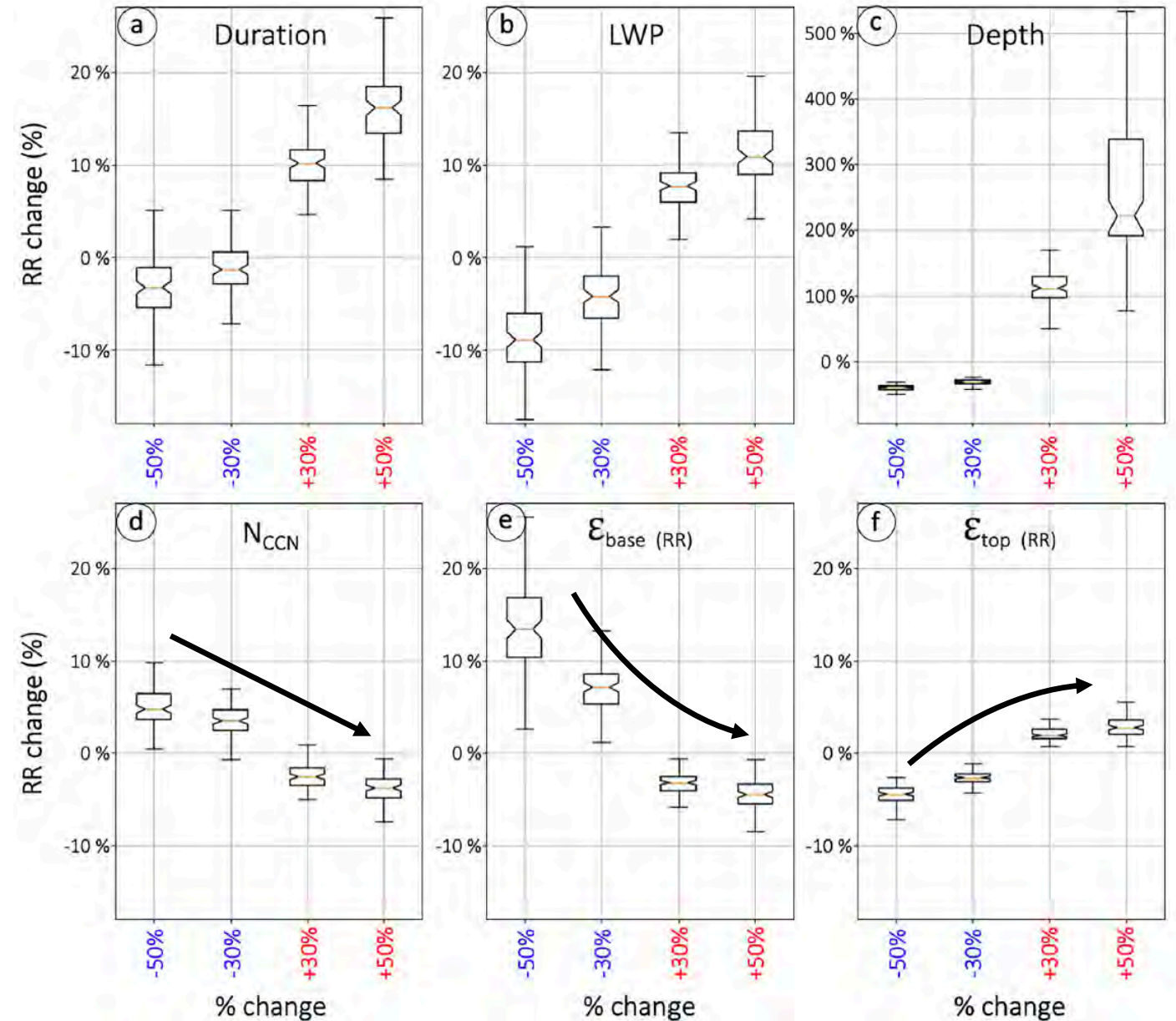
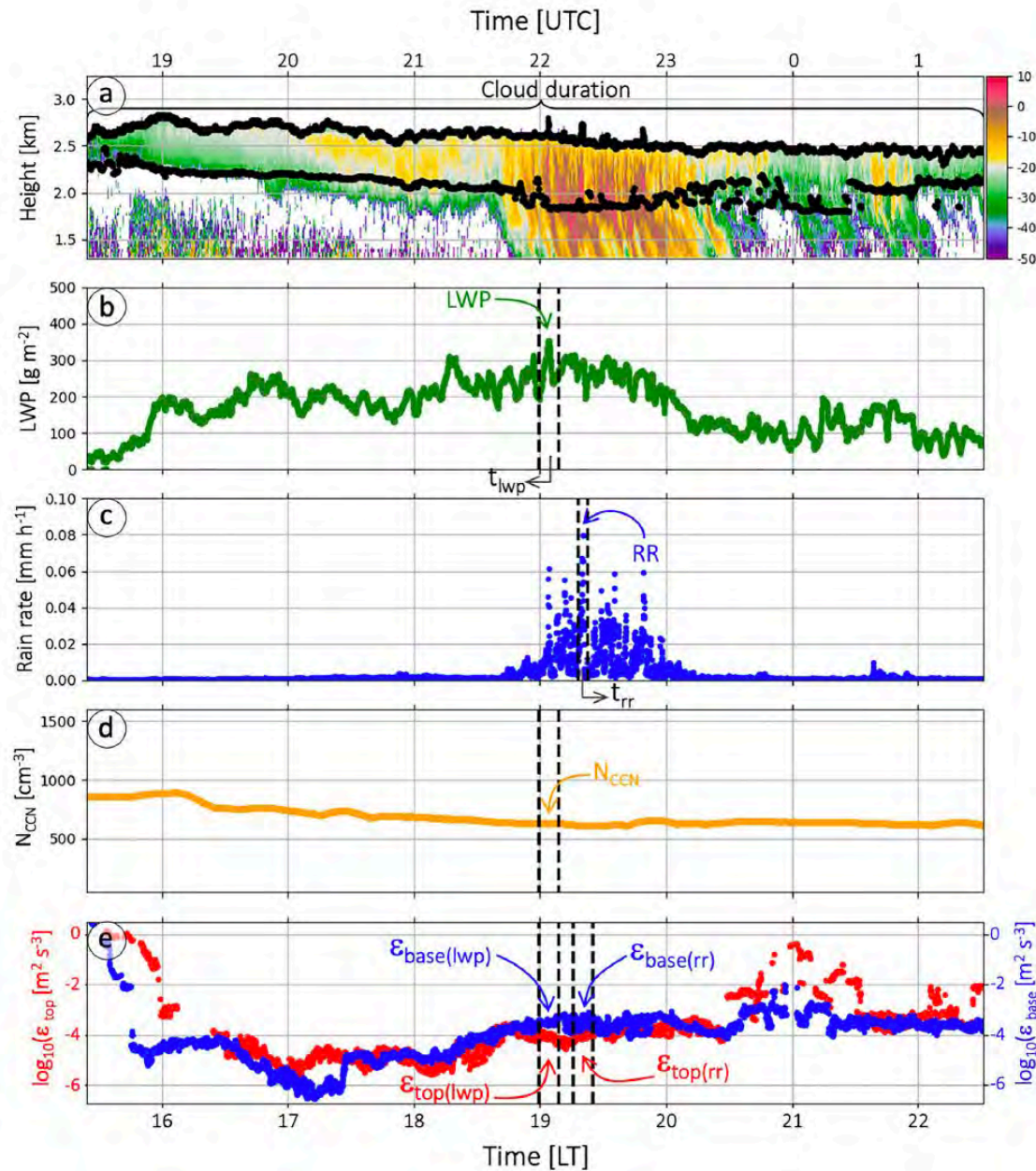


Aerosol and Turbulence Effects on Drizzle

Paloma Borque (PNNL)

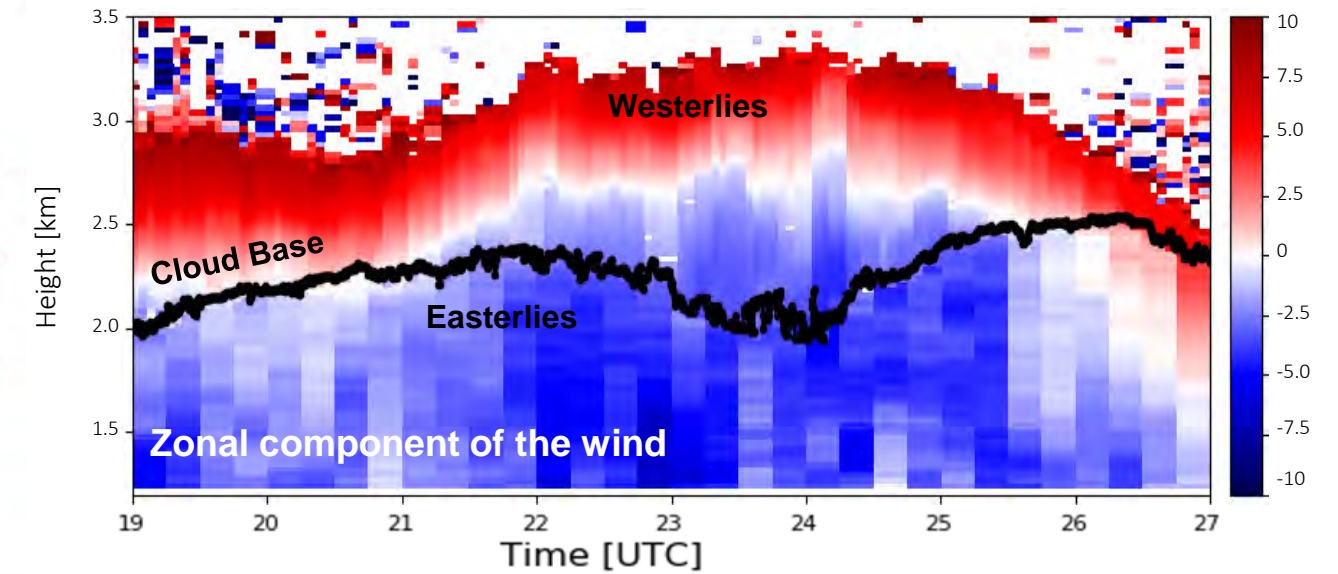
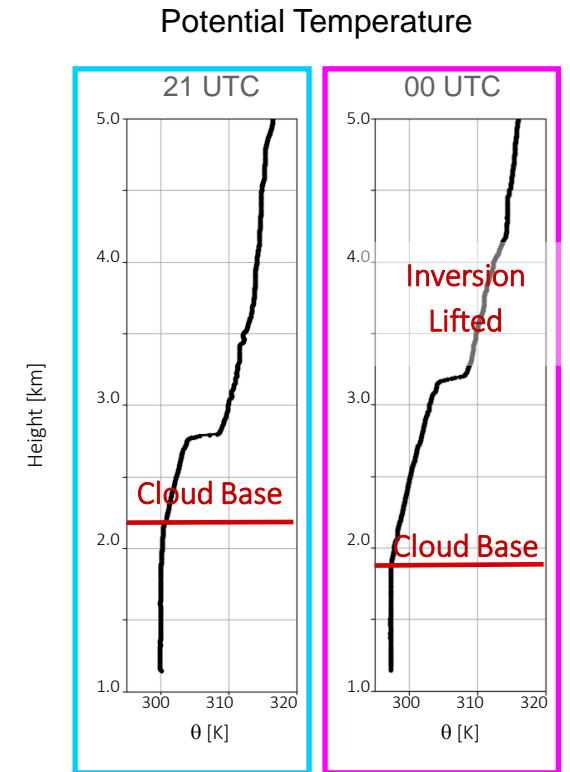
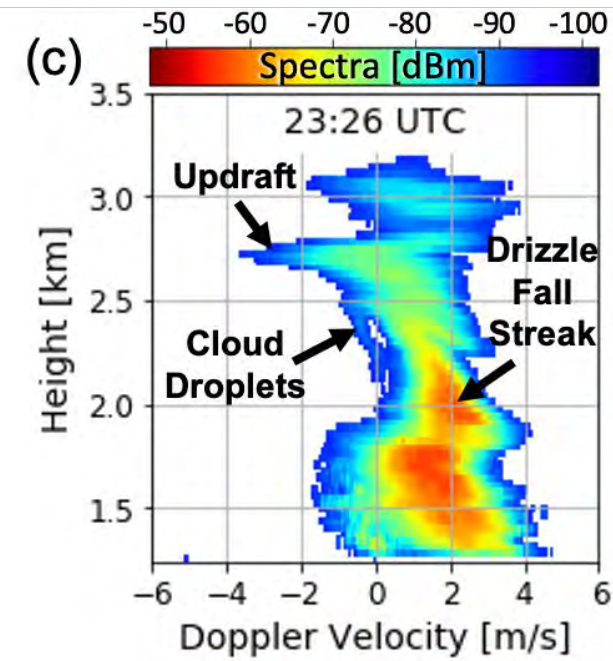
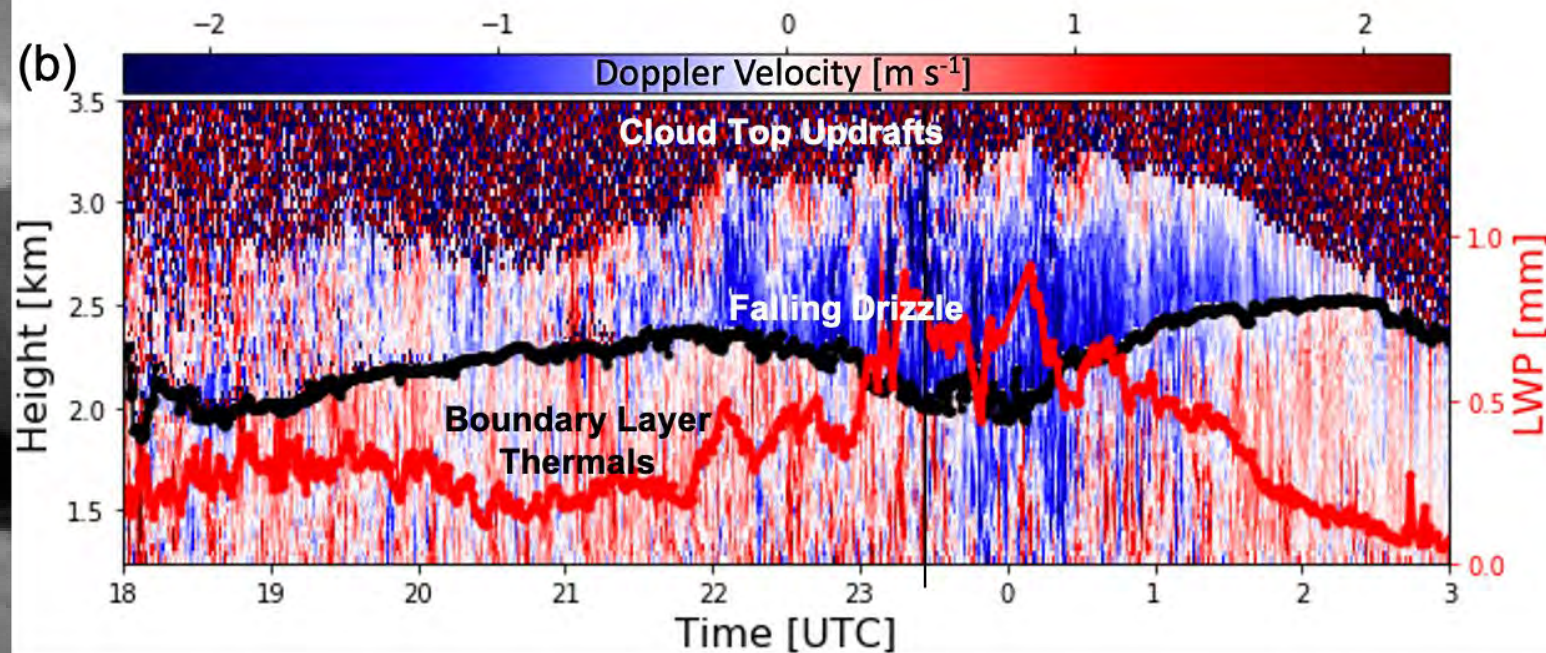
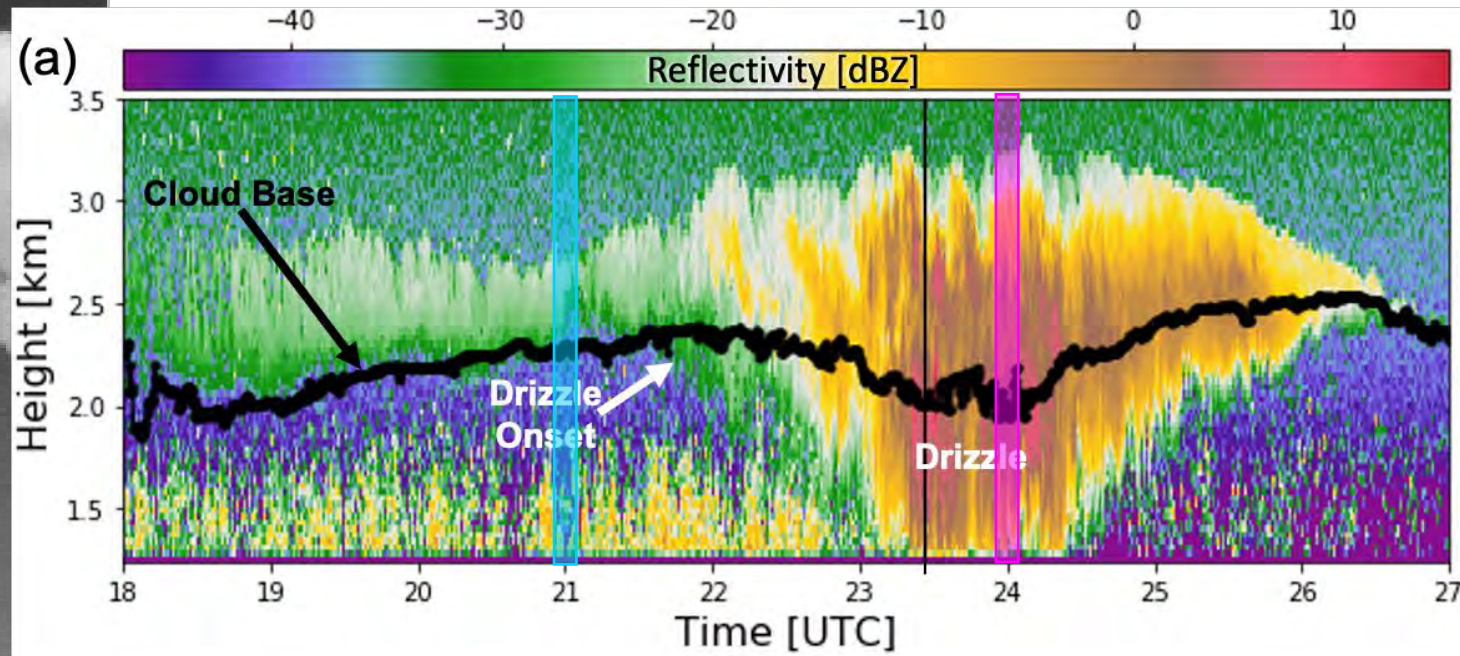
Borque, P., et al., 2022: Peak rain rate sensitivity to observed cloud condensation nuclei and turbulence in continental warm shallow clouds during CACTI. *JGR Atmos.*, doi:10.1029/2022JD036864.

3300 warm (1900 w/precipitation), 2200 mixed phase (extending below freezing), and 160 deep cloud time-height objects



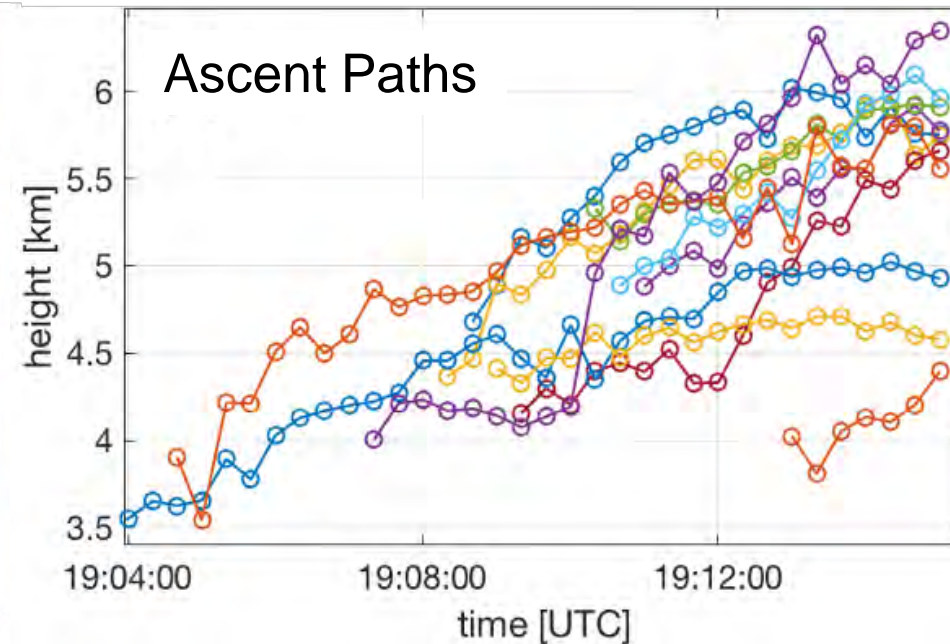
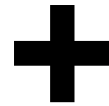
Further Shallow Cloud Research Opportunities

Courtesy Paloma Borque



Ongoing Research: Congestus Deepening Processes

Andrew Geiss (PNNL), Rusen Öktem and David Romps (LBL, UC-Berkeley)



How does cloud top ascent rate and max depth correlate with congestus width?

Does LES replicate observations, such that entrainment-driven dilution effects can be quantified?

Deep Convection Initiation Processes

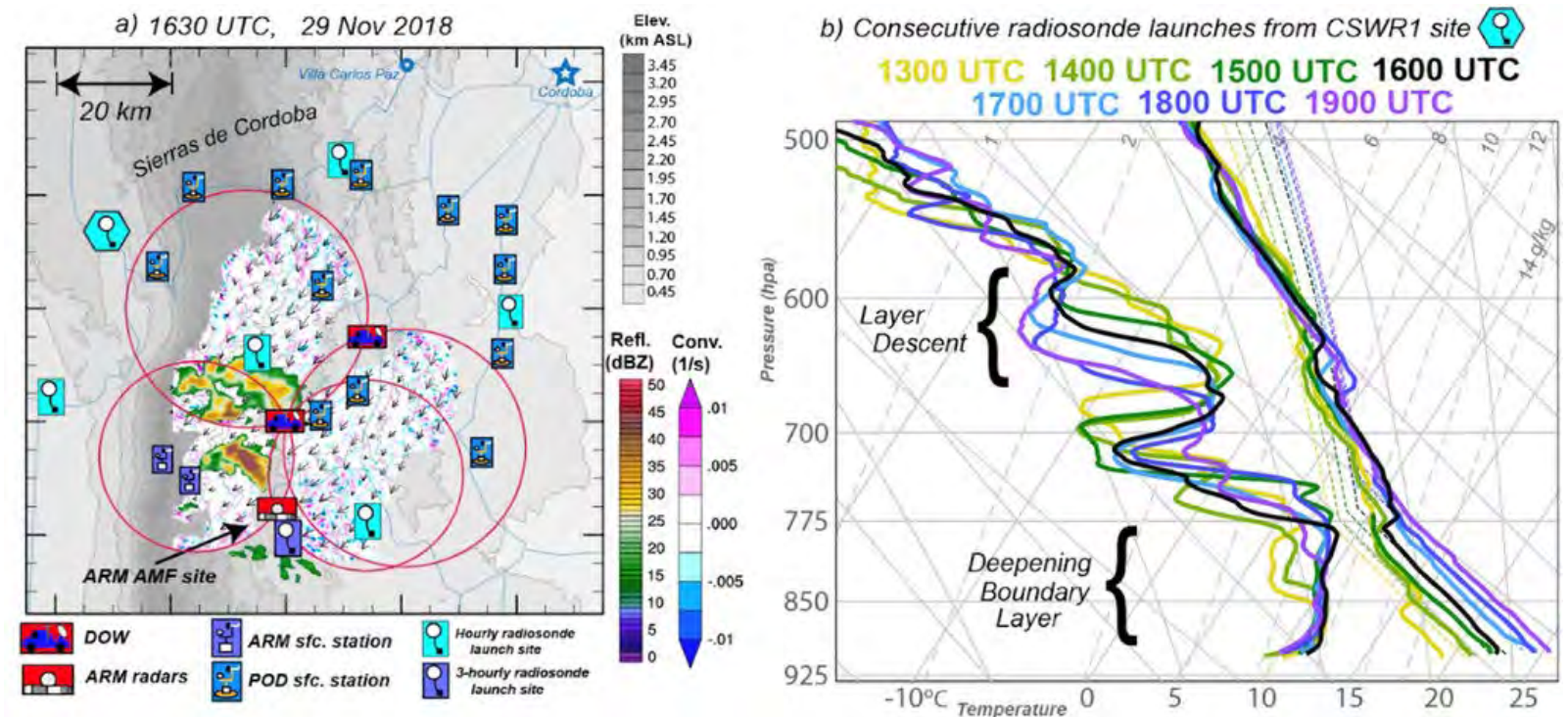
Jim Marquis (PNNL), Connor Nelson (U. Colorado)

With frequent orographic clouds and favorable deep convective thermodynamic conditions, many deep convection initiation (CI) success and failure cases were observed.

Marquis J. N., et al., 2021: Low-level Mesoscale and Cloud-scale Interactions Promoting Deep Convective Initiation. *MWR*, doi:10.1175/MWR-D-20-0391.1.

Nelson T. C., et al., 2021: Radiosonde Observations of Environments Supporting Deep Moist Convection Initiation during RELAMPAGO-CACTI. *MWR*, doi:10.1175/MWR-D-20-0148.1.

Marquis, J. N., et al., 2023: Near-cloud atmospheric ingredients for deep convection initiation, *MWR*, doi:10.1175/MWR-D-22-0243.1.



Updraft width is key to successful Deep CI

Jim Marquis (PNNL)

Max updraft widths on 29 Nov approach 5 km with coherence for 15-30+ minutes and correlate with the robust low level reflectivity areas downshear.

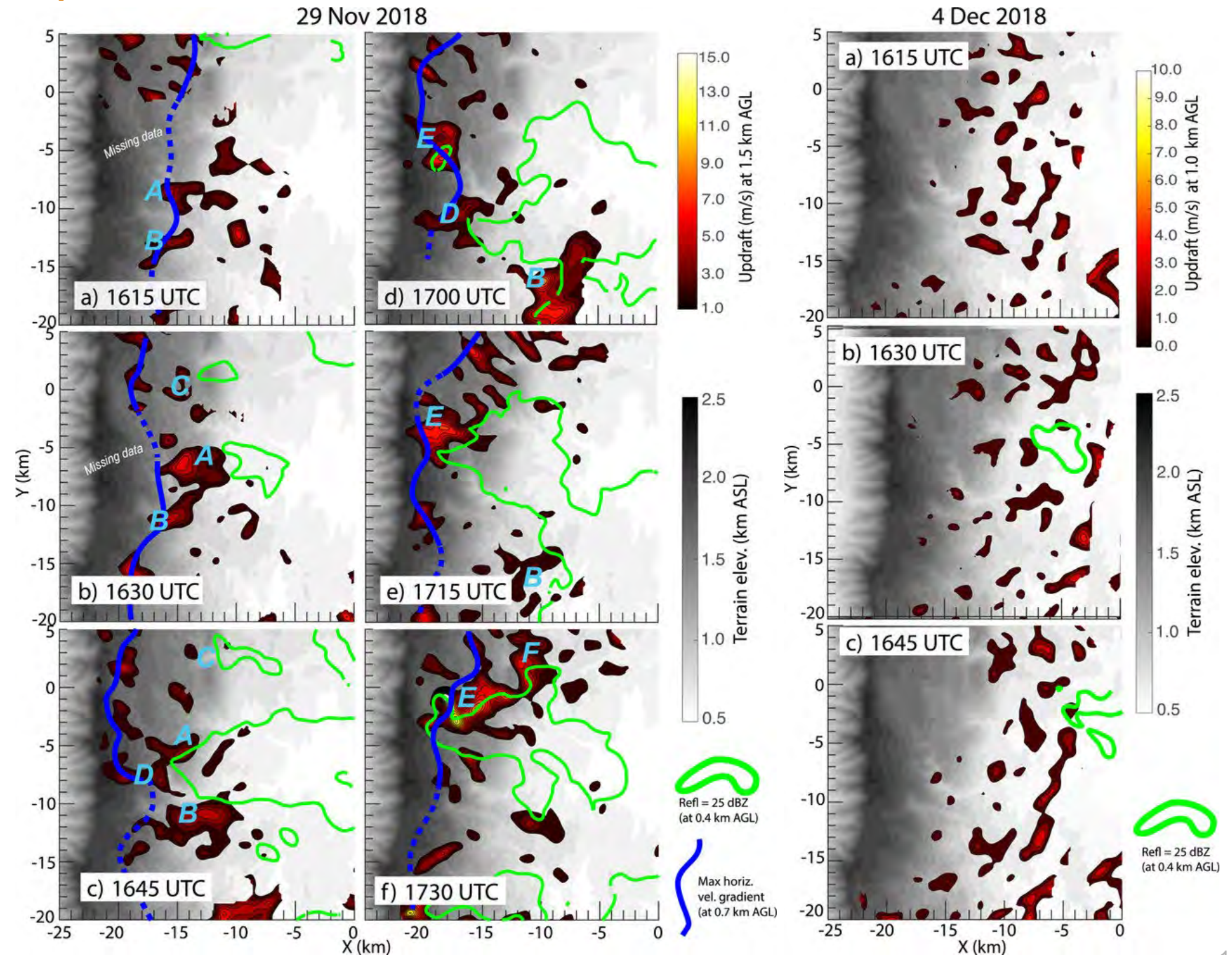
Max updraft widths on 4 Dec remain < 3 km, similar to the scale of boundary layer thermals.

Mesoscale convergence may promote wider updrafts that can overcome buoyancy dilution by entrainment aloft.

Mid-level humidity and large-scale ascent are also important (not shown)

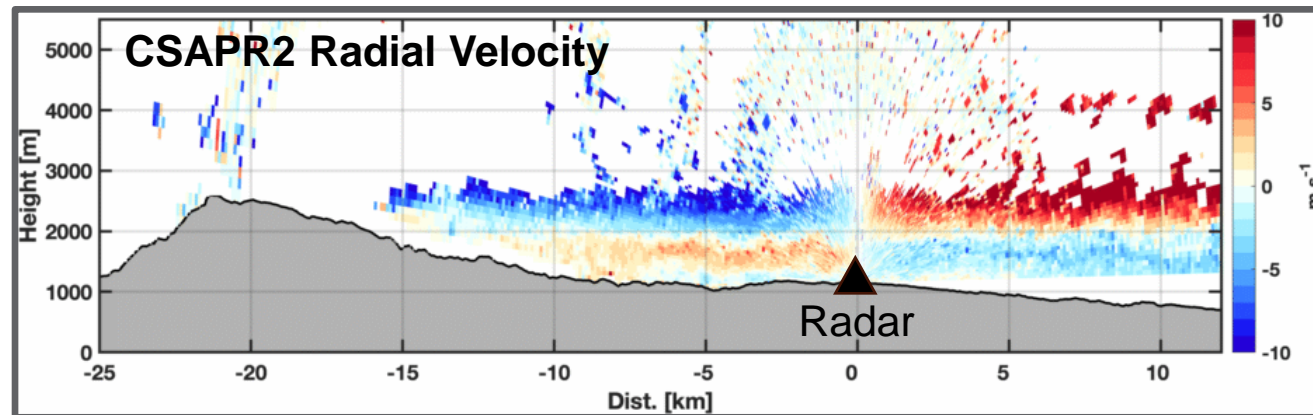
Marquis J. N., et al., 2021, *MWR*, doi:10.1175/MWR-D-20-0391.1.

Marquis, J. N., et al., 2023, *MWR*, doi:10.1175/MWR-D-22-0243.1.



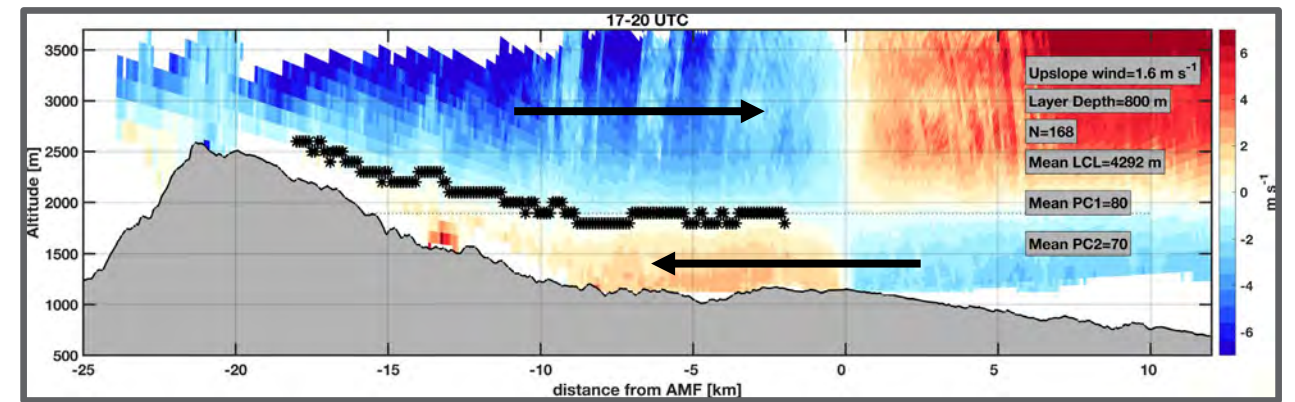
Ongoing Work: Orographic Flow Effects on Convective Clouds

Neil Lareau (U. Nevada, Reno)

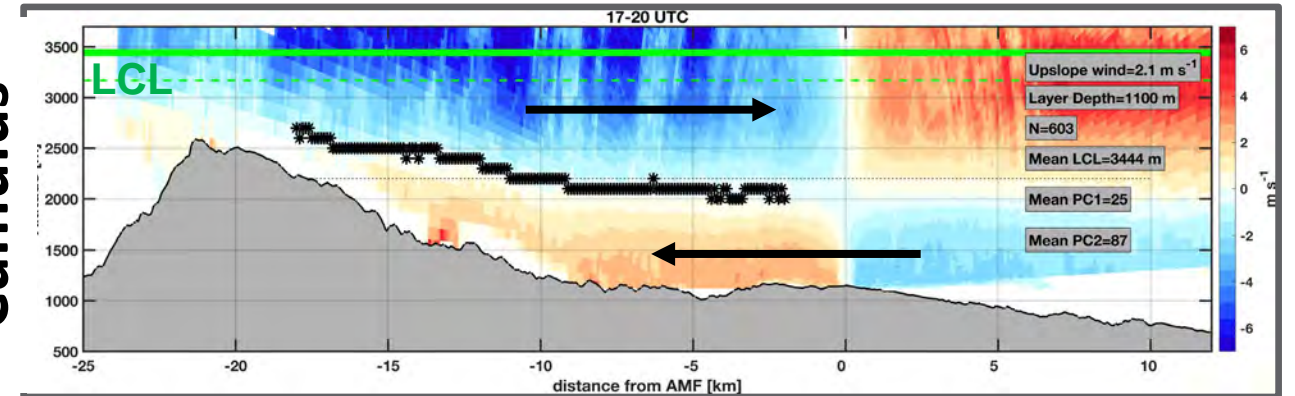


- Upslope flow deepens with increasing cloud development
- LCL lowers with increasing cloud development
- *Thermally forced* upslope flow increases from clear to congestus mode, then decreases for deep mode
- *Mechanically forced* east-to-west flow in the mid-levels increases on deep convective days
- Increasing stability suppresses the upslope flow but sensible heat flux has little correlation

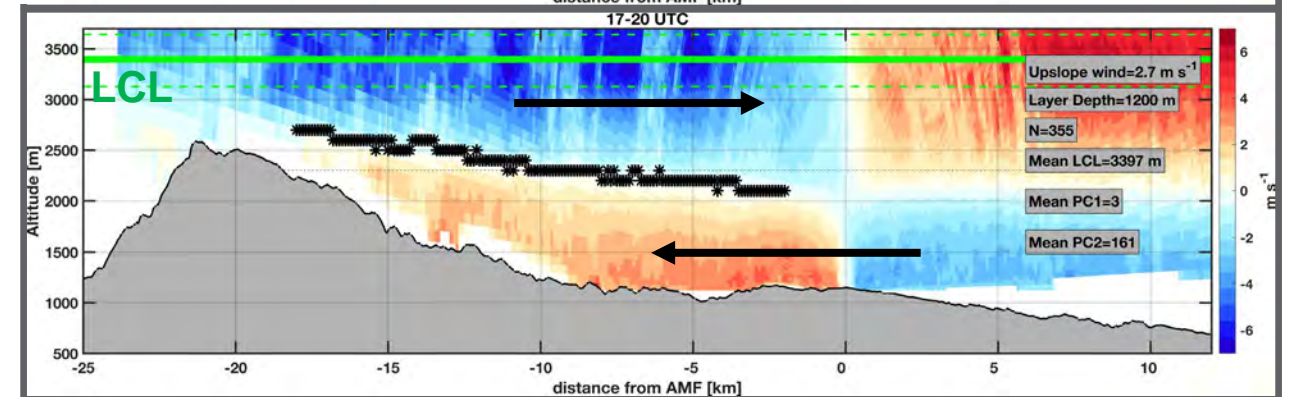
Clear Sky



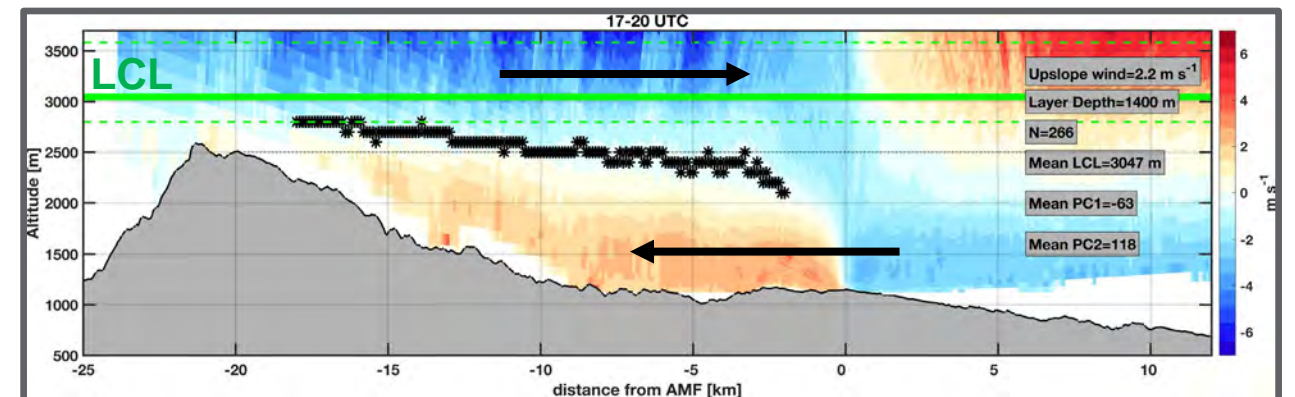
Shallow Cumulus



Congestus



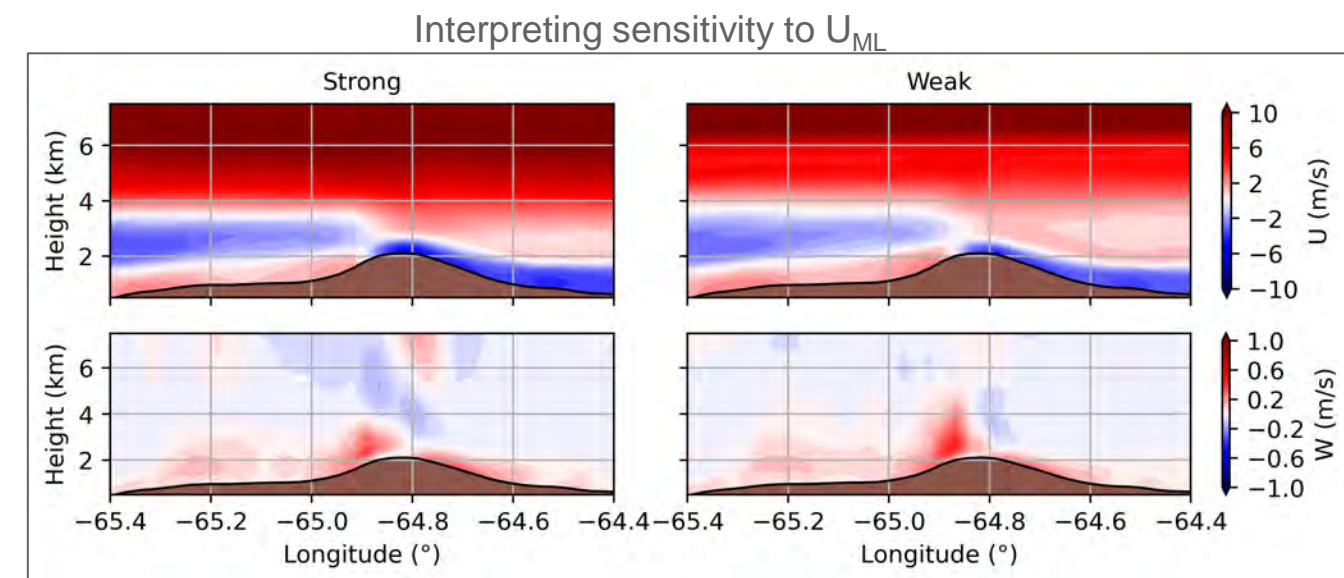
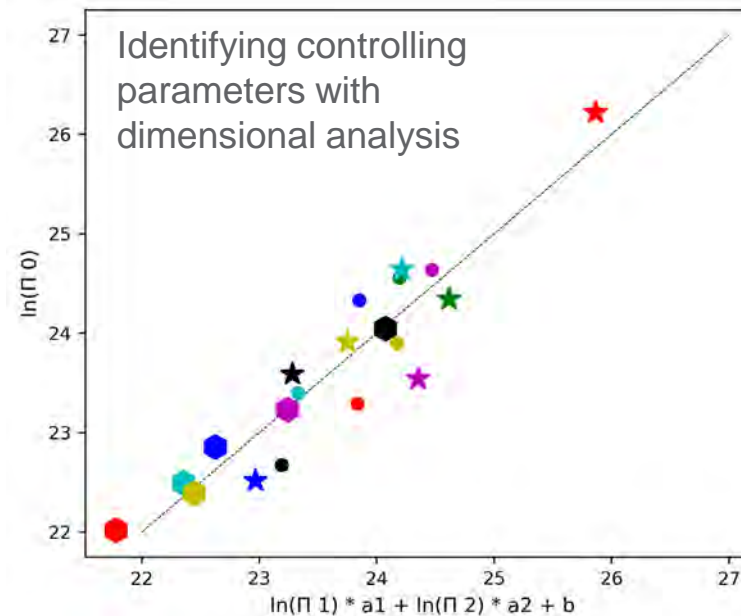
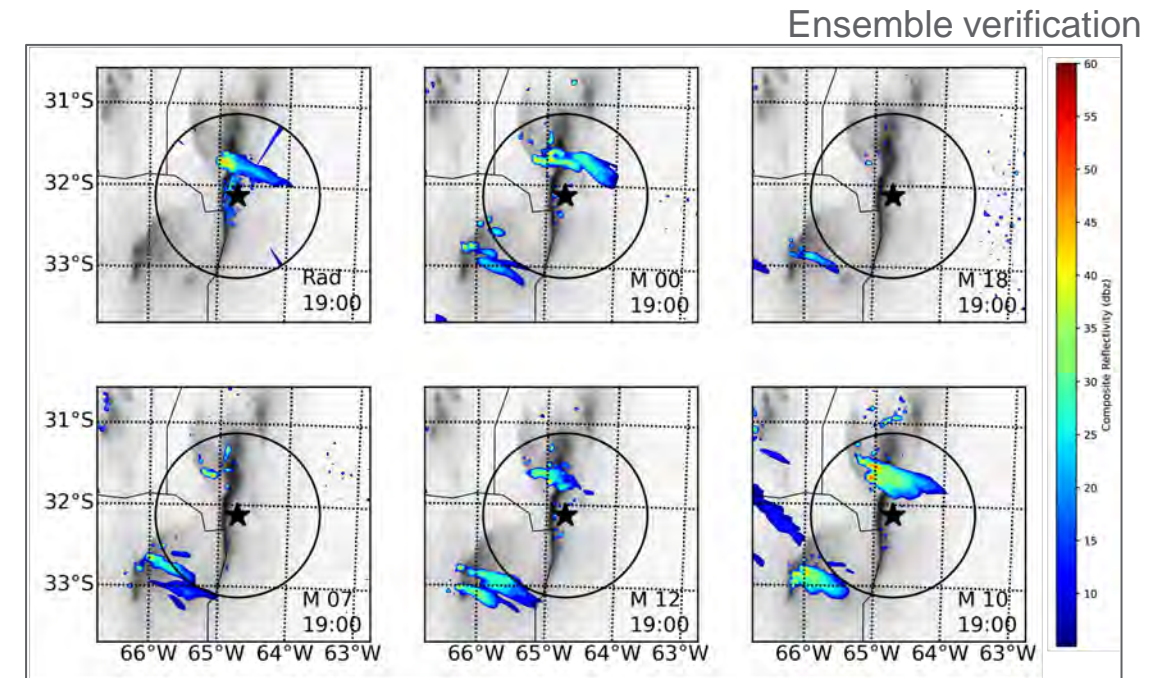
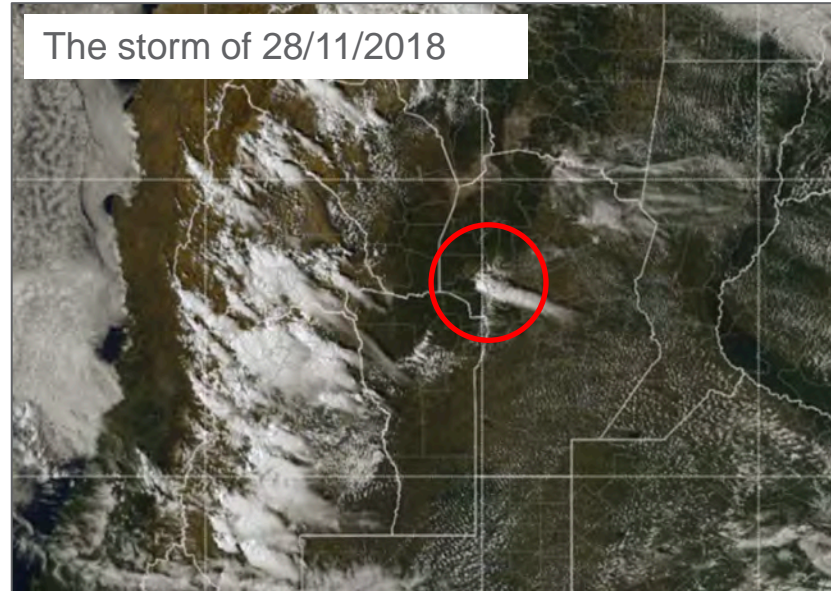
Deep Convection



Ongoing Work: Convective-scale ensemble predictability of an isolated thunderstorm

Andres Lopez, Dan Kirshbaum (McGill U.)

- 21 member, 2.5-km WRF initial-condition ensemble
- Using CACTI AMF1 observations, identified a major soil moisture bias
 - Rectification greatly improved verification
- Gained fundamental insight into mechanisms of convection initiation
 - Convective precipitation controlled by 3 pre-convective parameters: *CAPE, PBL upward mass flux, mid-level zonal wind*



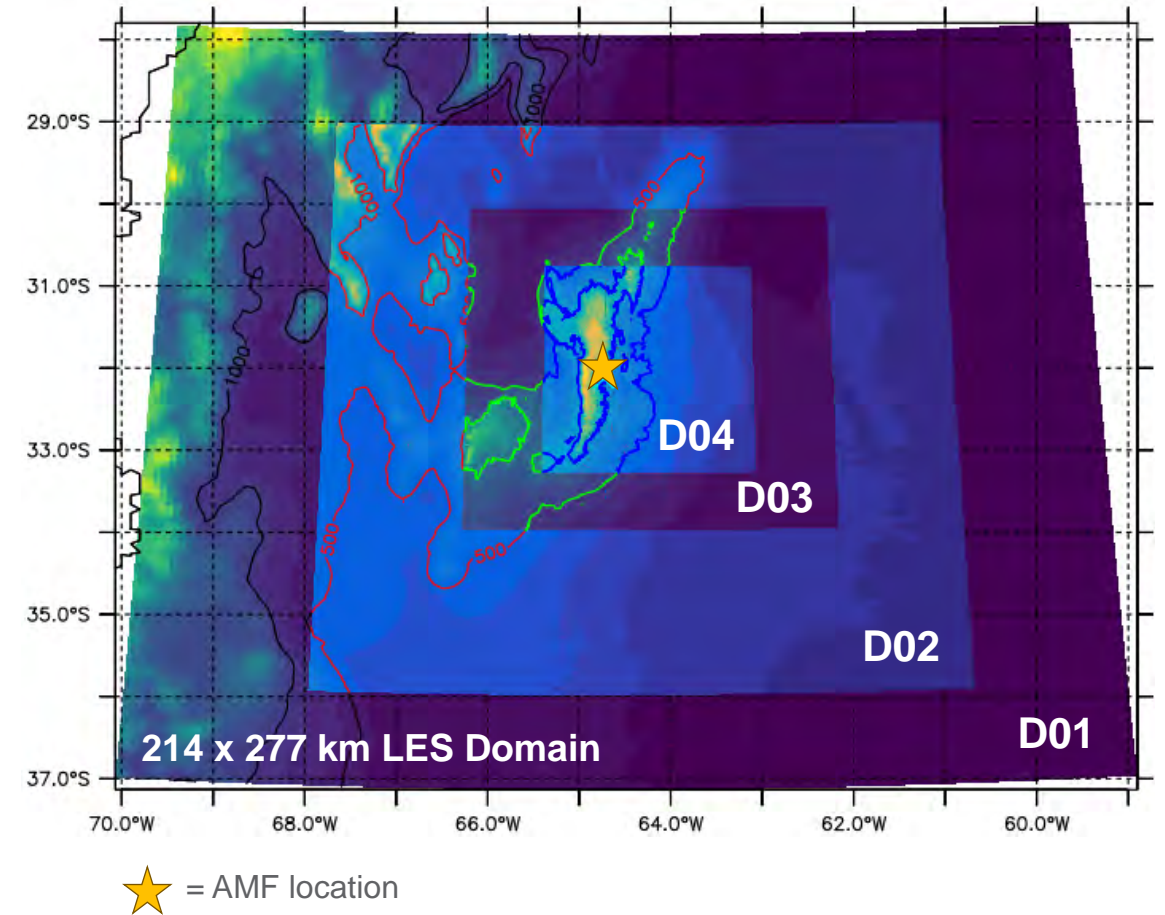


LASSO-CACTI

Bill Gustafson, Andy Vogelmann, and colleagues (PNNL, BNL)

- 20 cases with 33 ensemble members for the D02 domain (660 runs)
- 9 cases with D04 LES and multiple ensemble members (~35 total runs)
- Post-processed (subset, gridded) files and skill scores with observations
- Resides on ARM's Cumulus-2 cluster w/Jupyter; ARM is moving it for easier access (2 PB of data); email lasso@arm.gov for info
- Beta release: <https://discourse.arm.gov/t/lasso-cacti-beta-release-documentation/118>
- **Breakout: Today, 2-4 PM, Poster session 4, posters 40, 42**

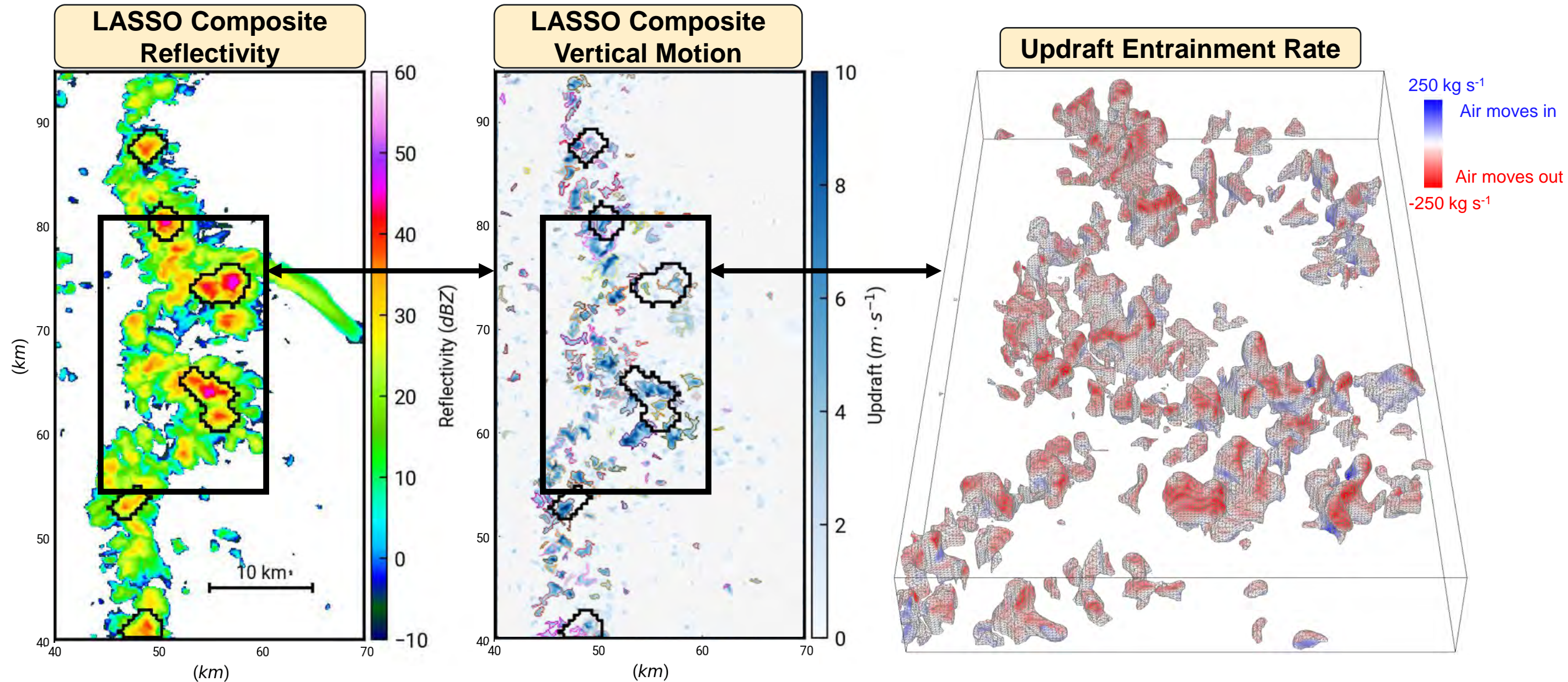
WRF Model Domains
 $\Delta x = 7.5 \text{ km}, 2.5 \text{ km}, 500 \text{ m}, \& 100 \text{ m}$



Category	Domain(s)	Δx	Frequency	Period	Purpose
Meso	D01, D02	7.5 km, 2.5 km	15 min	0–24 UTC	Full model state and diagnostics
Bridge	D03	500 m	15 min	6–24 UTC	Full model state and diagnostics
LES	D04	100 m	5 min	12–24 UTC	Full model state and diagnostics
Restart	D03, D04		30 min		Enable users to do restarts

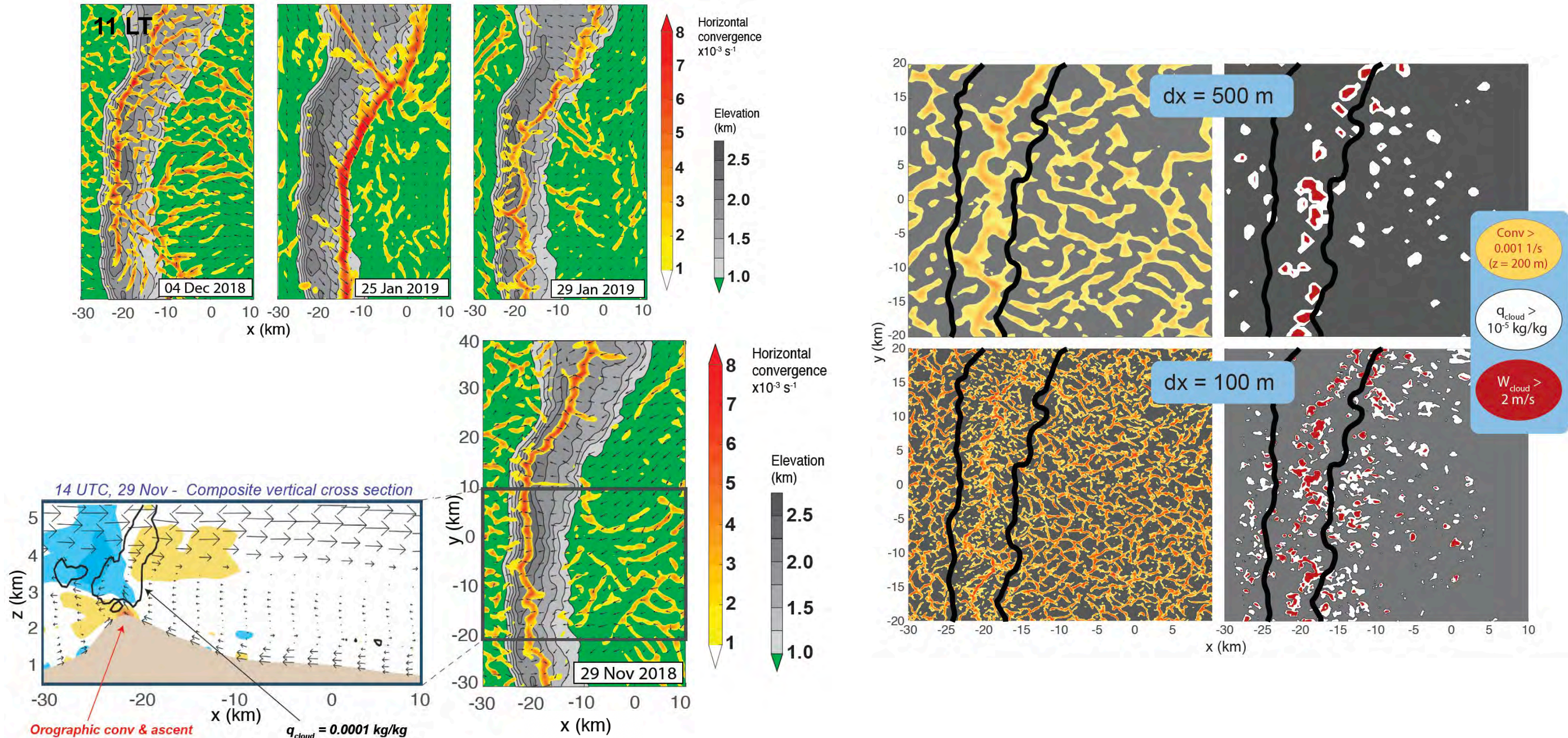
Ongoing Work: Entrainment effects on convective cell life cycles

Enoch Jo (PNNL); See session 4 poster 46



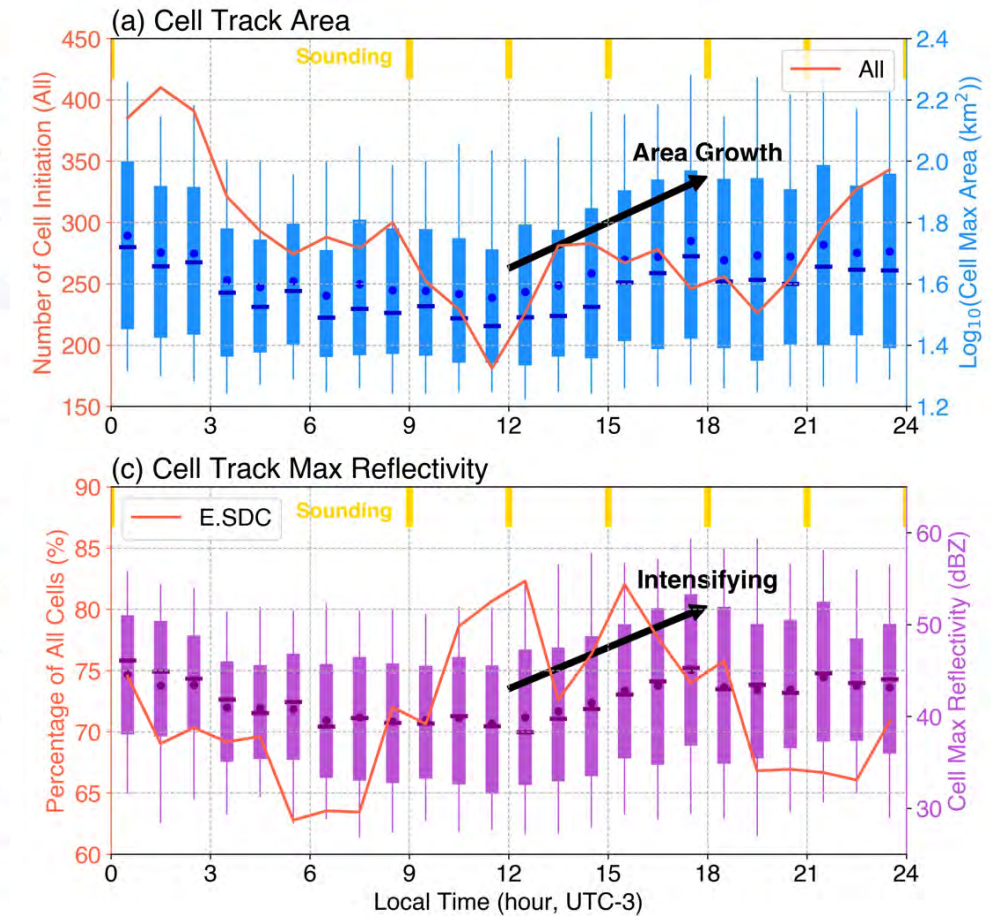
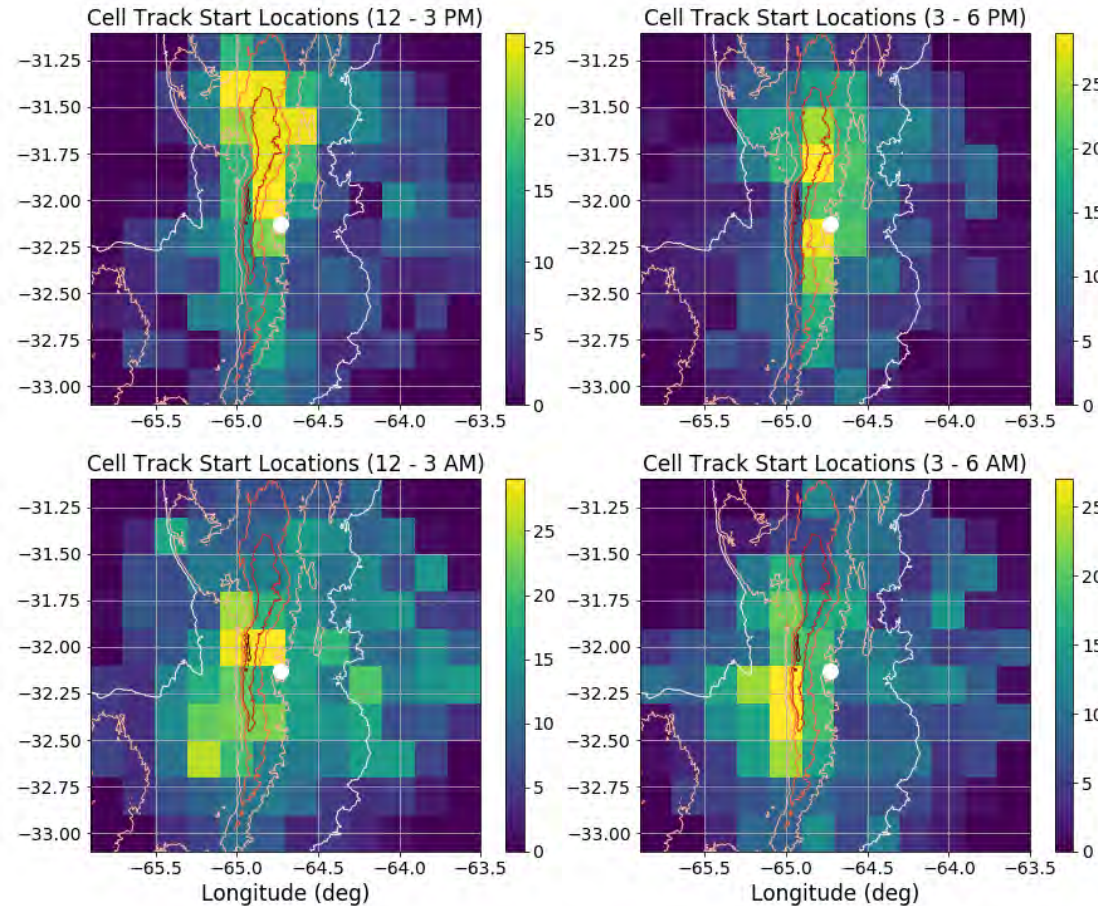
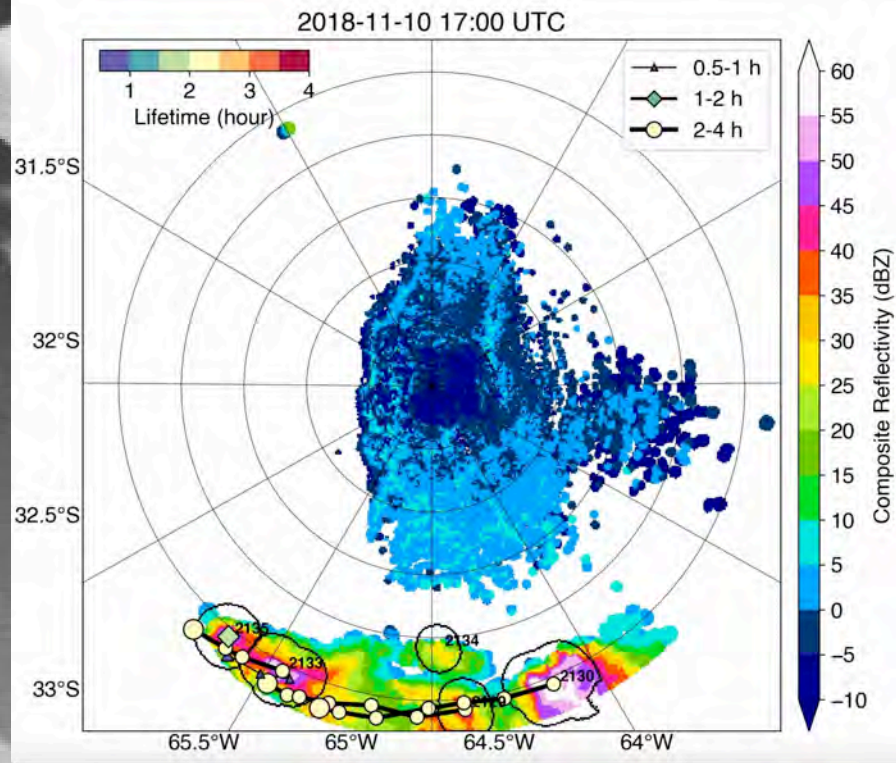
Ongoing Work: How mesoscale convergence facilitates deep convection initiation

Jim Marquis (PNNL); See session 4, poster 52



Convective Cell Track Database

*Zhe Feng (PNNL); Available as ARM PI product;
See session 1, poster 47*



PyFLEXTRKR was used to separate, track, and save properties (Profiles of Z_e , Z_{DR} , K_{DP} , rain rate, D_m , RWC, GOES cloud tops) of ~6,900 convective cells on 74 days, matching them to sounding-derived atmospheric conditions.

Feng, Z, et al., 2022: Deep Convection Initiation, Growth, and Environments in the Complex Terrain of Central Argentina during CACTI, *MWR*, doi:10.1175/MWR-D-21-0237.1.

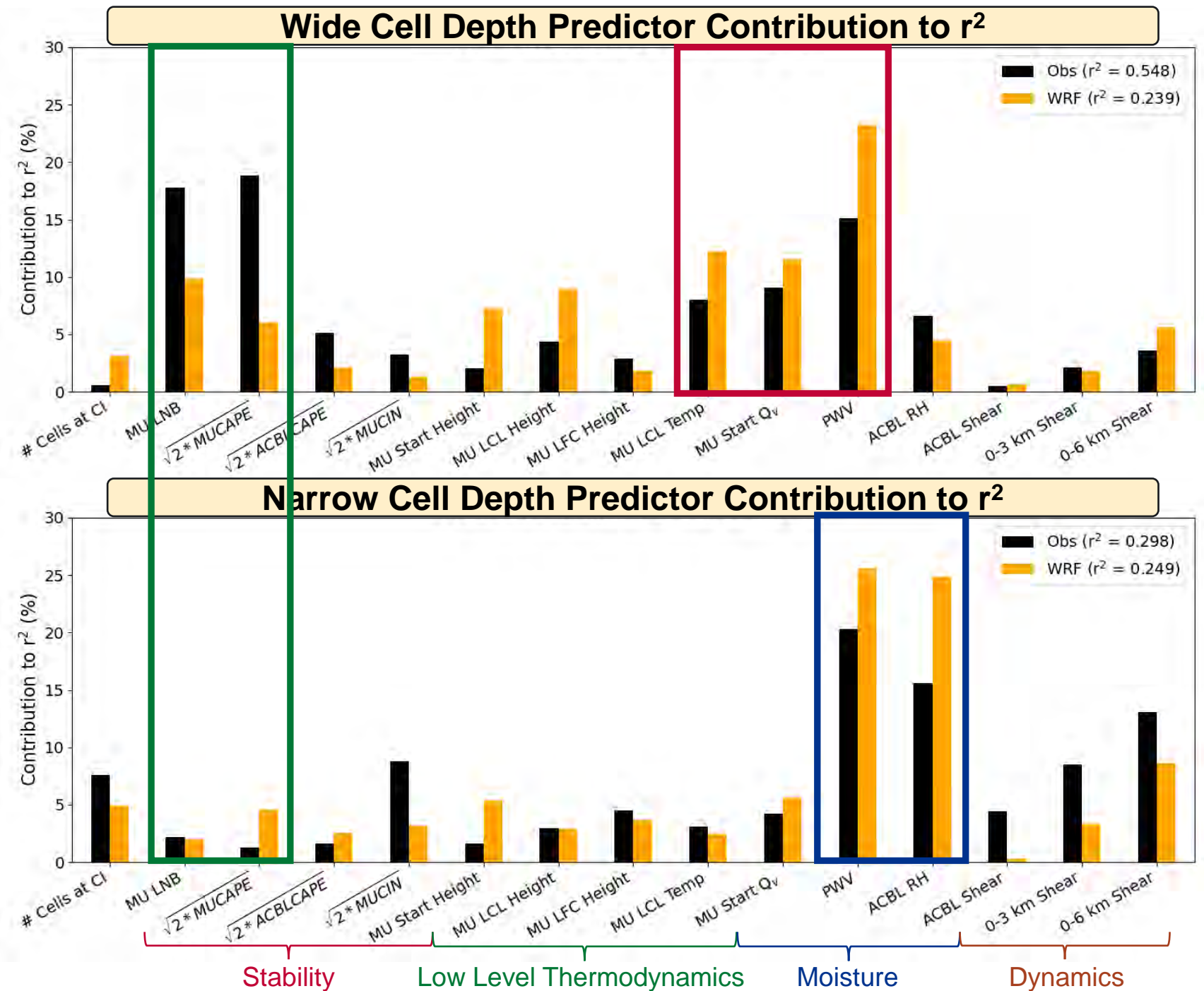
Feng, Z., et al., 2023: PyFLEXTRKR: A Flexible Python Feature Tracking Software for Convective Cloud Analysis. *GMD*, doi:10.5194/gmd-16-2753-2023.

<https://github.com/FlexTRKR/PyFLEXTRKR>

Ongoing Work: Controls on Convective Cell Growth

Adam Varble (PNNL); See session 1 poster 49

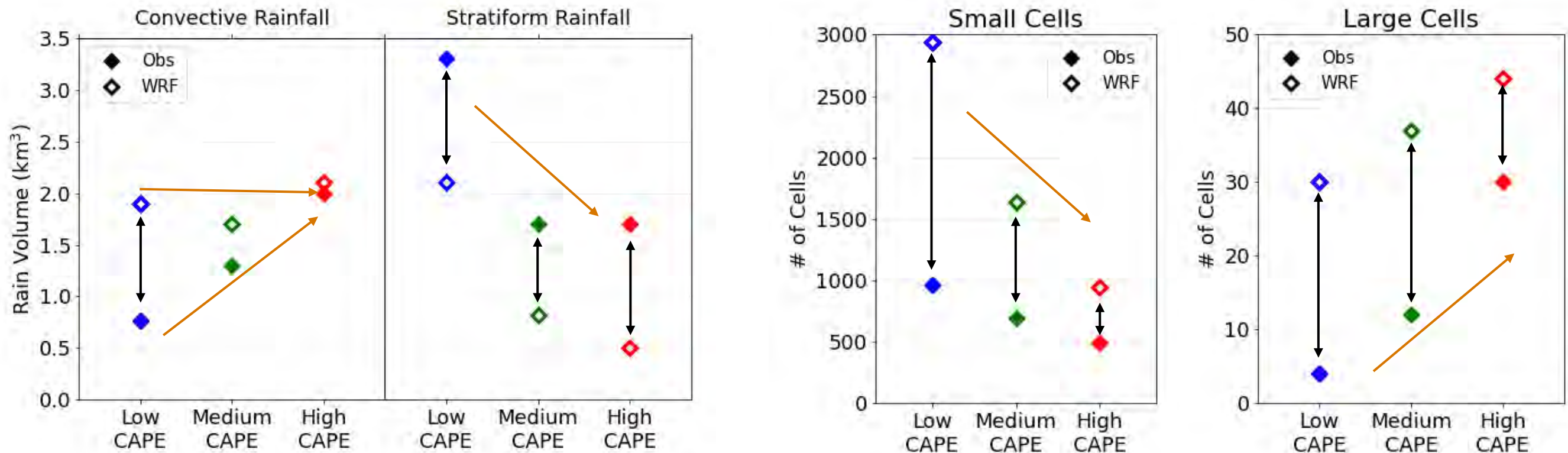
- MUCAPE and MU LNB are good predictors for wide cell growth but not narrow cell growth, which correlates better with ACBL RH
- PWV is a good predictor for all cells but manifests as low-level moisture changes for wide cells and mid-level moisture changes for narrow cells.
- This is observational support for entrainment-driven dilution mattering for narrow but not wide updrafts, as found in idealized modeling studies



Simulated Convective Cell and System Growth Biases

Zhixiao Zhang (U. Utah)

Zhang, Z., et al., 2023, to be submitted to *JGR-Atmospheres*.



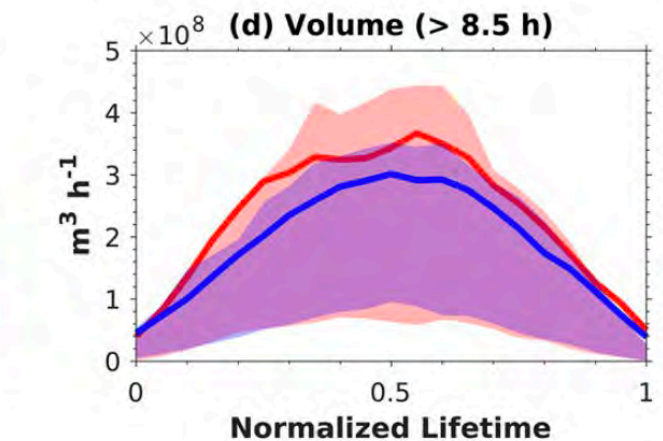
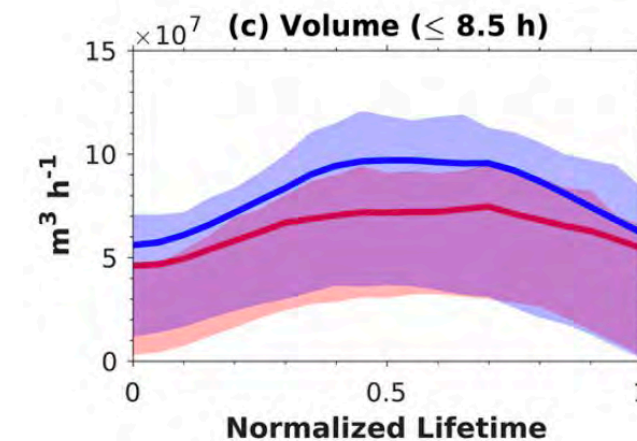
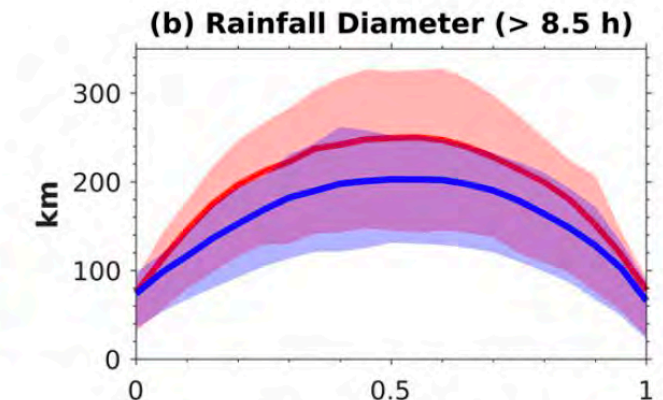
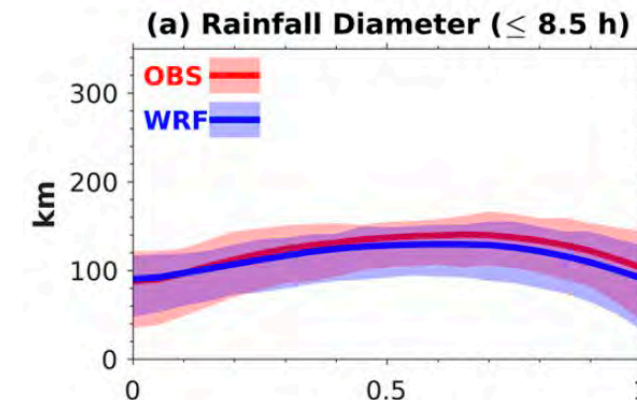
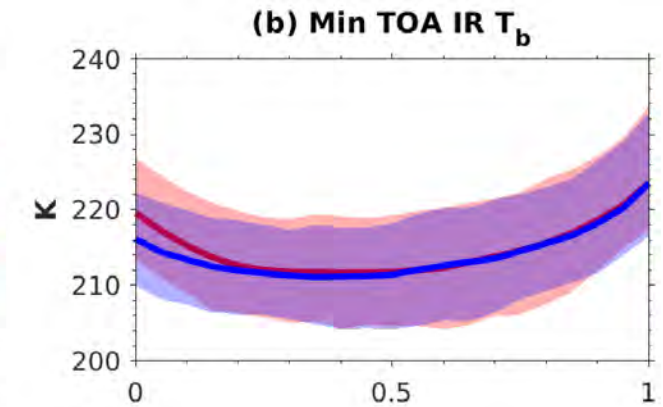
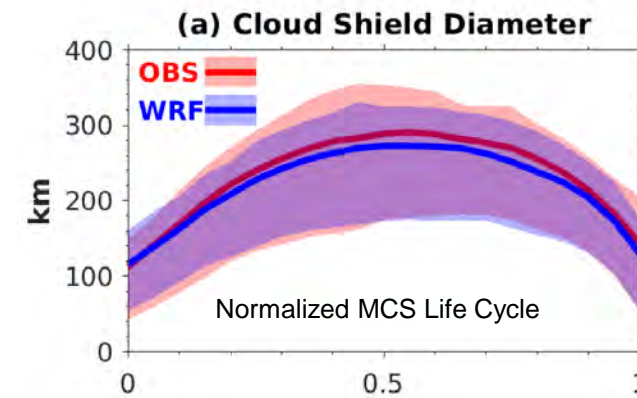
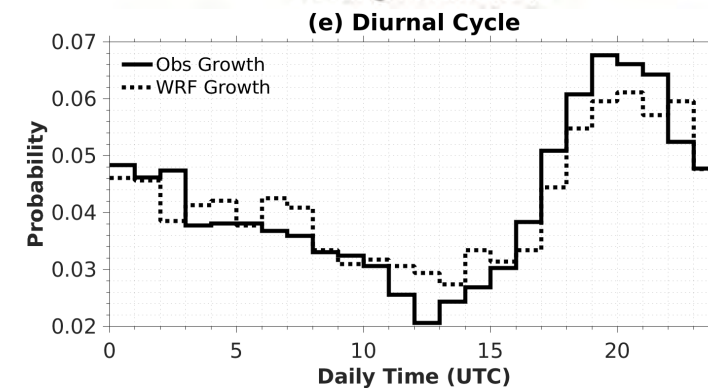
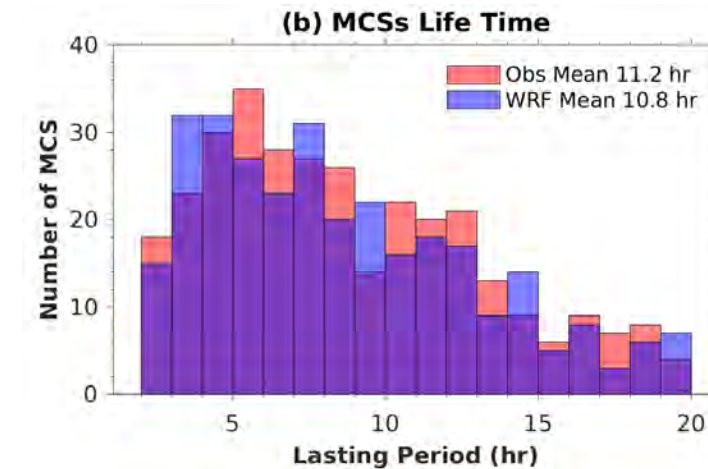
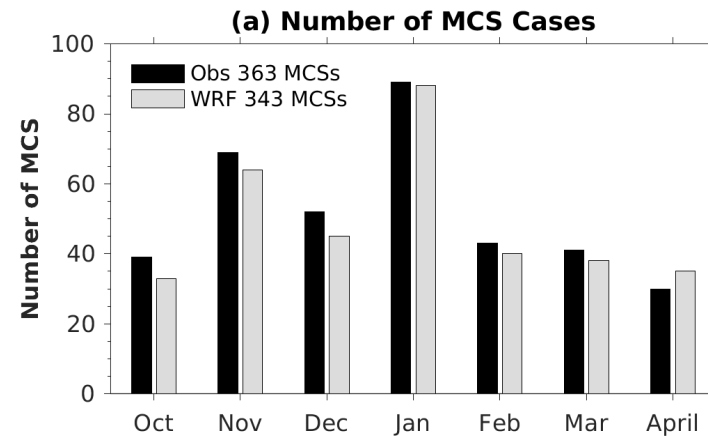
- Convection-permitting (3-km) WRF reproduces rainfall, but significantly underpredicts stratiform rainfall.
- WRF has far too many convective cells (not due to resolution).
- Large cells disproportionately contribute to convective rainfall in WRF.
- Convective biases tend to decrease as CAPE increases though stratiform biases do not.

Simulated MCS Growth Biases

Zhixiao Zhang (U. Utah)

Zhang, Z., et al., 2021: Growth of Mesoscale Convective Systems in Observation and a Seasonal Convection-Permitting Simulation over Argentina. *MWR*, doi:10.1175/MWR-D-20-0411.1.

- WRF replicates observed MCS numbers, timing, and lifetimes.
- WRF also reproduces MCS cloud shield area and temperature
- WRF rain rates tend to be too heavy with insufficient areal coverage of lighter precipitation, a bias that worsens as MCSs become larger and longer lived



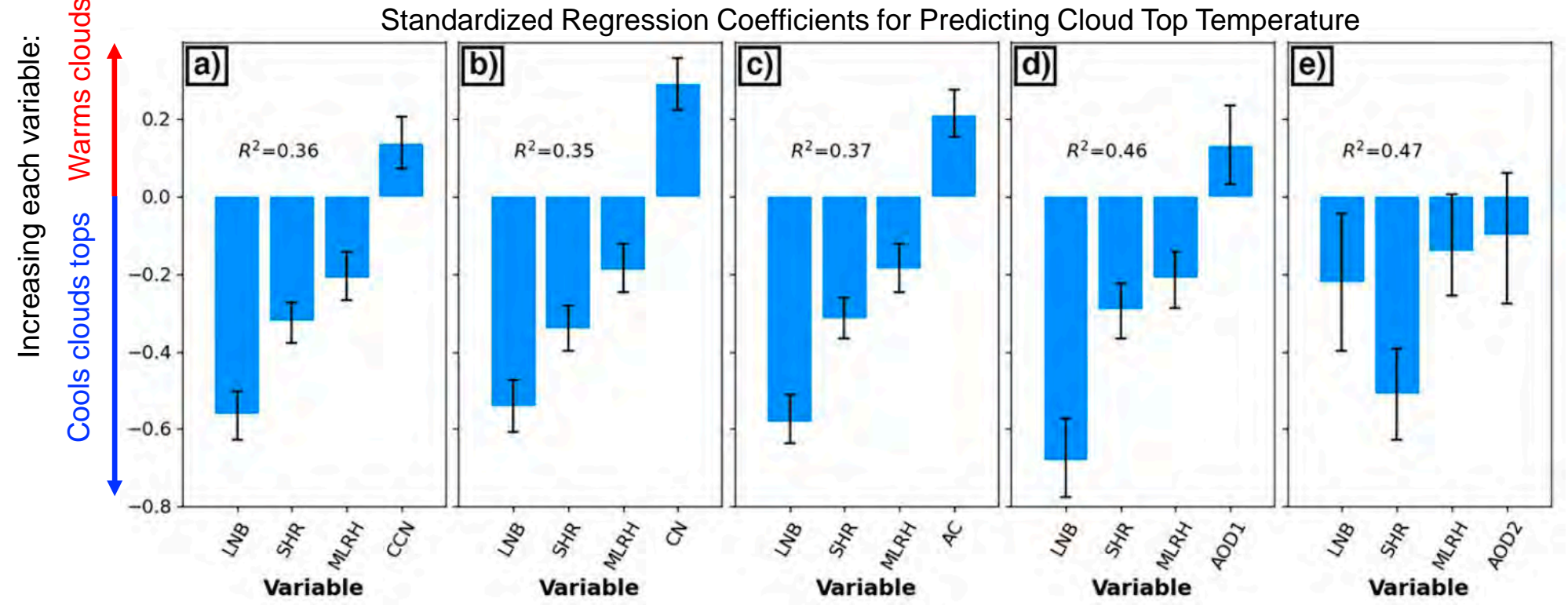
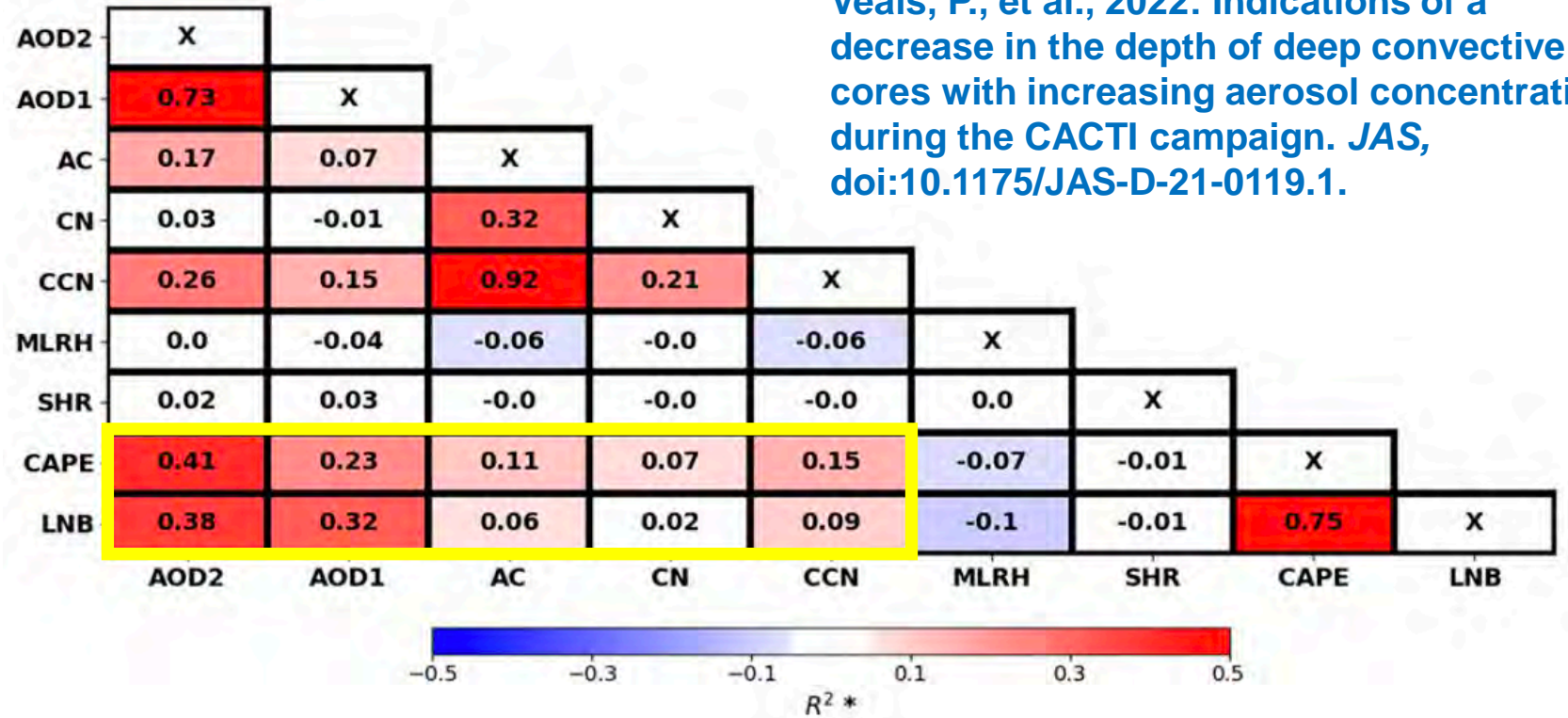
Aerosol Effects on Deep Convection

Peter Veals (U. Utah)

CCN negatively correlates with deep convective depth, but only if controlling for LNB or CAPE

Ongoing work at PNNL examining tracked cell microphysical modification by aerosols and modulation by intra-convective cell interactions

Veals, P., et al., 2022: Indications of a decrease in the depth of deep convective cores with increasing aerosol concentration during the CACTI campaign. *JAS*, doi:10.1175/JAS-D-21-0119.1.



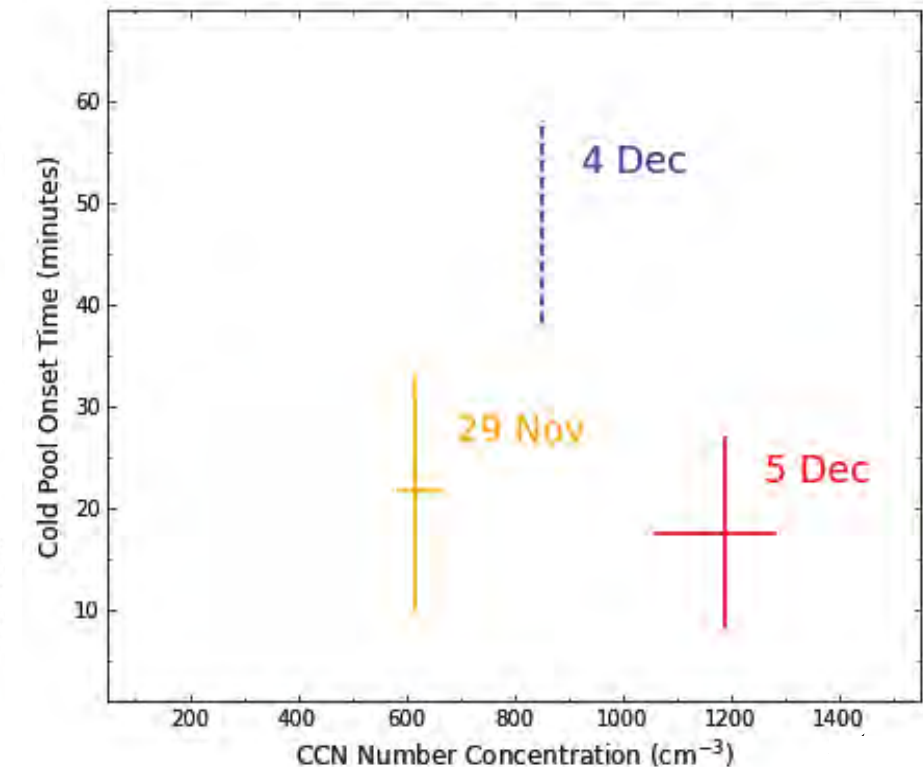
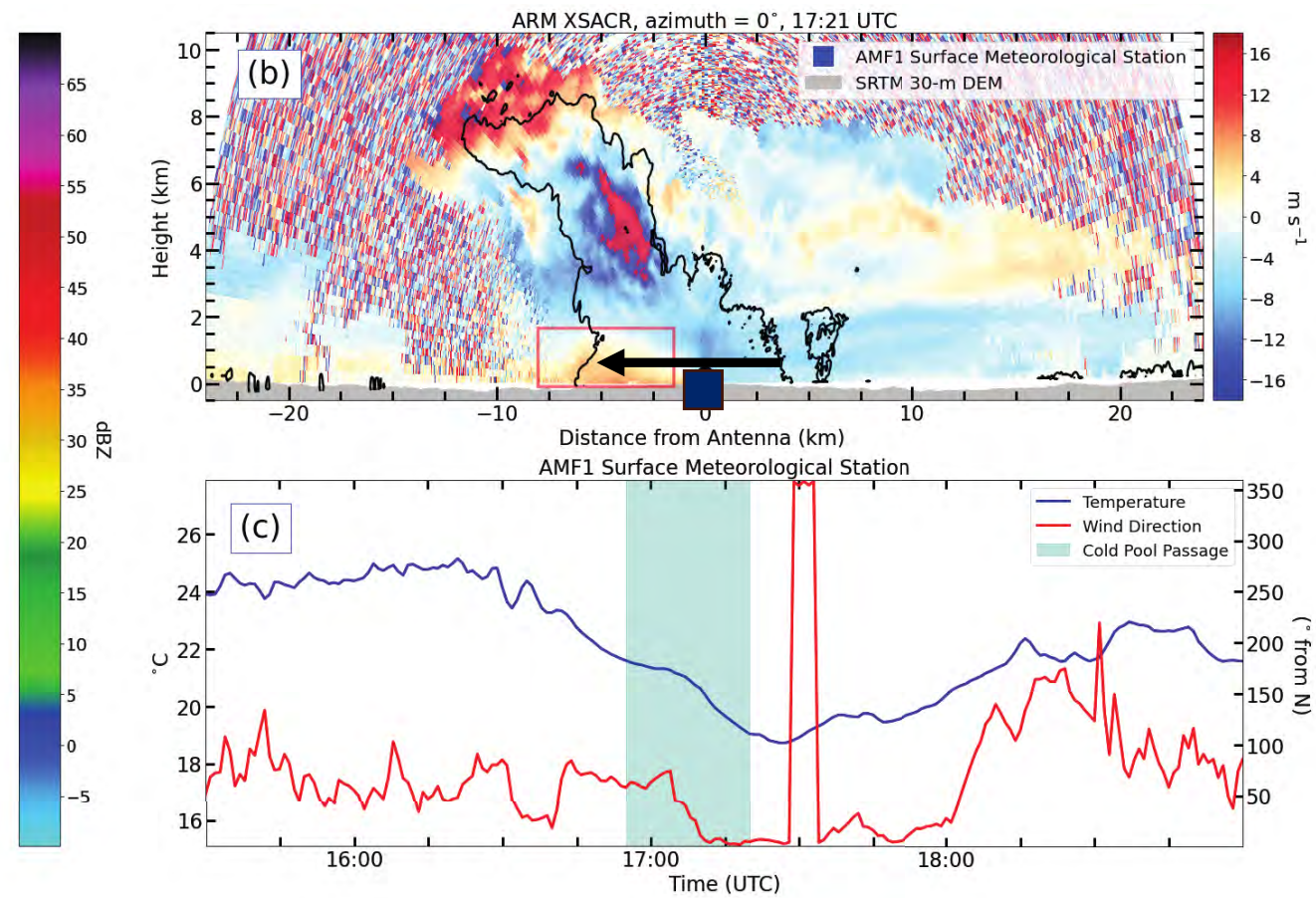
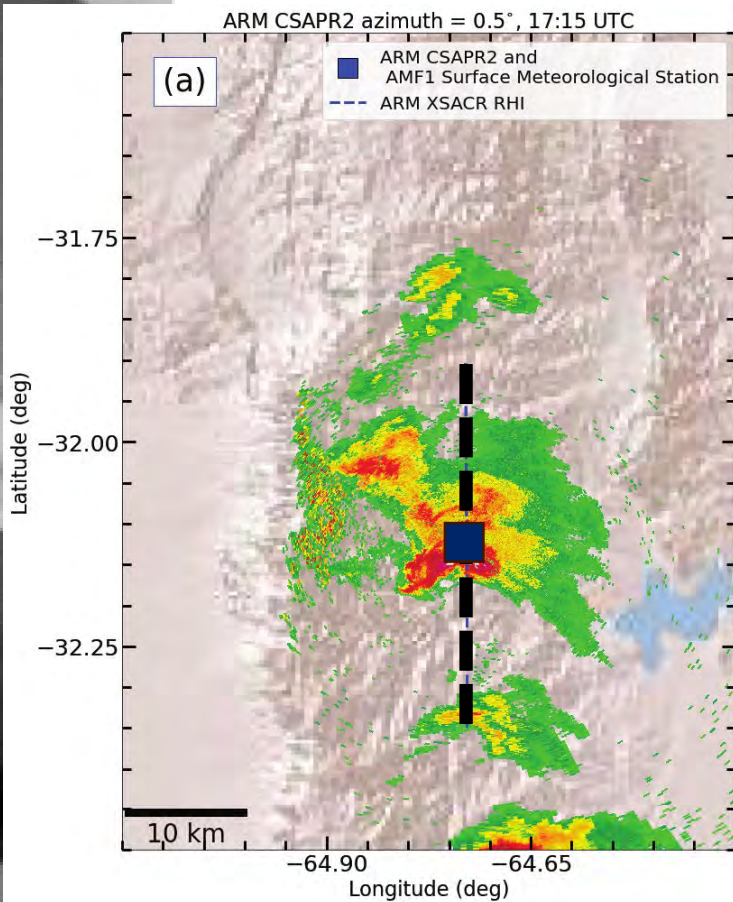
CCN Effects on Convective Cold Pools

Sonia Lasher-Trapp, Toby Ross (U. Illinois)

MWR paper in review: "On CCN Effects upon Convective Cold Pool Timing and Features"
See session 3 poster #49

Hypothesis: Storms ingesting more CCN have delayed precipitation and delayed cold pools

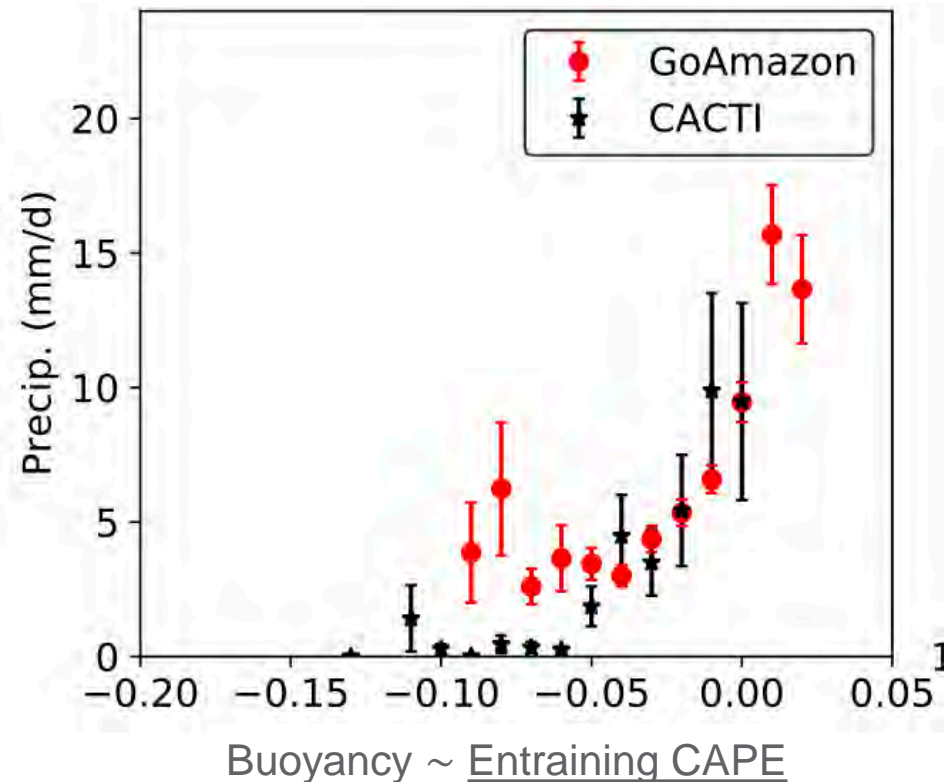
Results: Ordinary thunderstorms adhered to hypothesis, but the supercell (5 Dec) did not. Numerical modeling supported these results.



Ongoing Work: Thermodynamic controls on precipitation

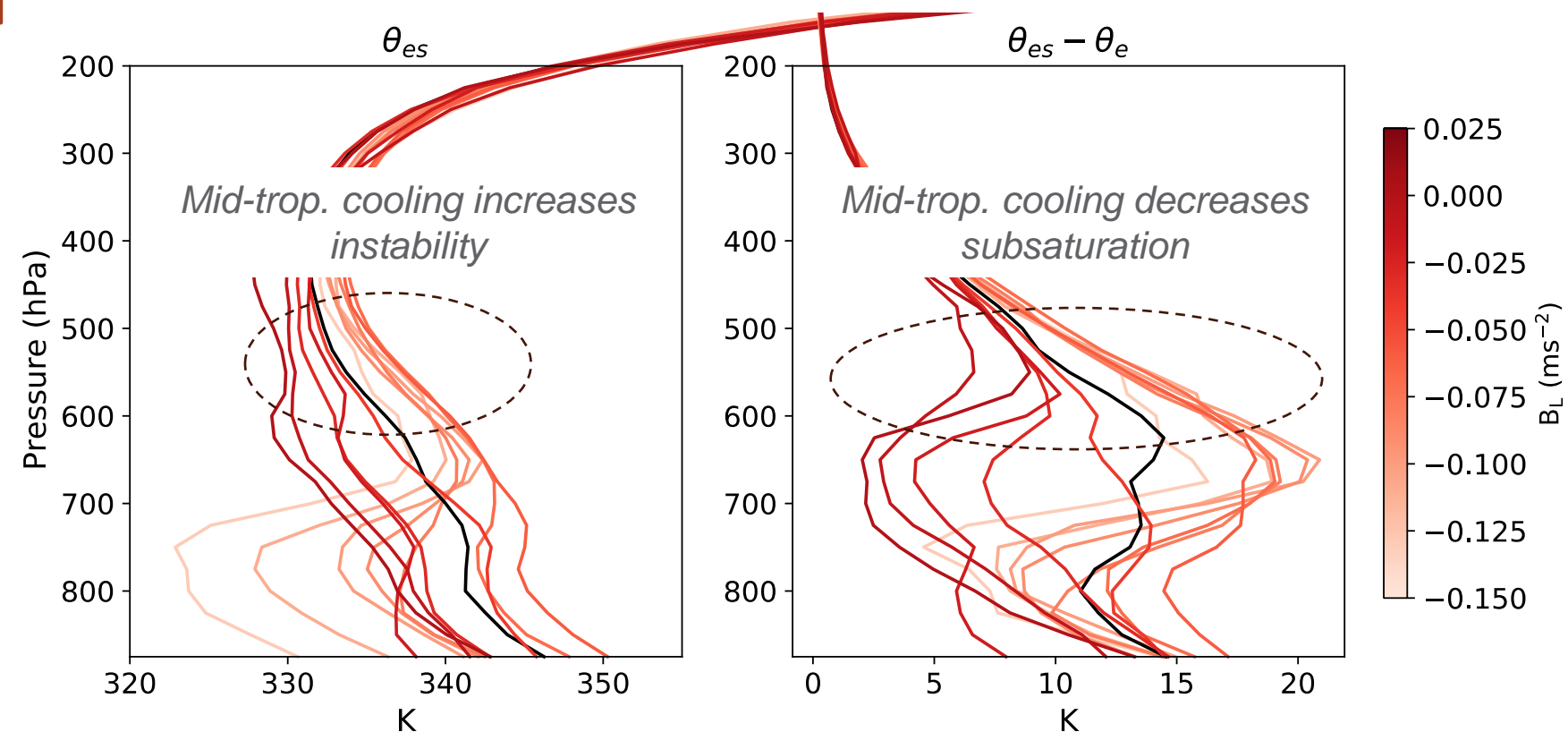
Fiaz Ahmed, Todd Emmenegger (UCLA); see session 2, poster 42

Precipitation relationship to thermodynamics broadly similar between GoAmazon and CACTI



Implication: orography does not impact precipitation, independent of thermodynamics.

Buoyancy increases during CACTI correspond to both surface warming and mid-tropospheric cooling.



Ongoing work aimed at understanding synoptic conditions that coincide with mid-tropospheric cooling.

A climatology of convective-storm environments

Russ Schumacher (CSU); Clayton Sasaki (U. Washington)

Schumacher, R., et al., 2021: Convective-storm environments in subtropical South America from high-frequency soundings during RELAMPAGO-CACTI. *MWR*, doi:10.1175/MWR-D-20-0293.1.

Sasaki, C., et al., 2023: Influences of the South American low-level jet on the convective environment in central Argentina, *MWR*, in review.

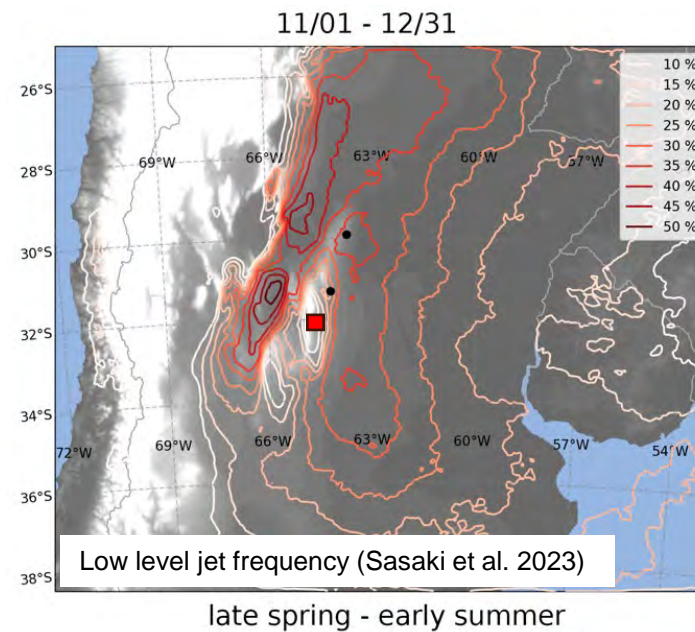
Over 2700 soundings were launched in RELAMPAGO-CACTI.

LLJs varied from 500 m to > 2000 m, weakening as they intersect the terrain. The more elevated LLJs may occur more frequently than over the Great Plains.

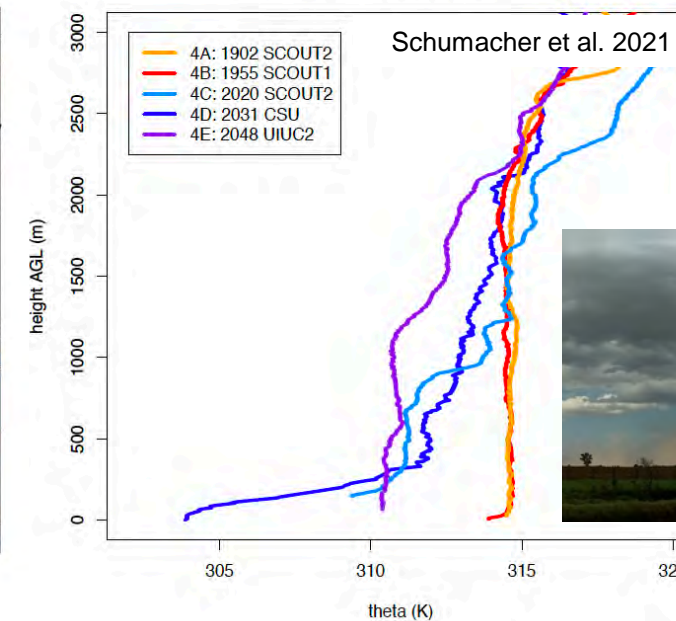
Cold pools varied greatly in depth and intensity, similar to the Great Plains.

Environments favorable to supercells and large hail were common, particularly in the immediate lee of the mountains.

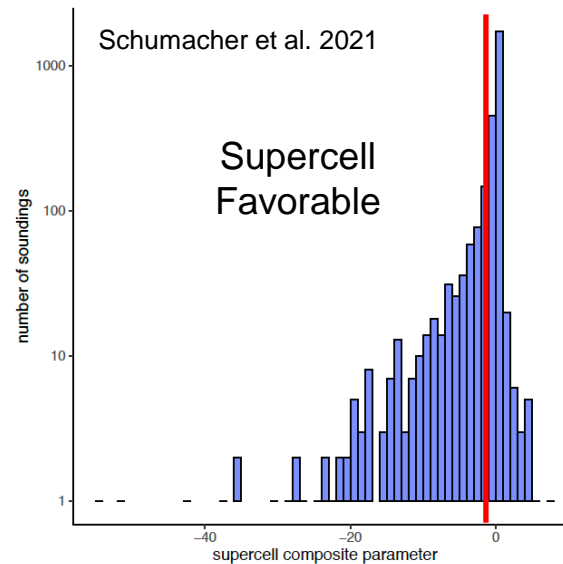
Tornado-supportive conditions were much rarer (insufficient low level vertical wind shear and storm-relative helicity).



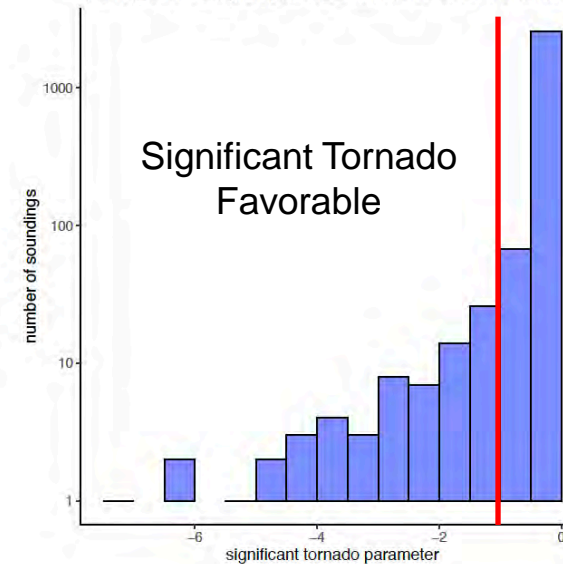
b) 10 November 2018 cold pool: virtual potential temperature (K)



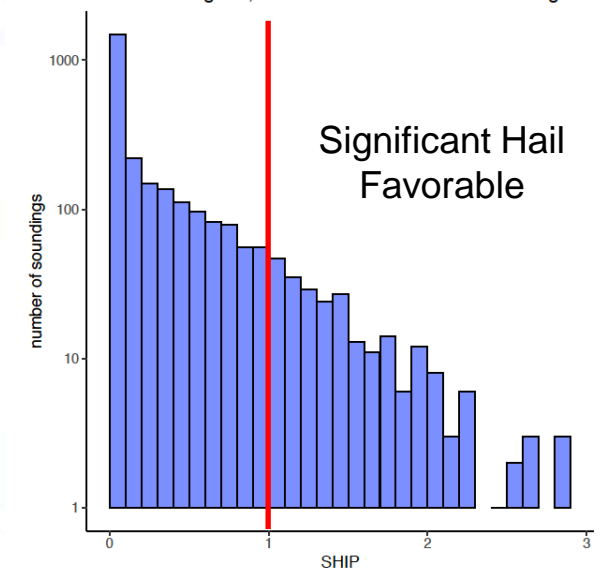
a) SCP histogram, all RELAMPAGO-CACTI soundings



b) STIP_CIN histogram, all RELAMPAGO-CACTI soundings

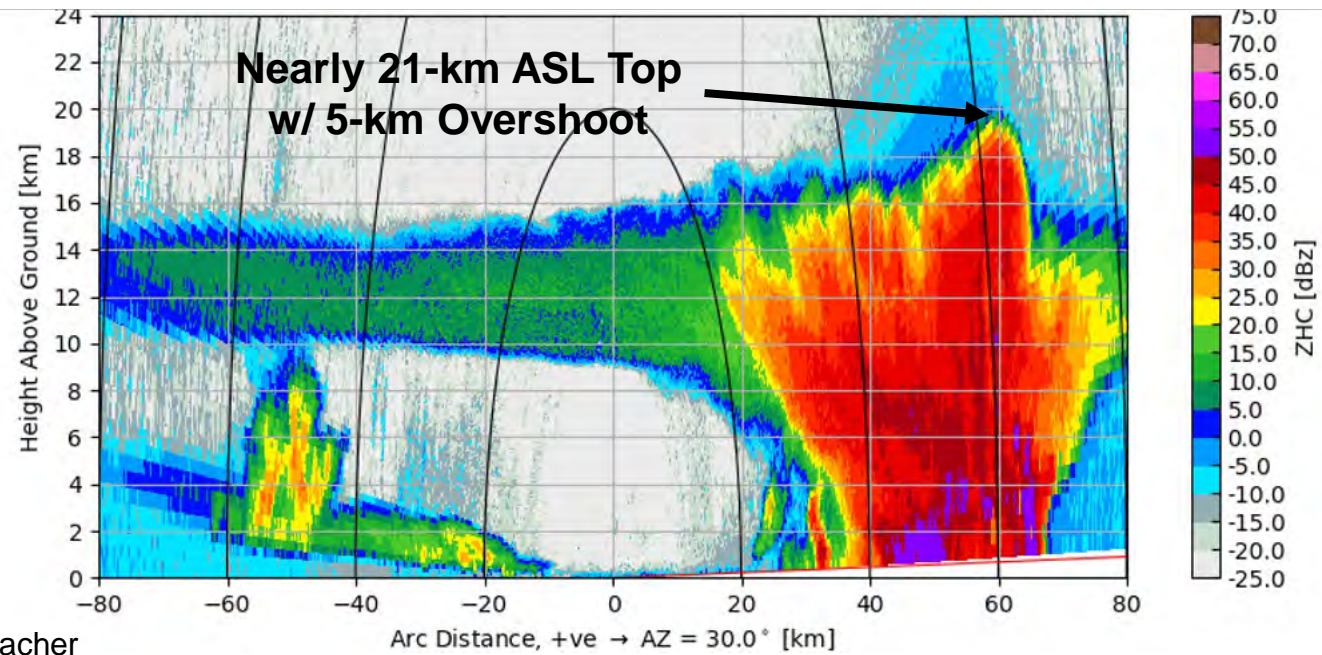
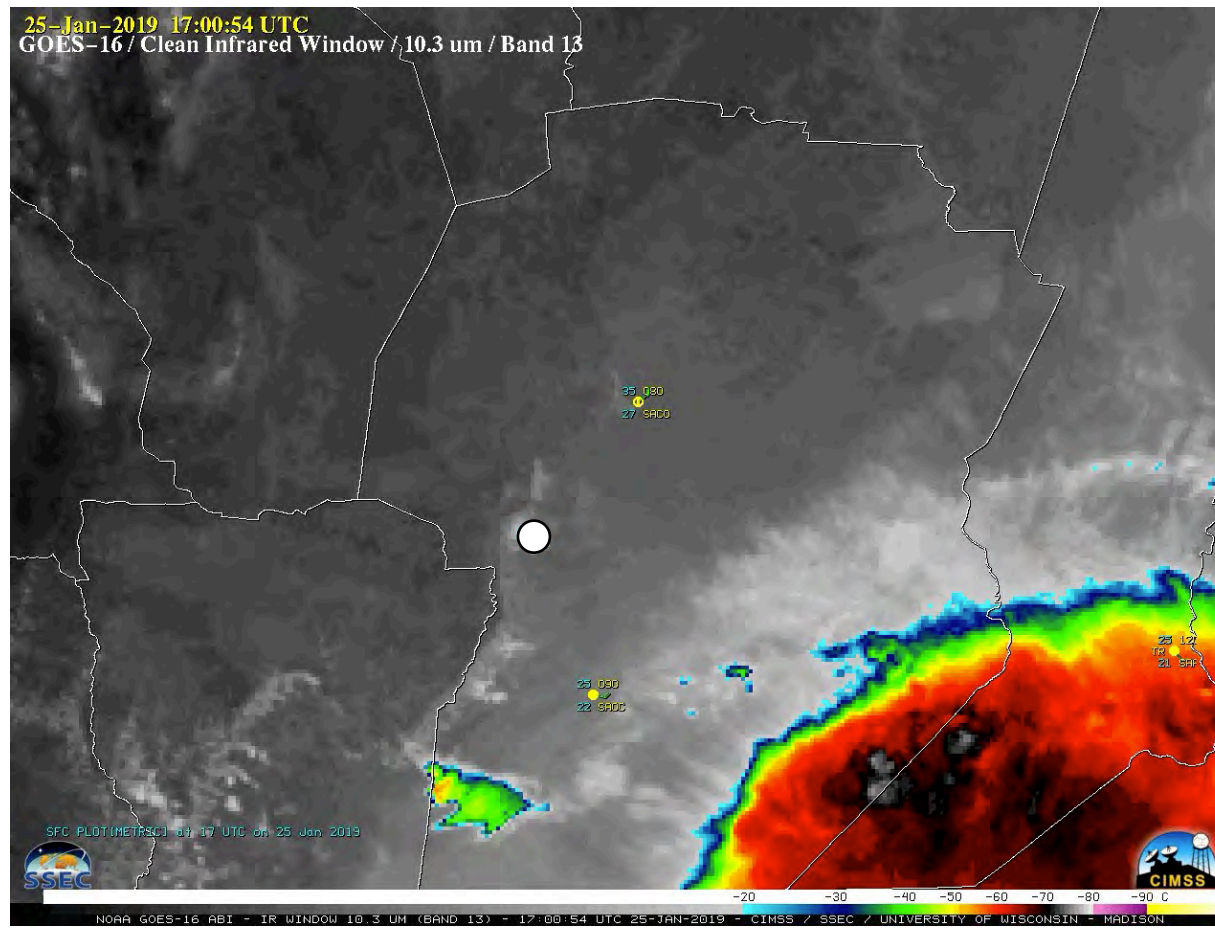


SHIP histogram, all RELAMPAGO-CACTI soundings





Extreme Deep Convection

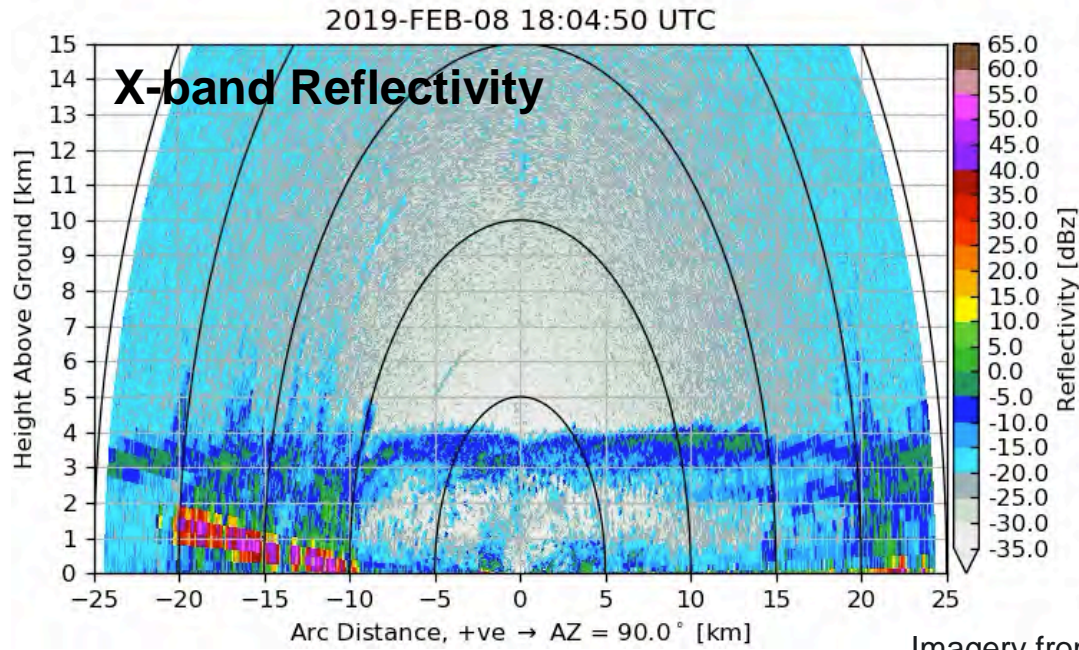
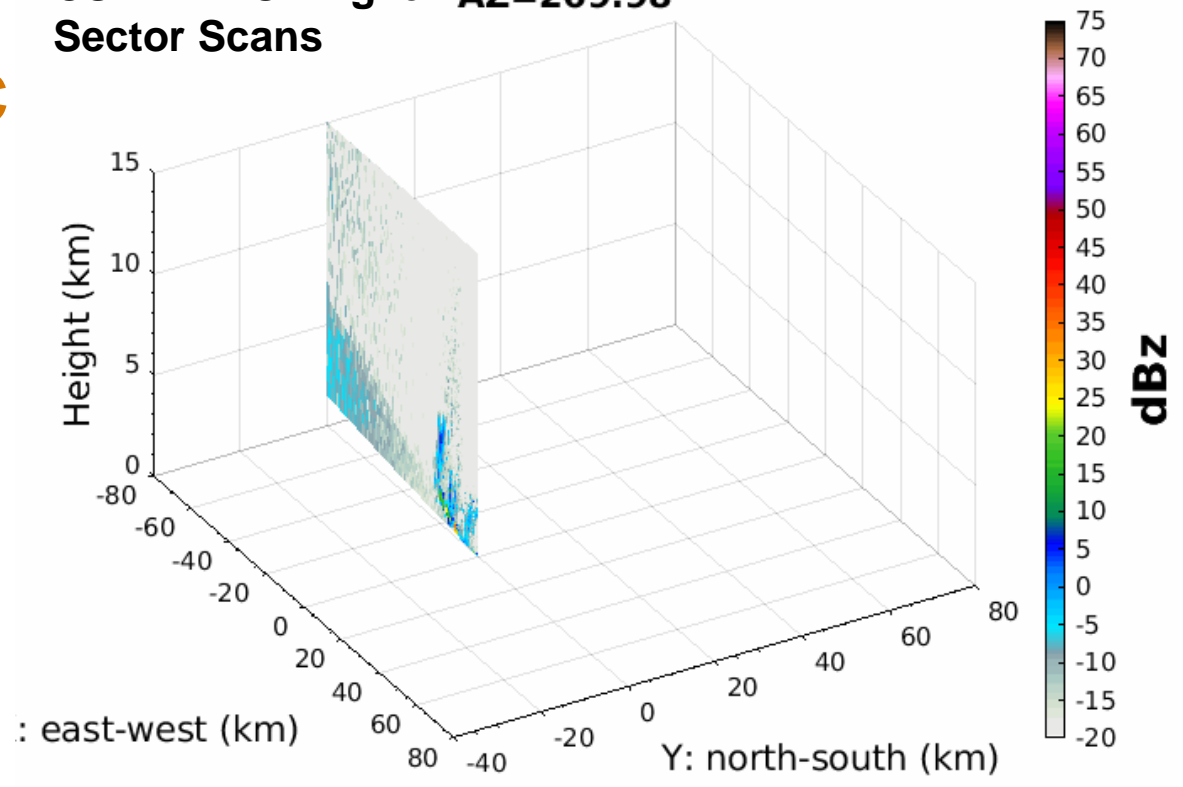


Courtesy of Paola Salio

Top: Courtesy Francina Dominguez; Bottom: Courtesy Russ Schumacher

Opportunity: Analyzing Microphysical and Kinematic Evolution in RHI Libraries

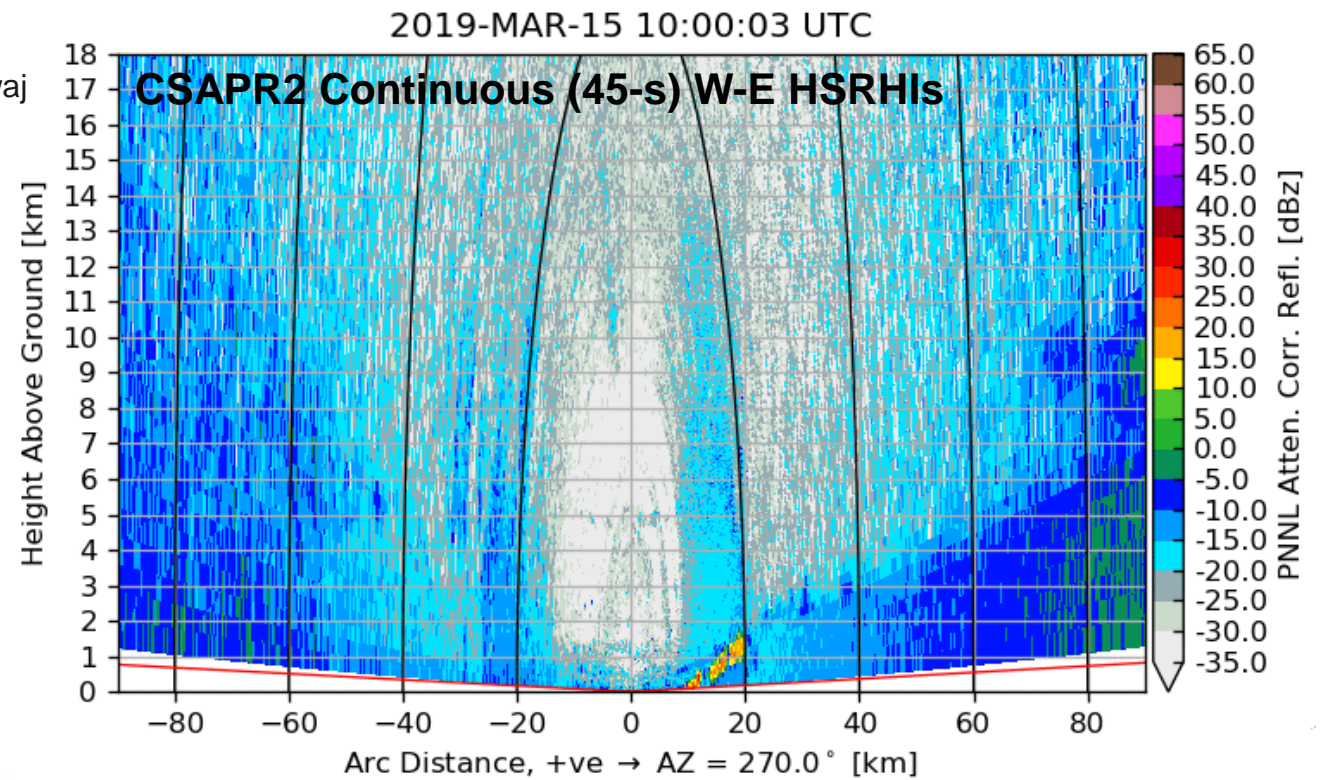
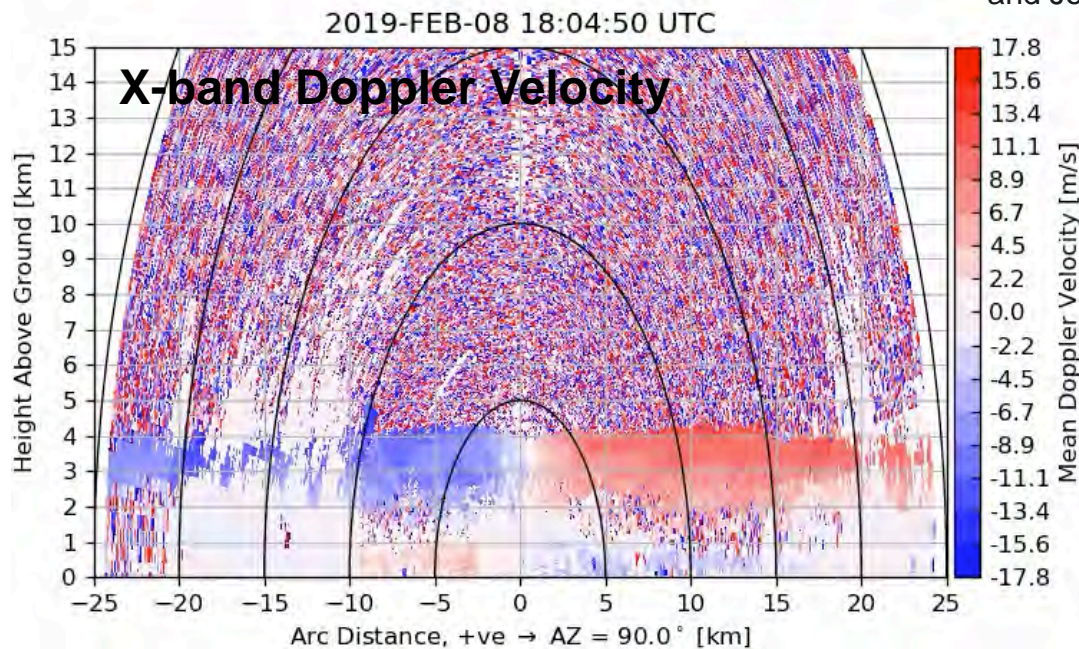
CSAPR2 IOP Agile AZ=269.98
Sector Scans



72 Ka/X-band HSRHIs per hour through Feb (48 in Mar-Apr) = ~330,000 HSRHIs

48 C-band HSRHIs per hour apart from select agile periods and Mar-Apr

Imagery from Nitin Bharadwaj and Joseph Hardin



Summary

CACTI's success is a result of **tremendous collaborative efforts by ARM staff, ASR investigators, in country support, NSF support, and many others**, much of which goes unnoticed behind the scenes.

Over 250 CACTI cloud, aerosol, radiation, and atmospheric state datastreams and products from the AMF1, CSAPR2, and G-1 are now available with most on the ARM archive **and LASSO output** is soon to follow (access available now through ARM Cumulus-2 cluster).



<https://www.arm.gov/research/campaigns/amf2018cacti>

Many research opportunities exist to build on the foundation laid by completed tools, products, and studies, particularly **related to the life cycles of clouds, aerosols, and their interactions.**



Thank You
adam.varble@pnnl.gov



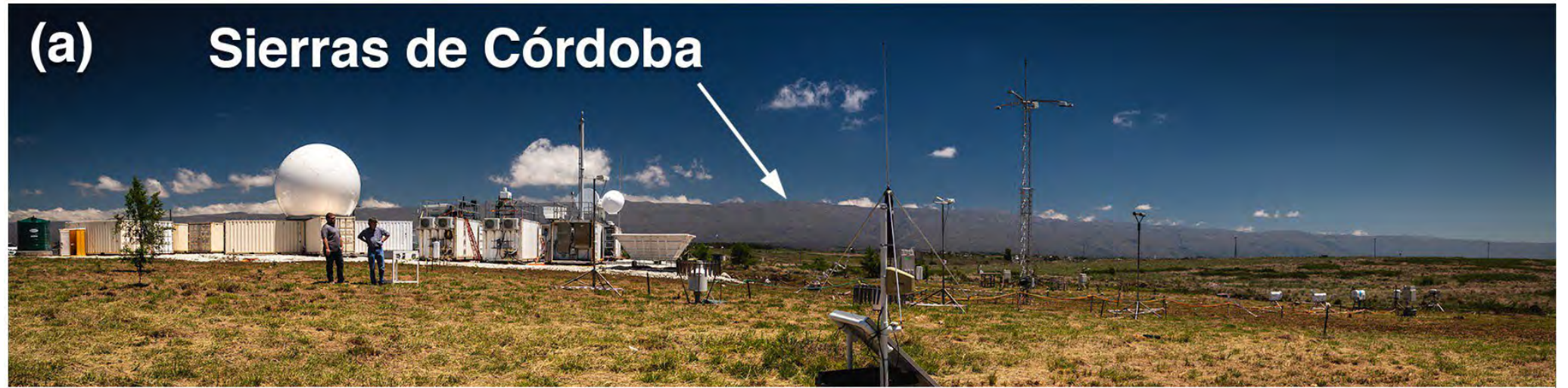


Pacific Northwest
NATIONAL LABORATORY

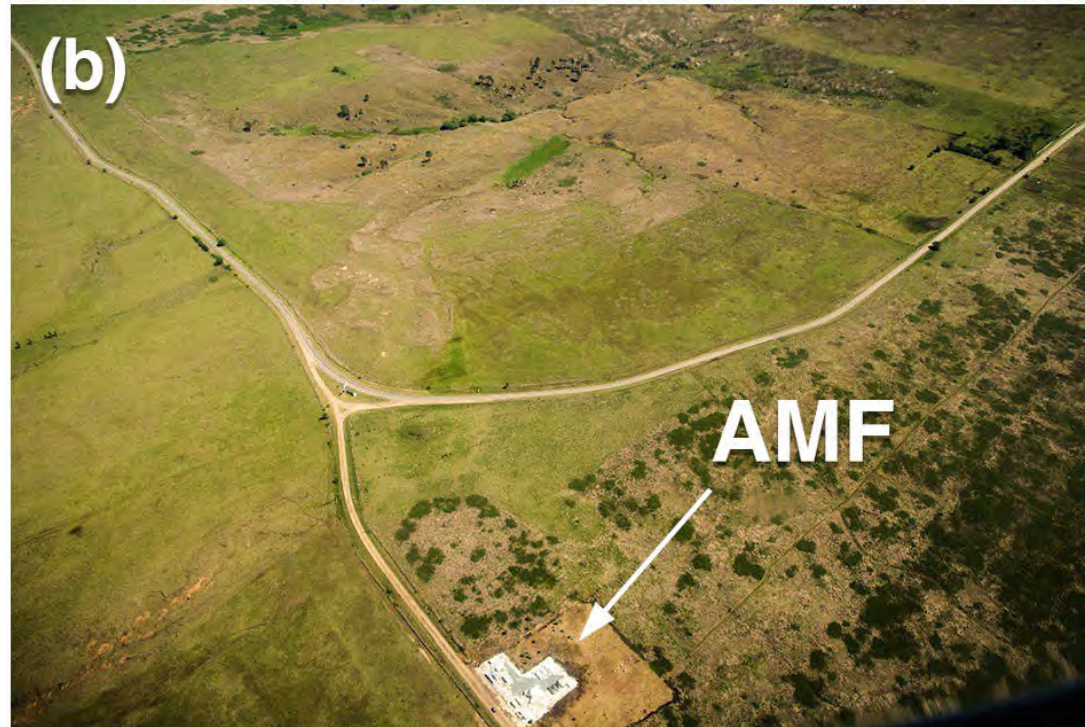
CACTI Observing Facilities (AMF1, G-1, CSAPR2)

Varble, A. C., et al., 2021,
BAMS, doi:10.1175/BAMS-
D-20-0030.1.

(a) Sierras de Córdoba



(b)



(c)

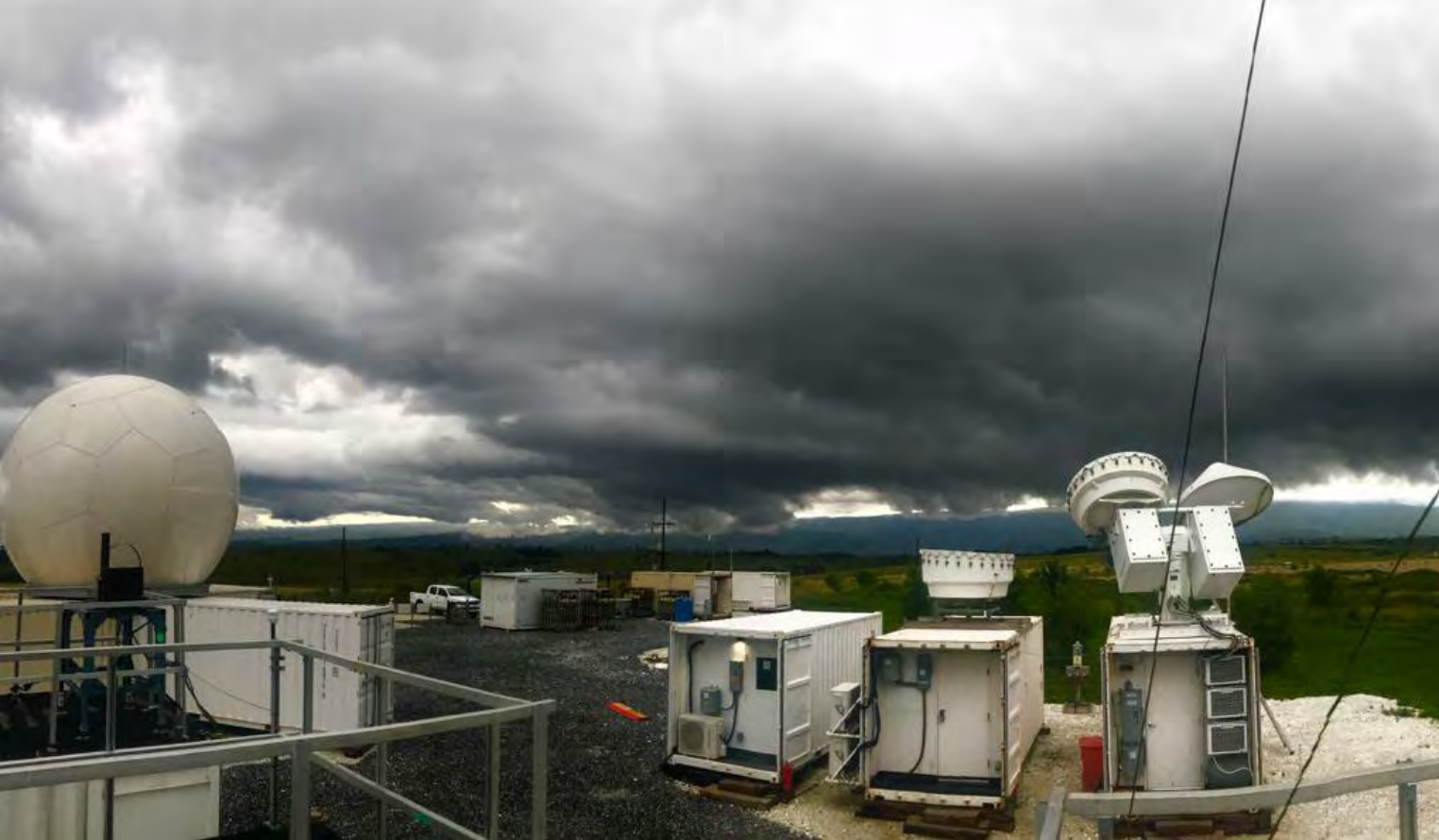


(b)



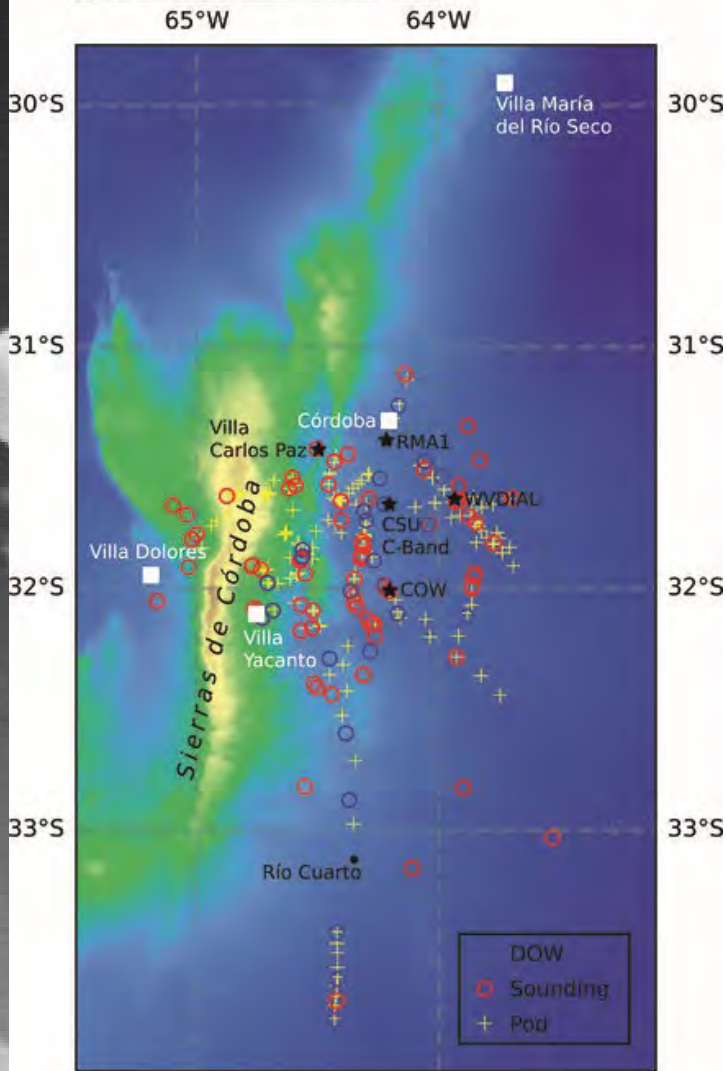
(c)



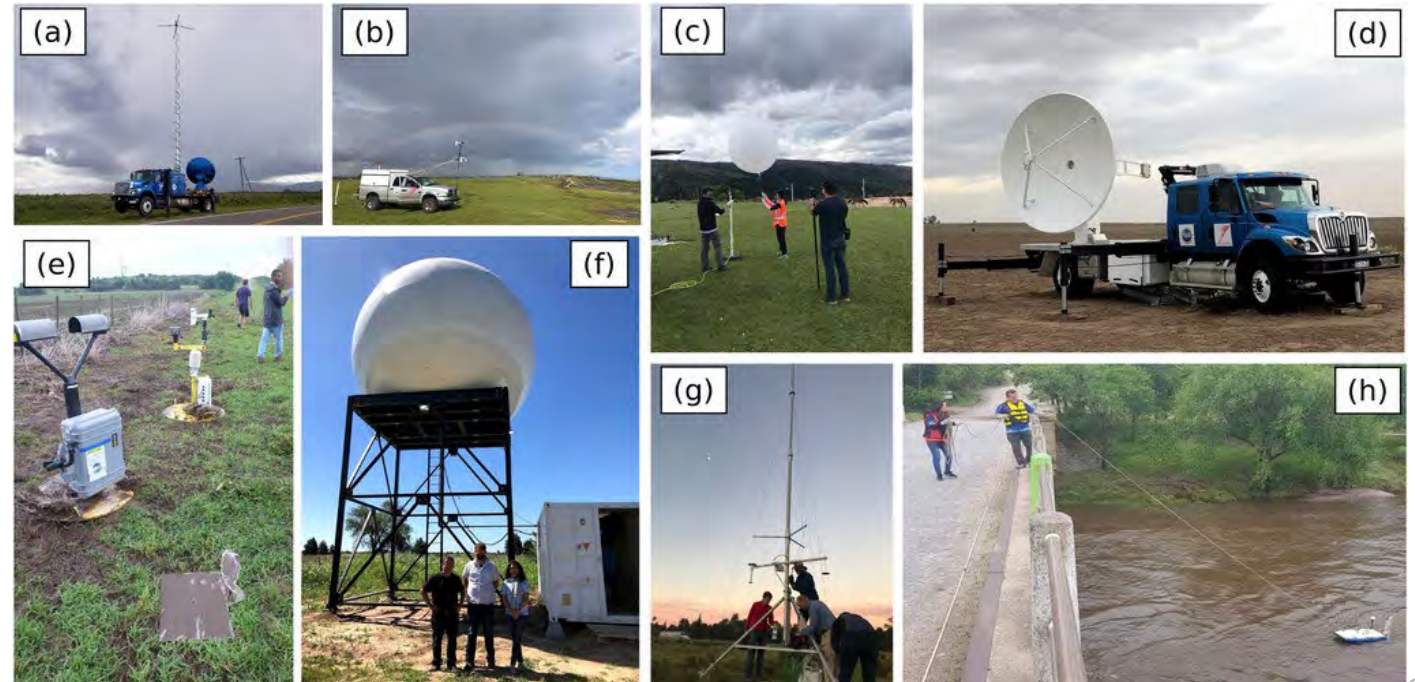
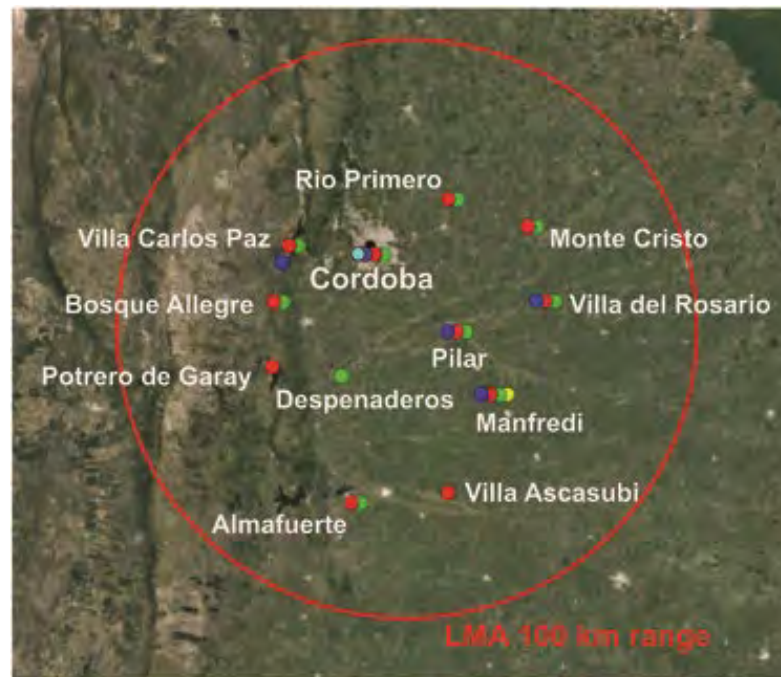
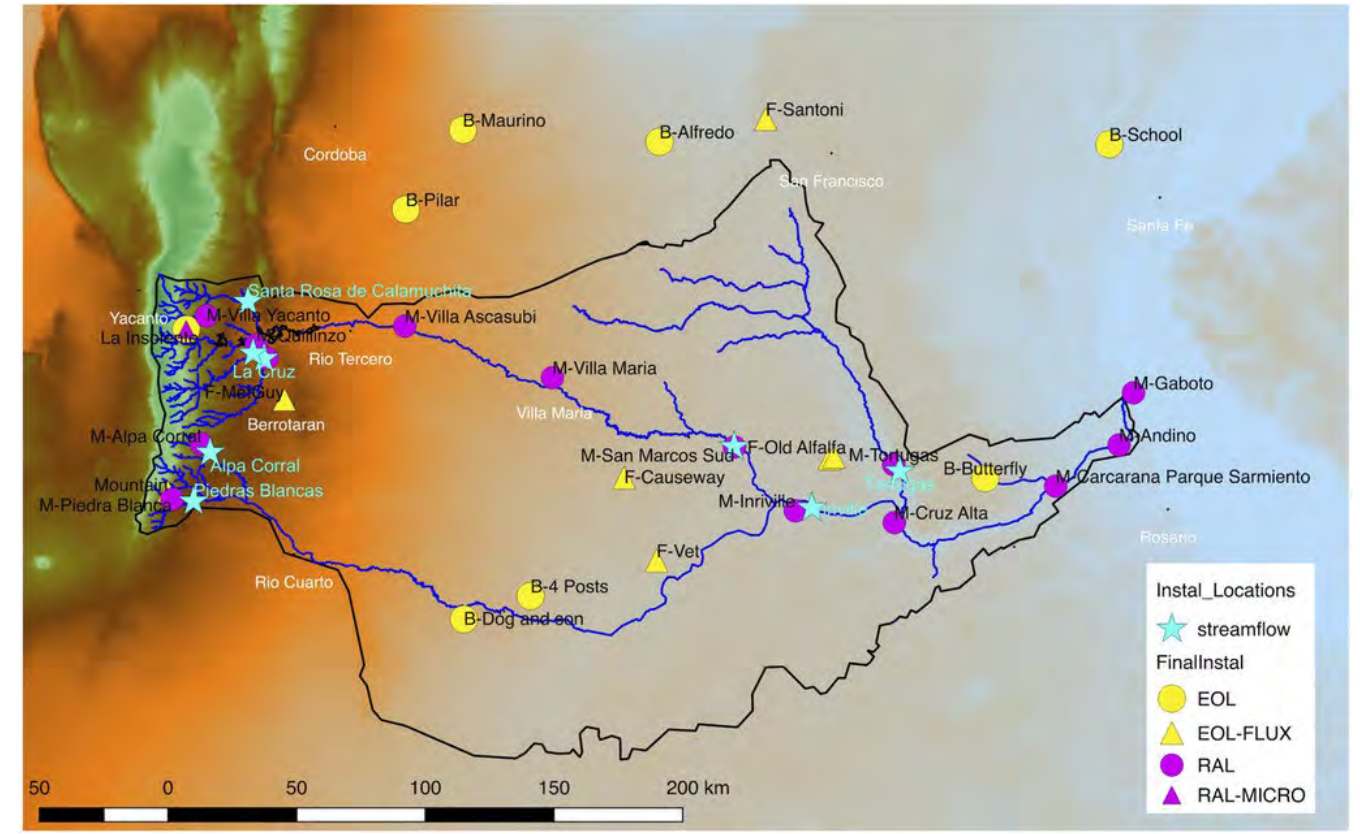
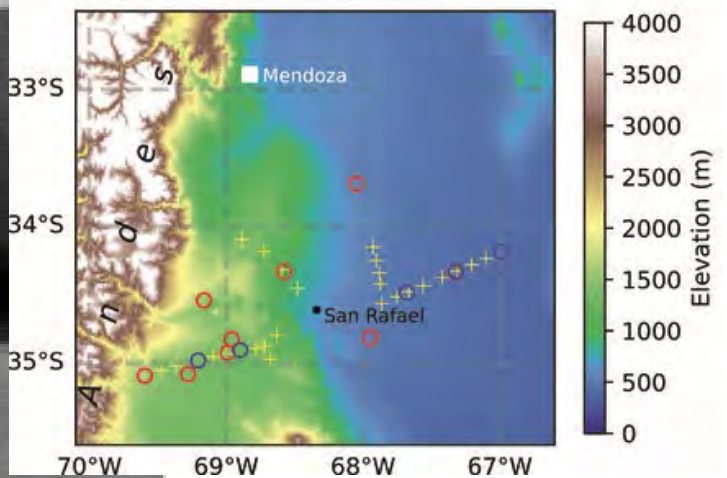


RELAMPAGO Operations

(a) Córdoba domain



(b) Mendoza domain



Surface-Based Measurements

Ground-Based Instruments and Measurements	
Cloud and Precipitation Measurements	Instrumentation
Cloud and Precipitation Kinematic and Microphysical Retrievals	C-band Scanning ARM Precipitation Radar, Ka/X-band Scanning ARM Cloud Radar, Ka-band ARM Zenith Radar, Radar Wind Profiler
Heights of Cloud Bases/Tops, Sizes, and Vertical Winds	ARM Cloud Digital Cameras
Cloud Base Height	Ceilometer, Micropulse Lidar, Doppler lidar
Cloud Scene/Fraction	Total Sky Imager
Raindrop Size Distribution, Fall Speeds, and Rainfall	Parsivel Laser and 2D Video Disdrometers, Tipping and Weighing Bucket Rain Gauges, Optical Rain Gauge, Present Weather Detector
Liquid Water Path	2-Channel, High-Frequency, and Profiling Microwave Radiometers
Atmospheric State Measurements	Instrumentation
Precipitable Water	2-Channel, High-Frequency, and Profiling Microwave Radiometers
Surface Pressure, Temperature, Humidity, Winds, and Visibility	Surface Meteorological Stations (4 sites)
Vertical Profiles of Temperature, Humidity, and Winds	Radiosondes (2 sites), Radar Wind Profiler, Profiling Microwave Radiometer, Atmospheric Emitted Radiation Interferometer
Boundary Layer Winds and Turbulence	Doppler Lidar, Sodar
Surface Condition Measurements	Instrumentation
Surface Heat Fluxes and Energy Balance, CO ₂ Flux, Turbulence, and Soil Temperature and Moisture	Eddy Correlation Flux Measurement System, Surface Energy Balance System
Aerosol and Trace Gas Measurements	Instrumentation
Aerosol Backscatter Profile	Micropulse Lidar, Doppler Lidar, Ceilometer
Aerosol Optical Depth	Cimel Sun Photometer, Multifilter Rotating Shadowband Radiometer
Cloud Condensation Nuclei (CCN) Concentration	Dual Column CCN counter
Condensation Nuclei (CN) Concentration	Fine and Ultrafine Condensation Particle Counters
Ice Nucleating Particle (INP) Concentration	Filters processed in Colorado State University Ice Spectrometer
Aerosol Chemical Composition	Aerosol Chemistry Speciation Monitor, Single Particle Soot Photometer
Aerosol Scattering and Growth	Ambient and Variable Humidity Nephelometers
Aerosol Absorption	Particle Soot Absorption Photometer
Aerosol Size Distribution	Ultra-High Sensitivity Aerosol Spectrometer, Scanning Mobility Particle Sizer, Aerodynamic Particle Sizer
Trace Gas Concentrations	O ₃ , CO, N ₂ O, H ₂ O Monitoring Systems
Radiation Measurements	Instrumentation
Radiative Fluxes	Broadband Direct, Diffuse, and Total Downwelling Downwelling Radiation Radiometers, Broadband Upwelling Radiation Radiometers, Ground and Sky Infrared Thermometers, AERI, Narrow Field of View 2-Channel Zenith Radiometer, Hemispheric and Zenith Shortwave Array Spectroradiometers, Multifilter Radiometer, Multifilter Rotating Shadowband Radiometer, Cimel Sun Photometer, Surface Energy Balance System, 2-Channel, High-Frequency, and Profiling Microwave Radiometers

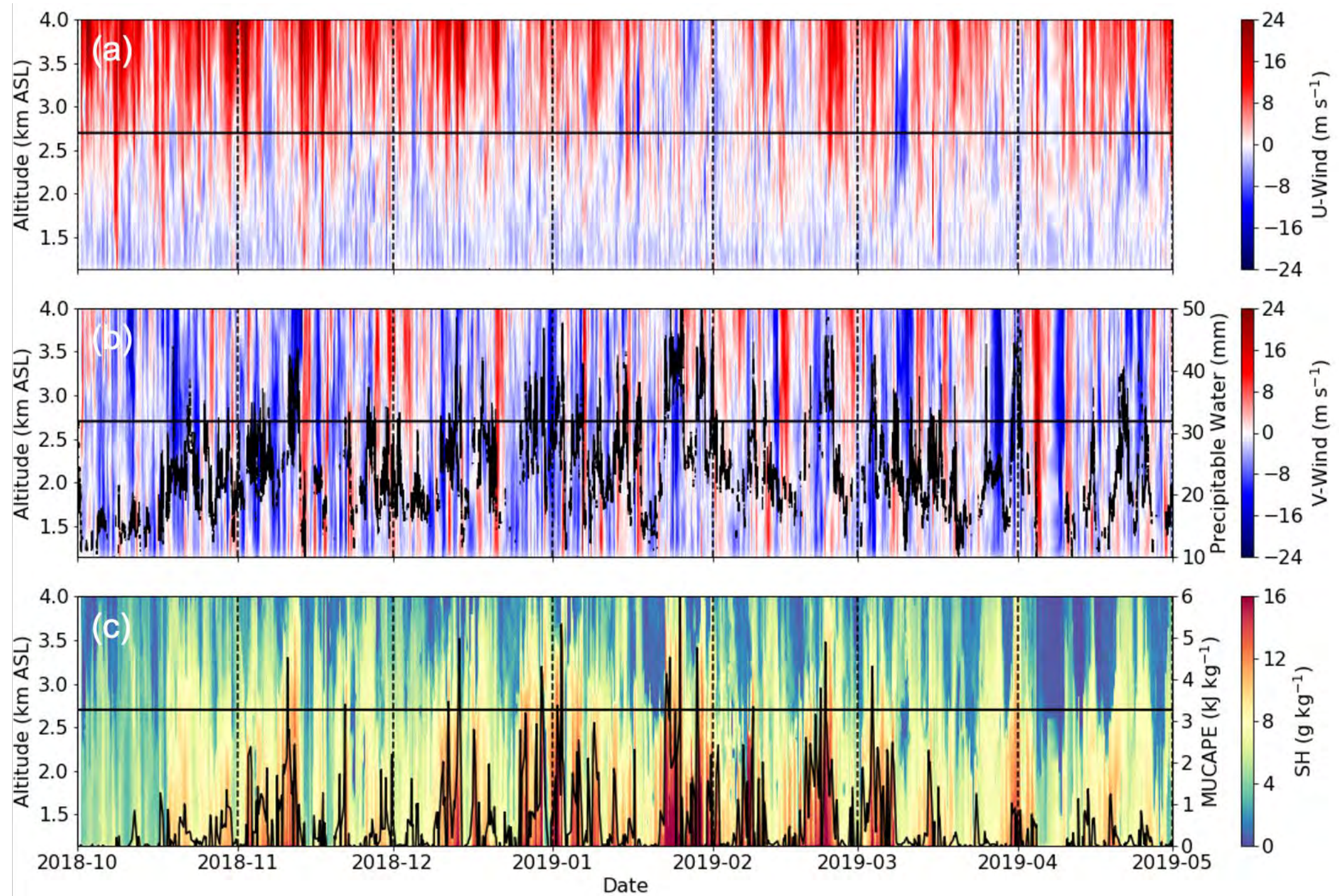
G-1 Flights

Flight	Time (UTC)	Situation
1	13:02–17:01 Nov 4	Deepening orographic cumulus
2	13:09–17:05 Nov 6	Deep convection initiation; likely warm rain
3	12:10–16:10 Nov 10	Deepening orographic cumulus prior to deep convection initiation
4	16:48–20:00 Nov 12	Elevated deep convection, low-level stable cumulus and stratus
5	14:00–18:00 Nov 14	Clear air aerosol sampling
6	13:05–16:00 Nov 15	Clear air aerosol sampling
7	14:05–18:00 Nov 16	Boundary layer and elevated orographic cumulus
8	12:18–16:30 Nov 17	Congestus along cold front; wind-blown dust; mountain wave
9	15:10–19:06 Nov 20	Orographic cumulus; strong inversion
10	18:22–20:27 Nov 21	Orographic congestus and deep convection initiation
11	14:31–18:11 Nov 22	Stratiform anvil sampling along radar north-south scans
12	16:17–20:25 Nov 24	Orographic cumulus line; strong inversion
13	15:51–19:07 Nov 25	Orographic cumulus line; potential decoupling from boundary layer
14	15:08–18:50 Nov 28	Orographic congestus and deep convection initiation
15	14:16–16:32 Nov 29	Orographic congestus and deep convection initiation
16	16:20–18:47 Dec 1	Elevated drizzle in orographic stratocumulus; possible ice
17	12:06–16:11 Dec 2	Elevated drizzle in widespread clouds; possible ice; gravity waves in cloud layer
18	16:03–20:09 Dec 3	Boundary layer coupled orographic cumulus; strong inversion
19	17:51–19:45 Dec 4	Deepening congestus and some deep convection initiation
20	12:04–15:28 Dec 5	Mid-level clouds; congestus and some deep convection initiation
21	15:01–19:01 Dec 7	Orographic cumulus; strengthening inversion
22	16:06–19:30 Dec 8	Clear air aerosol sampling

G-1 Measurements

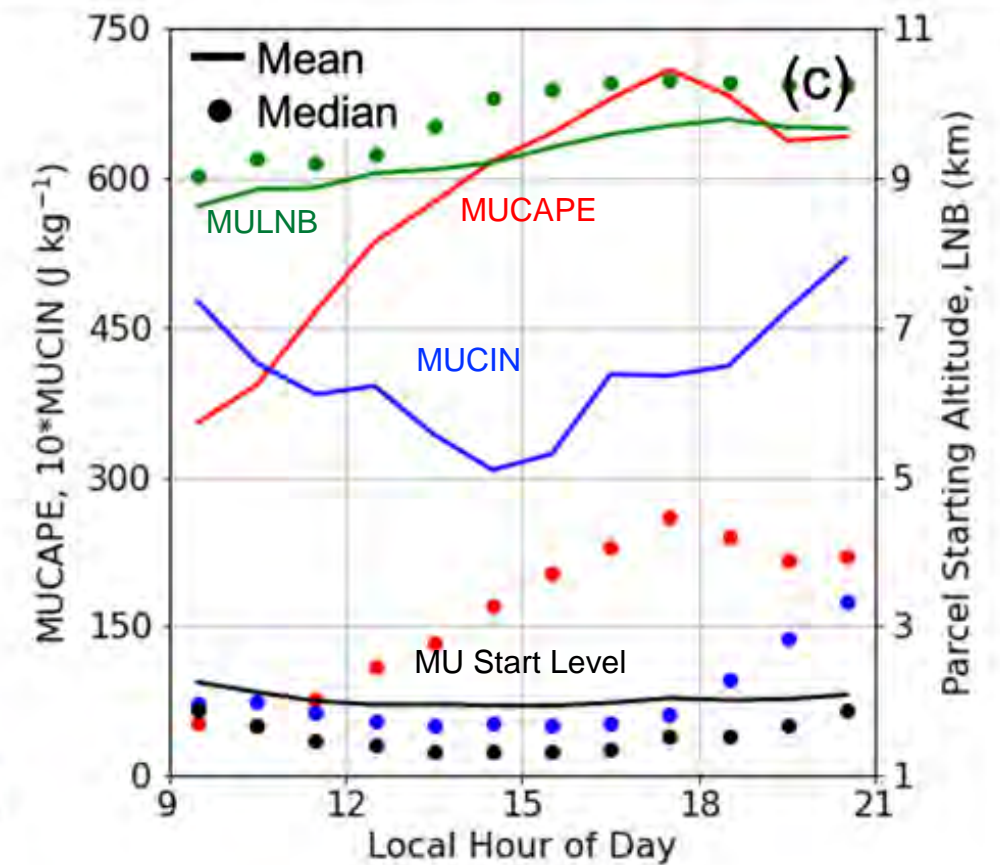
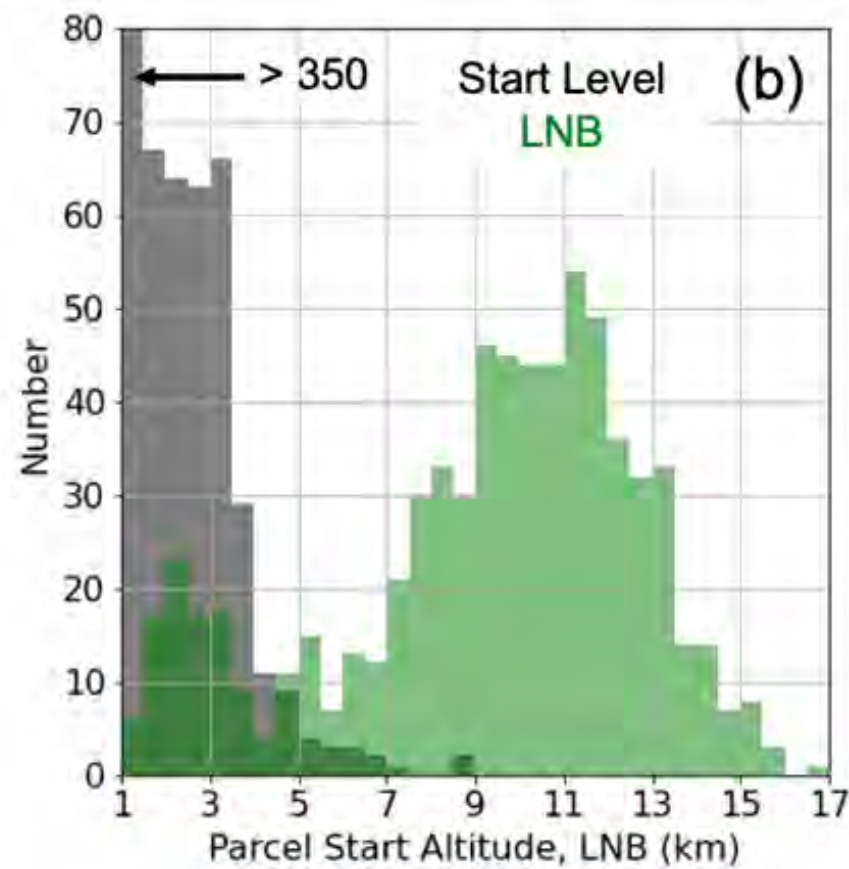
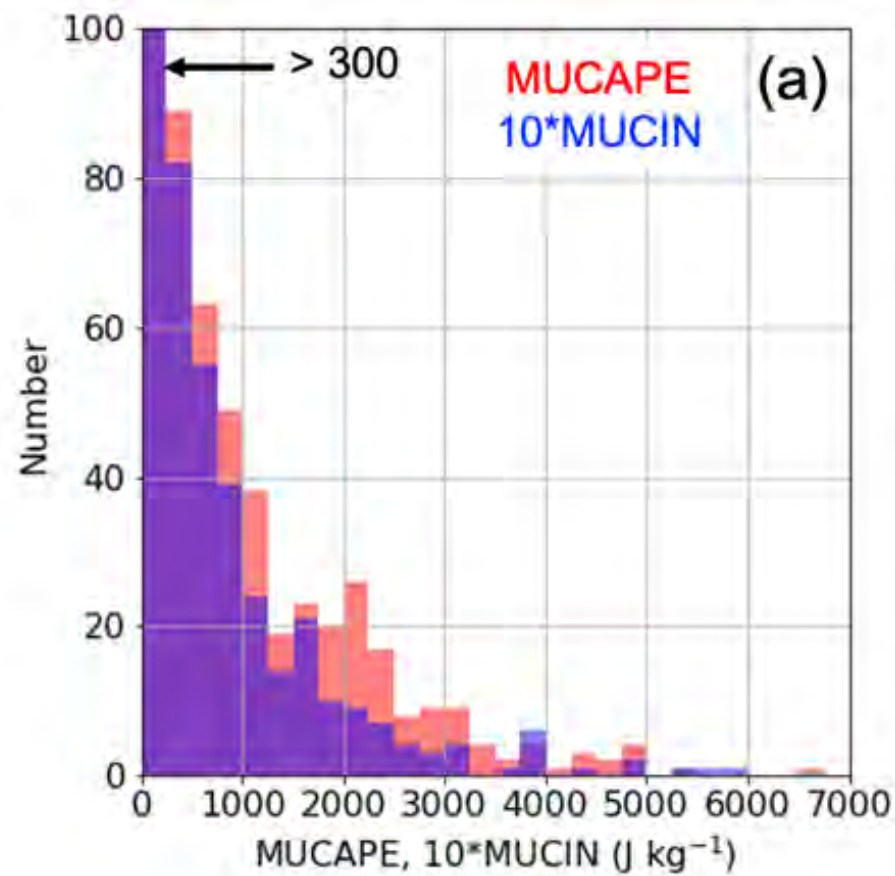
Aircraft Instruments and Measurements	
Positioning Measurements	Instrumentation
Position/Aircraft parameters	Aircraft Integrated Meteorological Measurement System-20, Global Positioning System (GPS) DSM 232, C-MIGITS III (Miniature Integrated GPS/INS Tactical System), VectorNav-200 GPS/INS, Video Camera P1344
Atmospheric State Measurements	Instrumentation
Pressure, Temperature, Humidity, Winds, Turbulence	Gust Probe, Rosemount 1221F2, Aircraft Integrated Meteorological Measurement System-20, Tunable Diode Laser Hygrometer, GE-1011B Chilled Mirror Hygrometer, Licor LI-840A, Rosemount 1201F1 and E102AL
Aerosol and Trace Gas Measurements	Instrumentation
Aerosol Sampling	Aerosol Isokinetic Inlet, Counterflow Virtual Impactor (CVI) Inlet
Aerosol Optical Properties	Single Particle Soot Photometer, 3-wavelength Integrating Nephelometer, 3-wavelength Particle Soot Absorption Photometer, 3-wavelength Single Channel Tricolor Absorption Photometer
Aerosol Chemical Composition	Single Particle Mass Spectrometer (miniSPLAT)
Aerosol Size Distribution	Ultra-High Sensitivity Aerosol Spectrometer, Scanning Mobility Particle Sizer, Passive Cavity Aerosol Spectrometer, Optical Particle Counter Model CI-3100, Dual Polarized Cloud and Aerosol Spectrometer (CAS)
CN Concentration	Fine (1 on Isokinetic Inlet and 1 on CVI Inlet) and Ultrafine CPCs
CCN Concentration	Dual-column CCN counter
INP Concentration	Filter Collections for Colorado State University Ice Spectrometer
Trace Gas Concentrations	N ₂ O, CO, O ₃ , and SO ₂ Monitoring Systems
Cloud and Precipitation Measurements	Instrumentation
Hydrometeor Size Distribution	Fast Cloud Droplet Probe, 2-Dimensional Stereo Probe, High Volume Precipitation Sampler 3, Cloud and Aerosol Precipitation Spectrometer (CAPS; includes Cloud Imaging Probe, CAS, and Hotwire Sensor)
Hydrometeor Imagery	Cloud Particle Imager
Liquid Water Content	Particle Volume Monitor 100-A, Multi-Element Water Content Meter, Hotwire Sensor from CAPS

Environmental Conditions During CACTI



Varble, A. C., et al., 2021, *BAMS*, doi:10.1175/BAMS-D-20-0030.1.

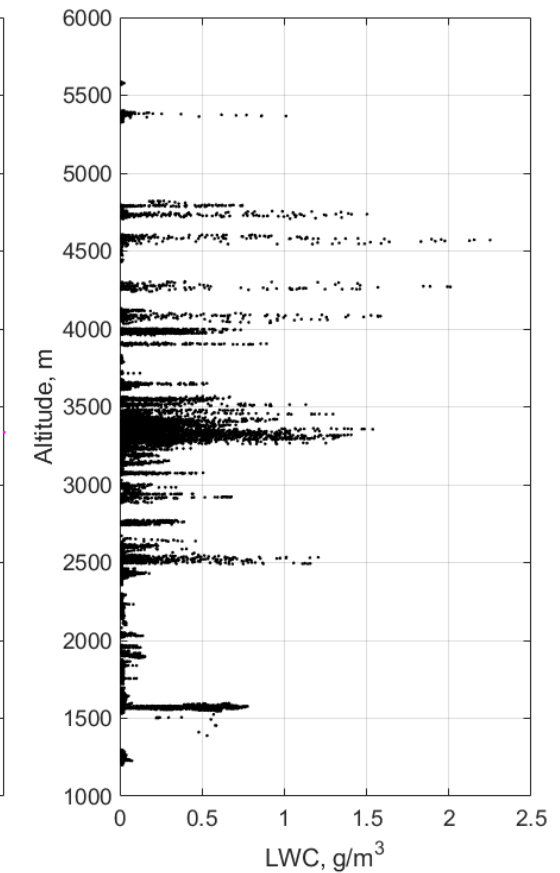
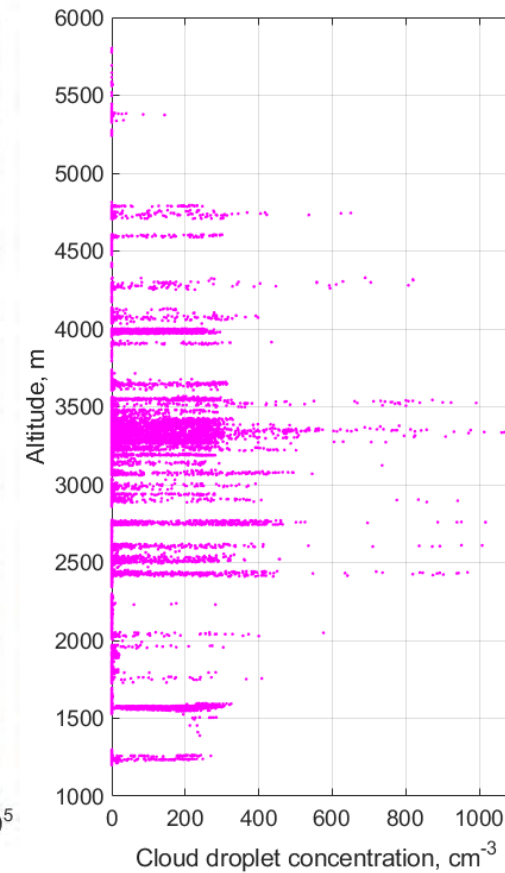
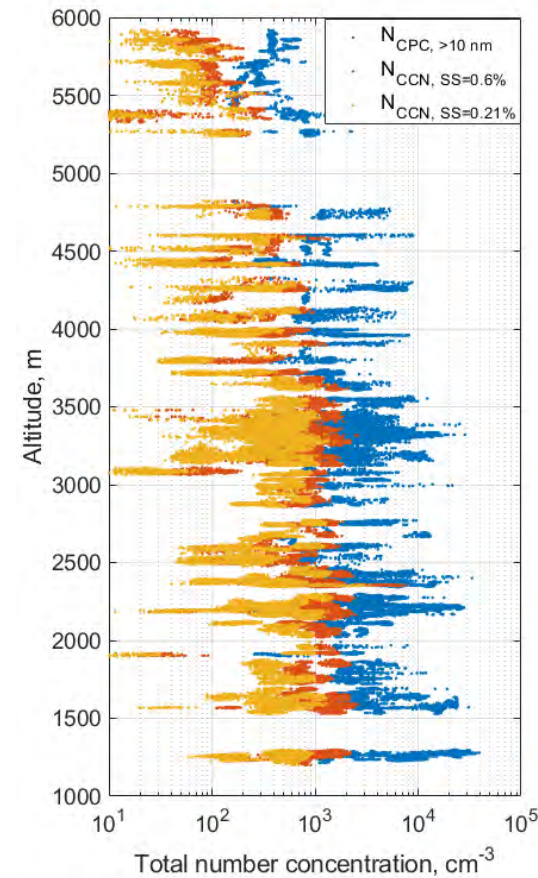
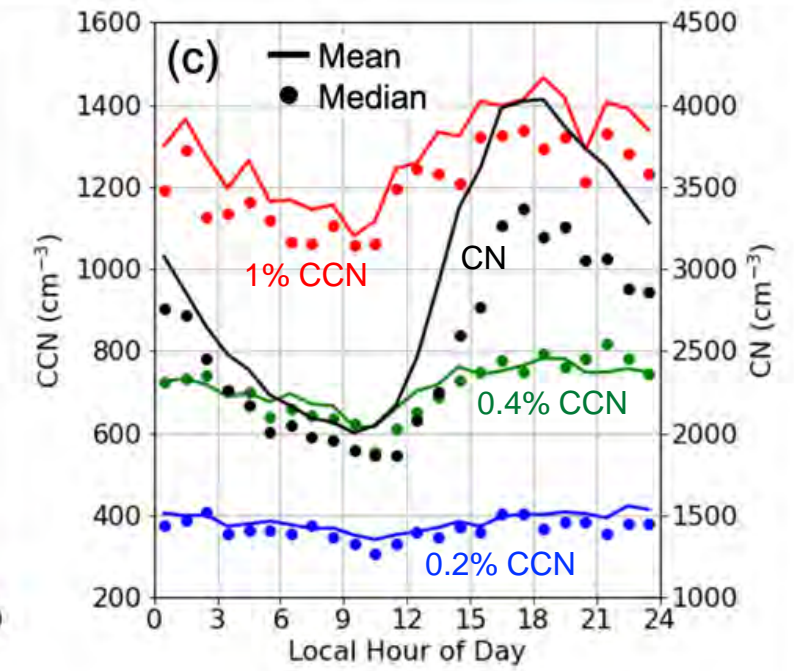
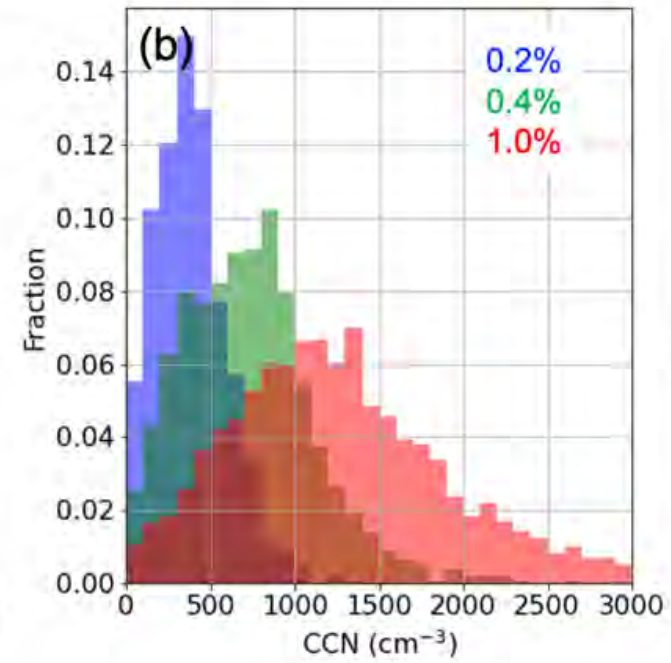
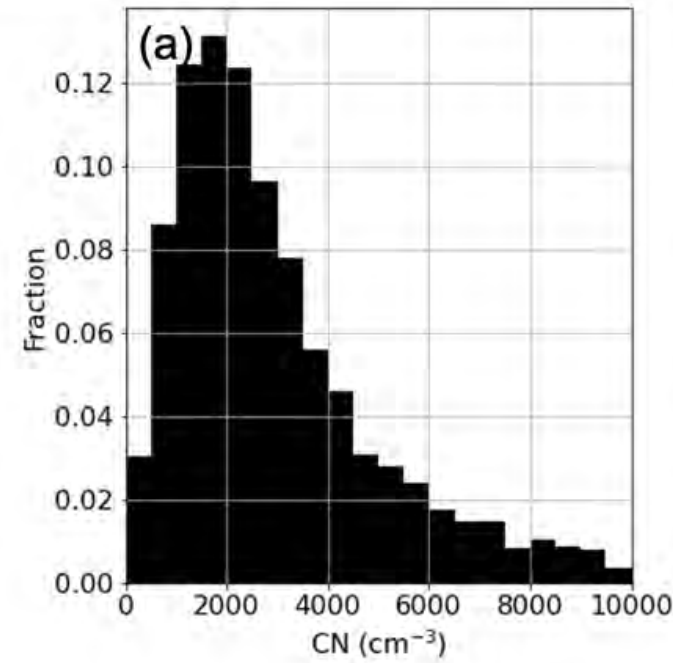
Convective Environmental Condition Distributions and Diurnal Cycles



Varble, A. C., et al., 2021, *BAMS*, doi:10.1175/BAMS-D-20-0030.1.

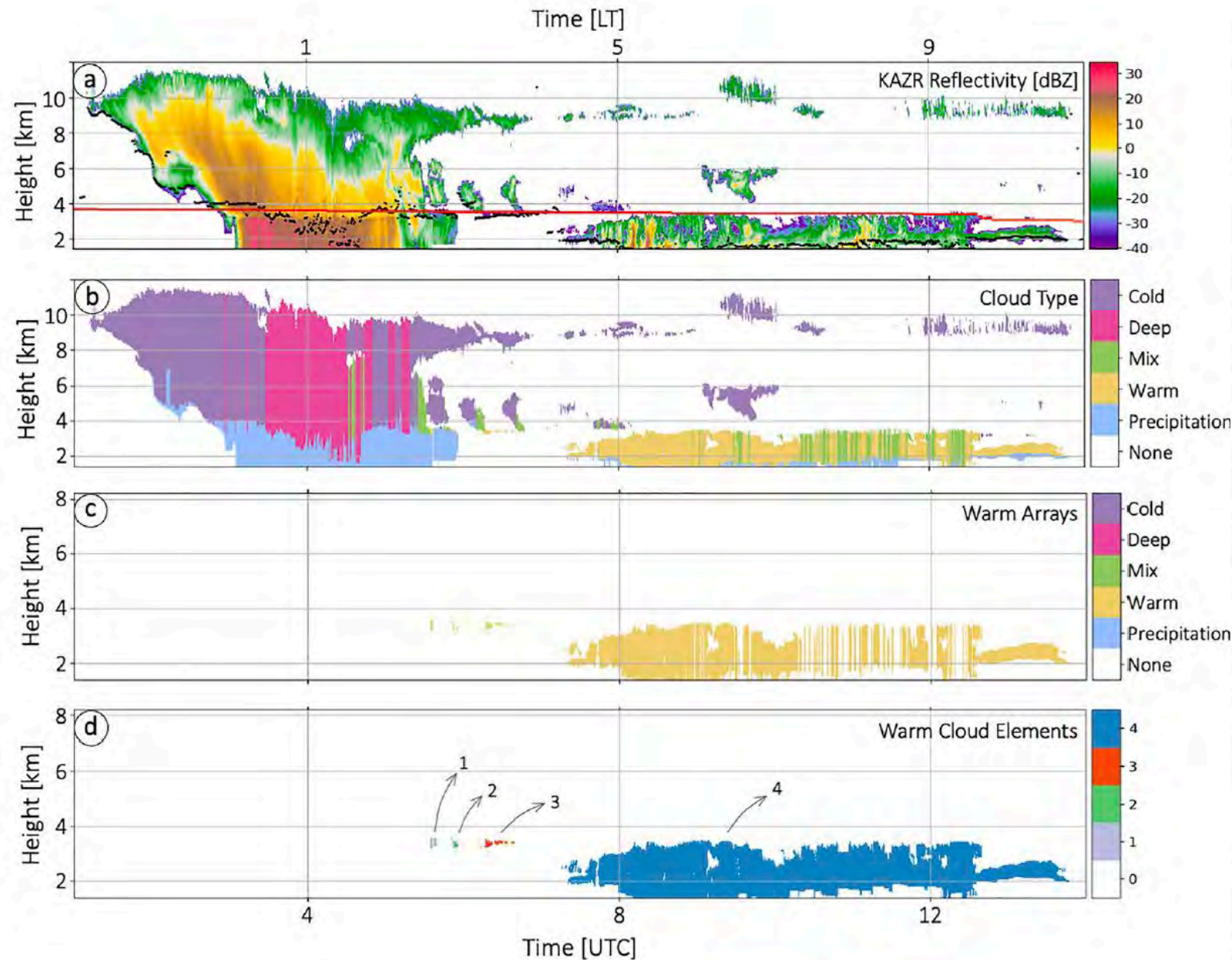
Aerosol and Aerosol- Cloud Interaction Observations

Varble, A. C., et al., 2021, *BAMS*,
doi:10.1175/BAMS-D-20-0030.1.

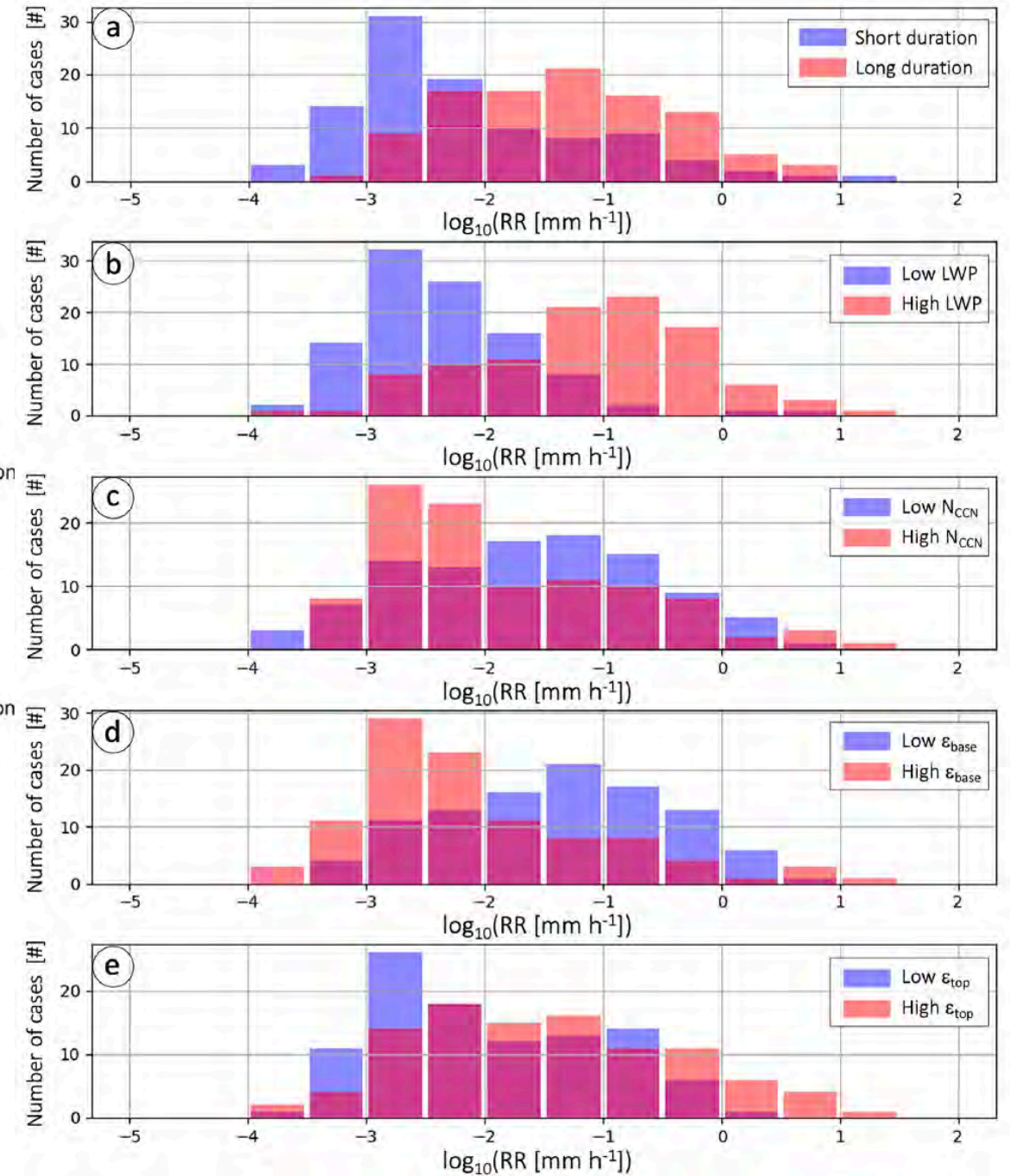


Warm Cloud Processes

Borque, P., et al., 2022: Peak rain rate sensitivity to observed cloud condensation nuclei and turbulence in continental warm shallow clouds during CACTI. *J. Geophys. Res. Atmos.*, 127, doi:10.1029/2022JD036864.



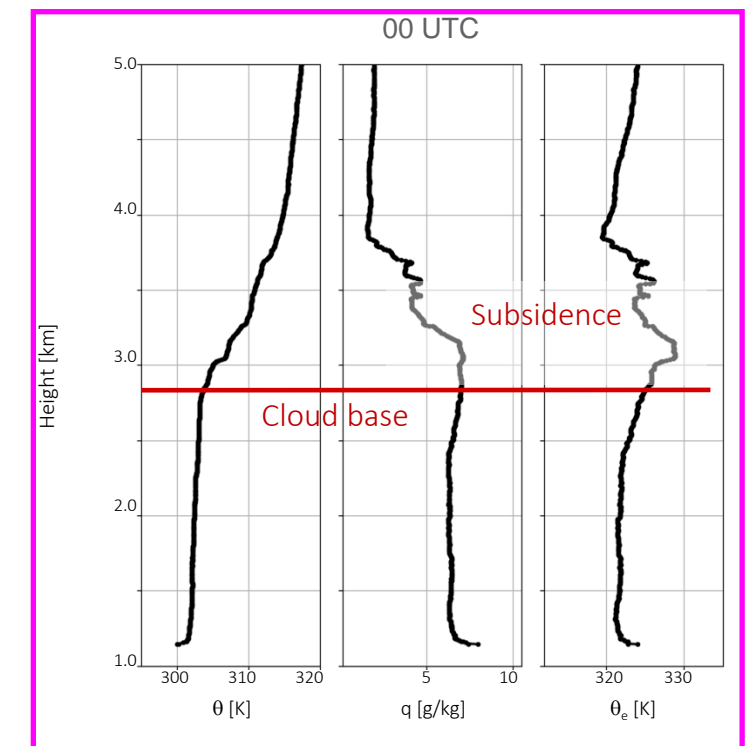
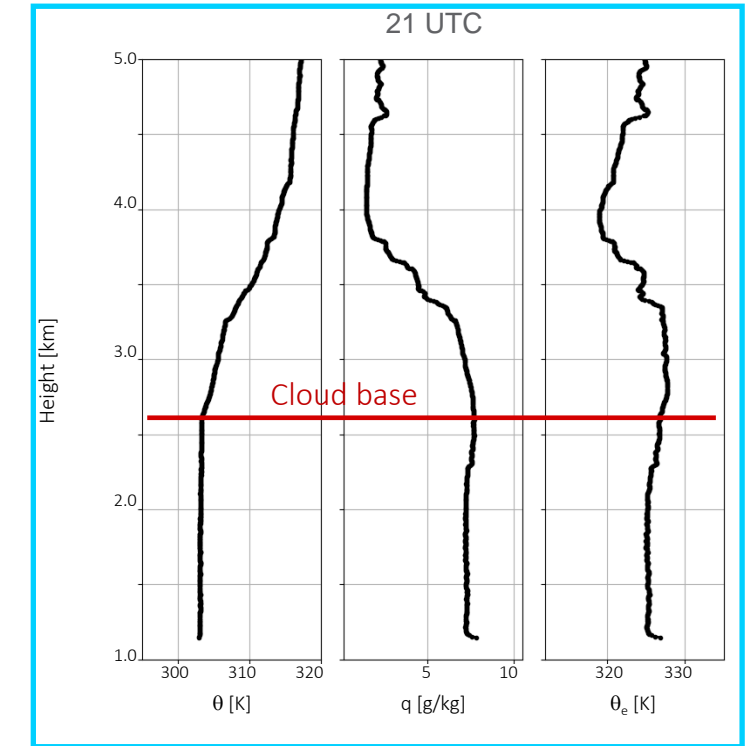
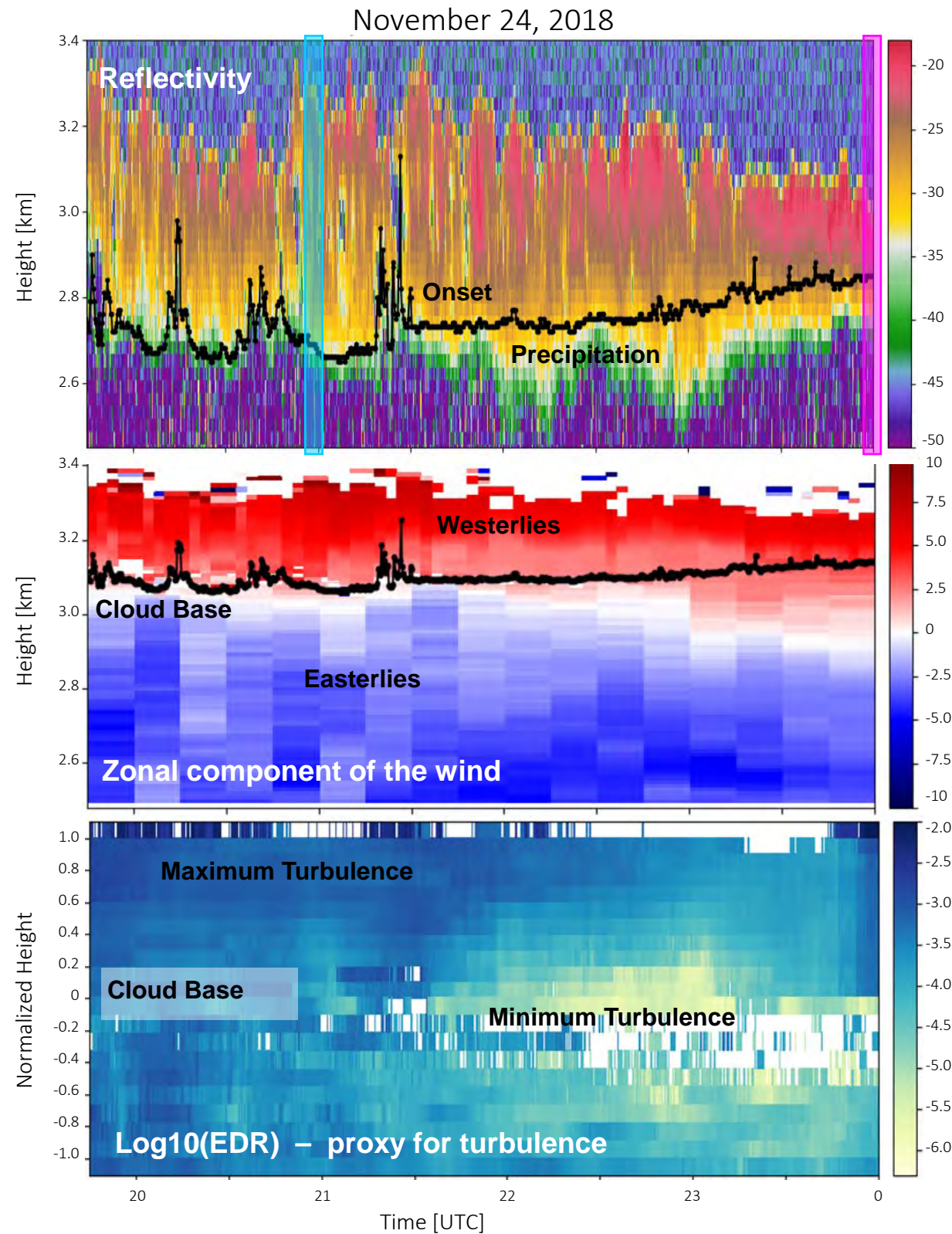
3342 warm cloud objects, 2173 mixed cloud objects, 152 deep cloud objects merged with cold clouds



Stratocumulus Drizzle Case

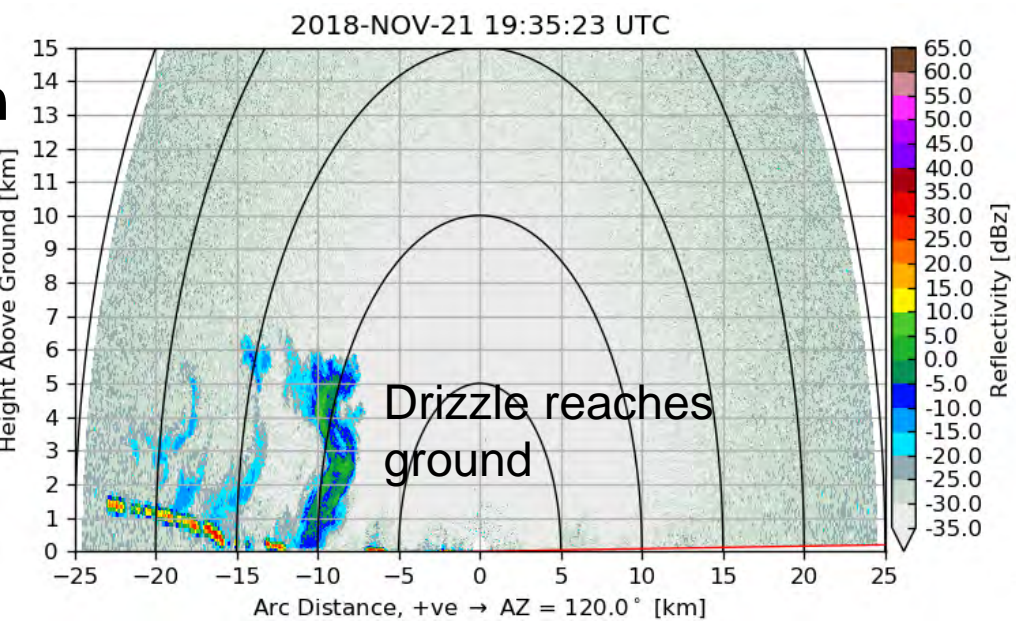
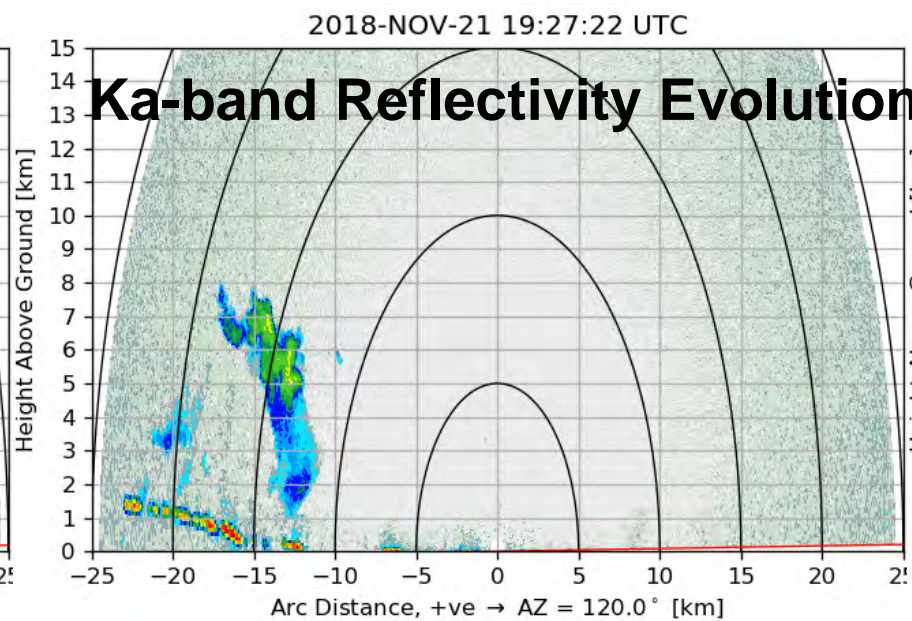
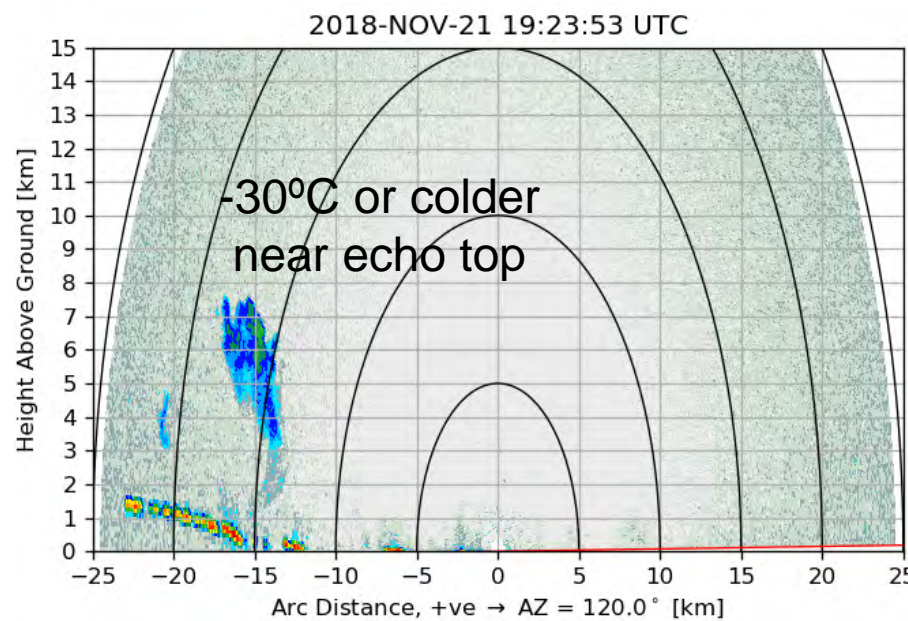
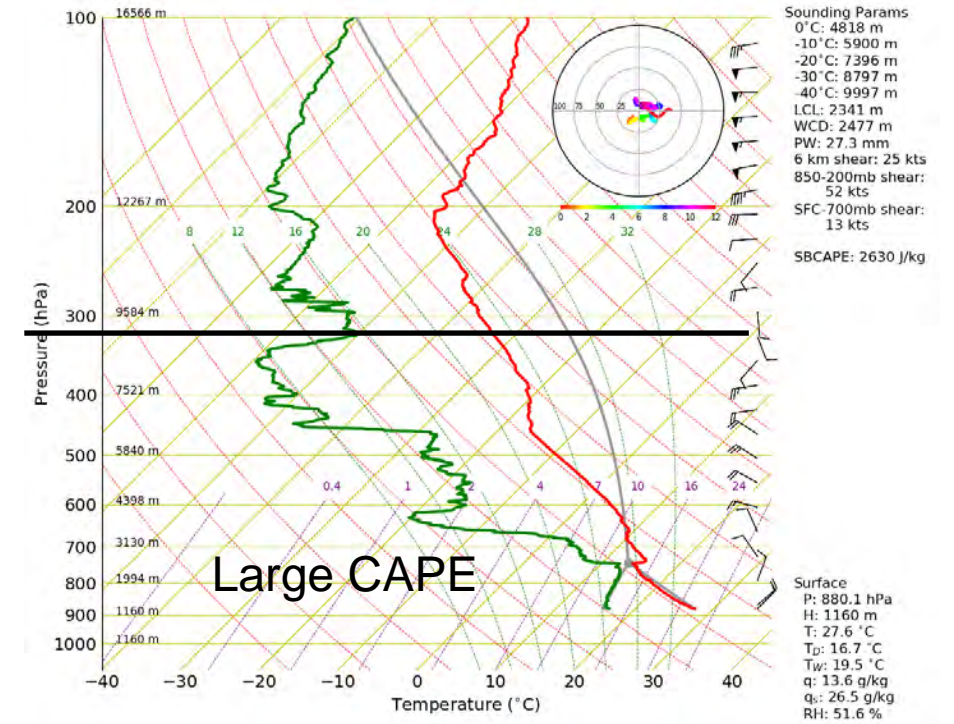
Paloma Borque

Wind shear layer remains constant and cloud depth does not increase during drizzle onset. The cloud decouples from the boundary layer during drizzle onset, indicating a potential role for lower CCN concentrations aloft.



Deep Convection Initiation (CI) Fail Case

21 November 2018



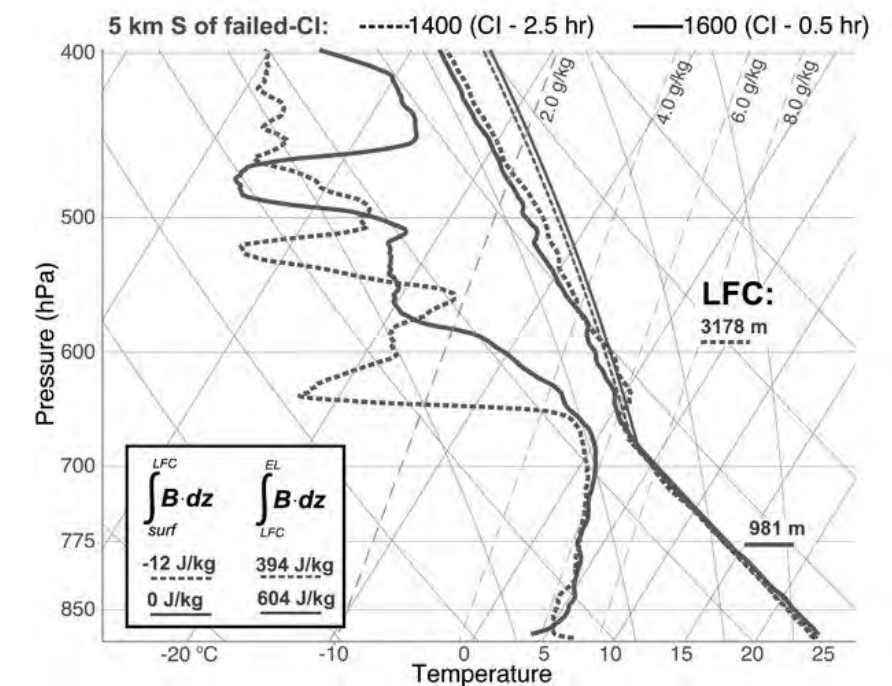
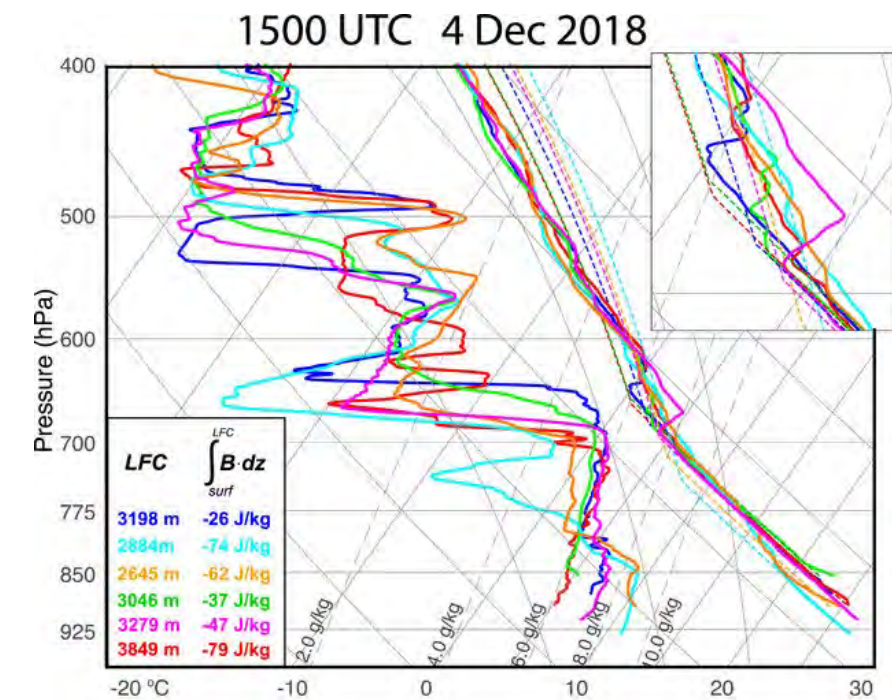
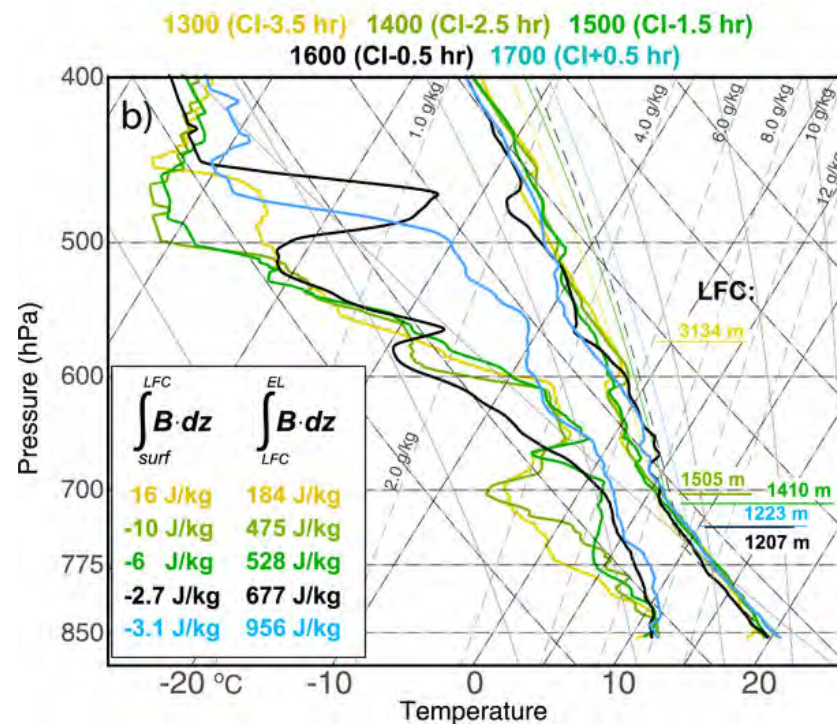
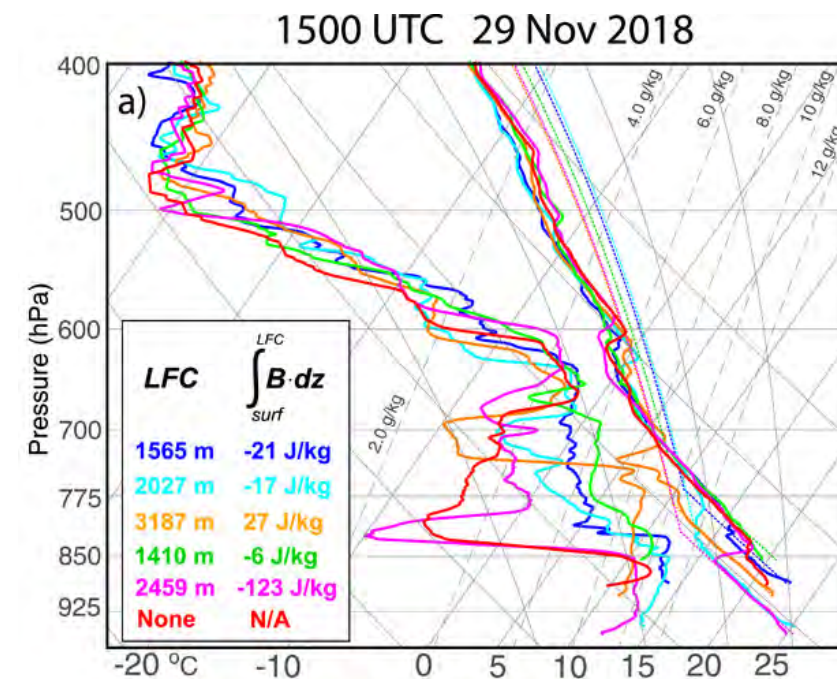
Success vs. Failure Thermodynamic Variability

Dense sounding networks during RELAMPAGO-mobile missions show considerable low level thermodynamic, particularly moisture, variability that greatly impacts convective inhibition and the level of free convection.

Upper PBL to lower troposphere moisture changes rapidly in time prior to deep convection initiation.

Just before deep convection initiation, CAPE and CIN are similar for both success and fail cases.

Marquis J. N., et al., 2021, *MWR*, doi:10.1175/MWR-D-20-0391.1.

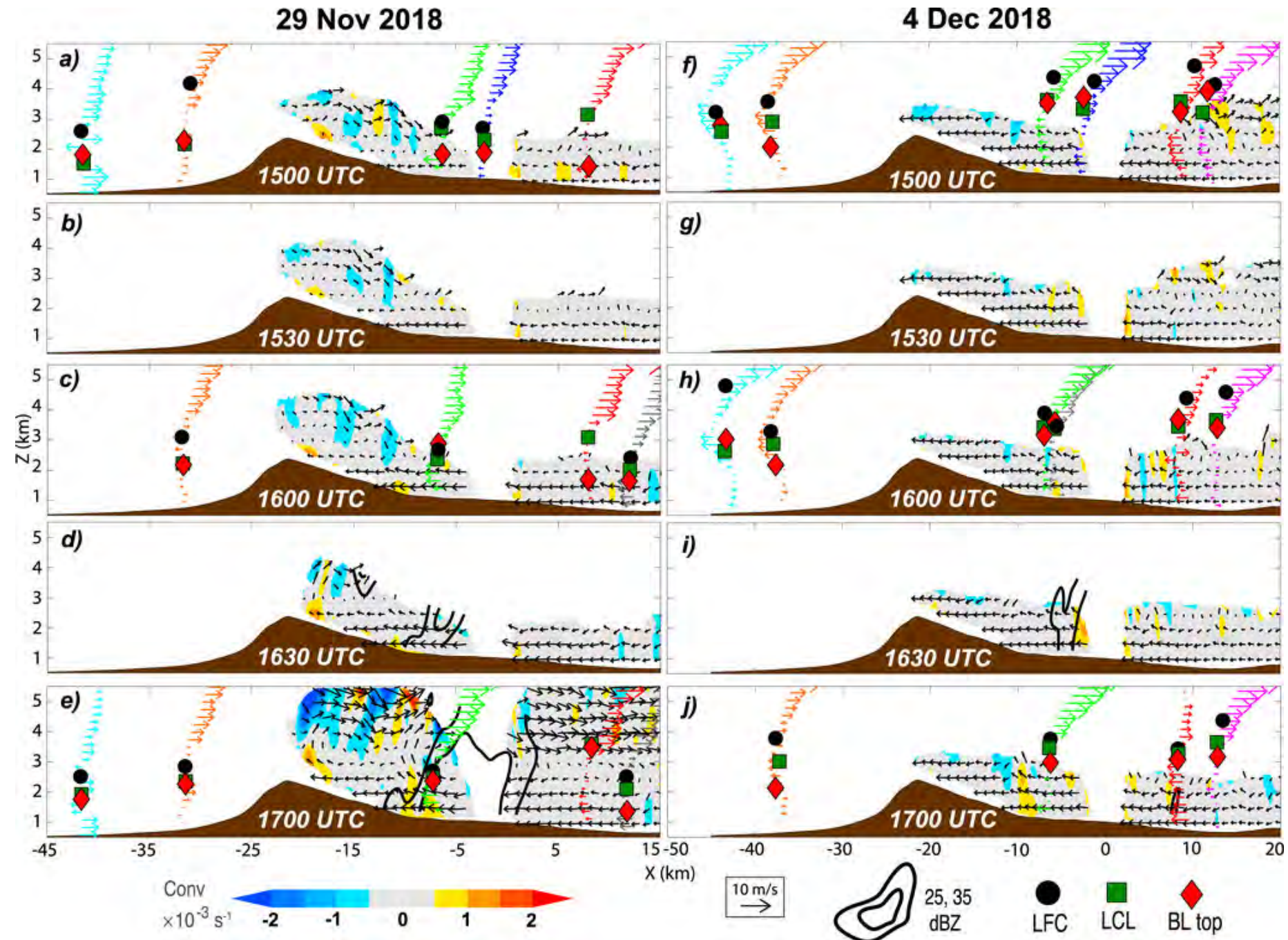


Success vs. Failure Circulations

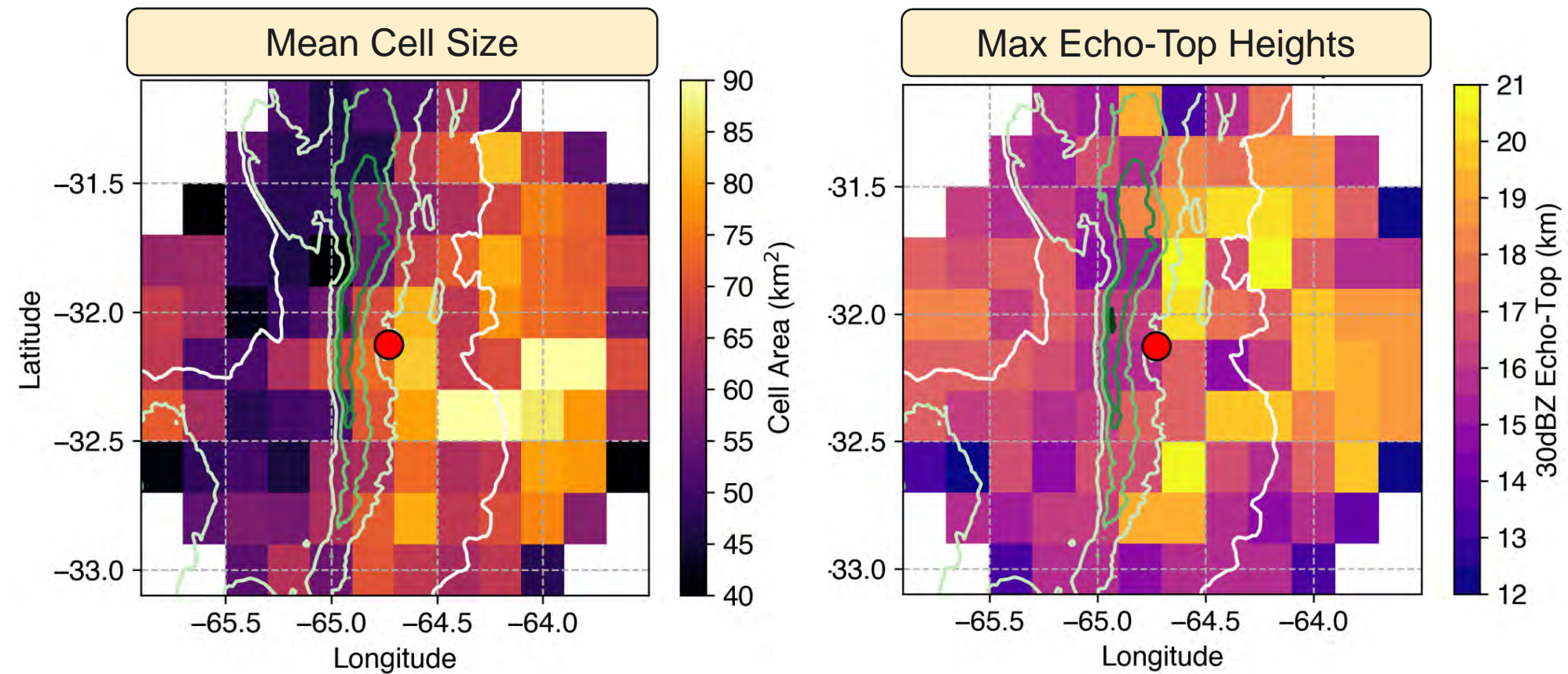
Dual-Doppler analyses and soundings highlight significantly different low level kinematic conditions on 29 Nov and 4 Dec.

29 Nov has a much shallower easterly upslope flow and regions of enhanced meridional-mean convergence indicating more robust mesoscale convergence that is also suggested by more widespread orographic congestus coverage.

Marquis J. N., et al., 2021, *MWR*, doi:10.1175/MWR-D-20-0391.1.



Tracked Cell Upscale Growth

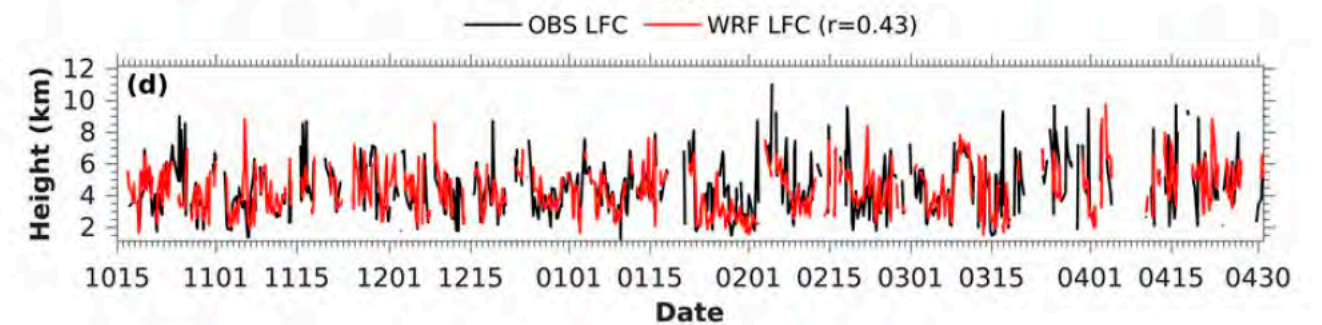
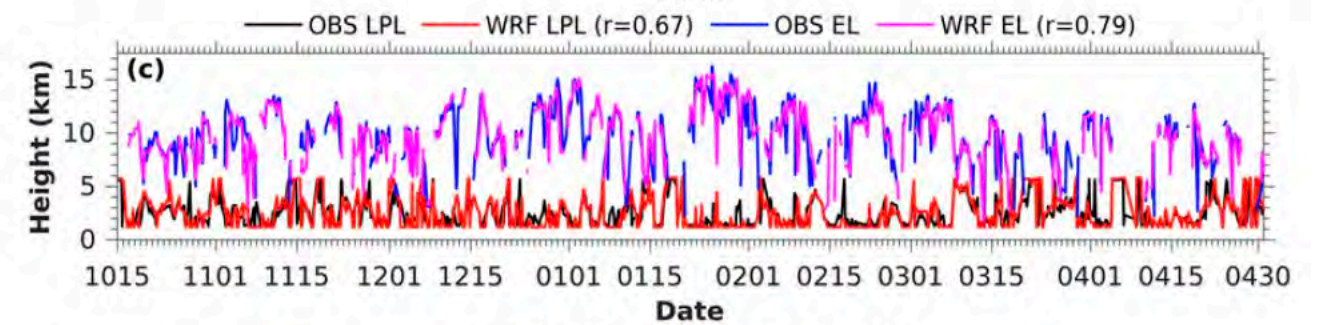
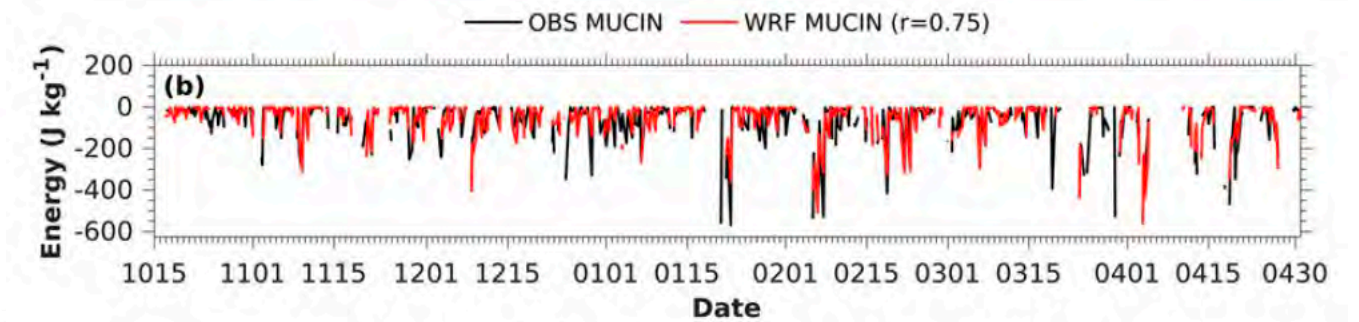
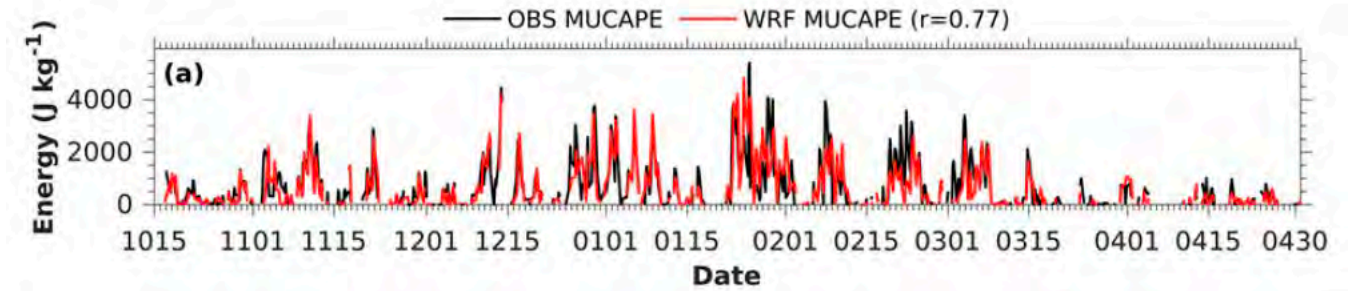
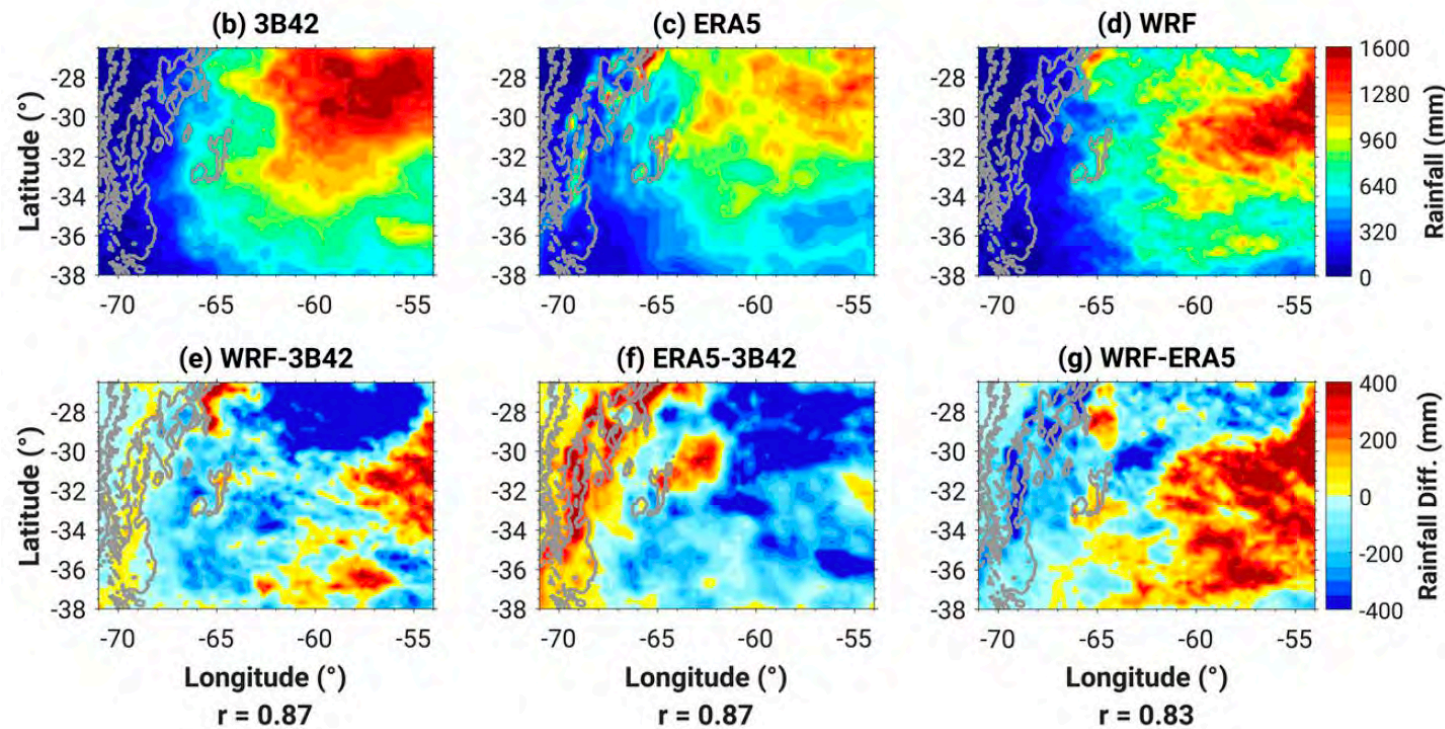
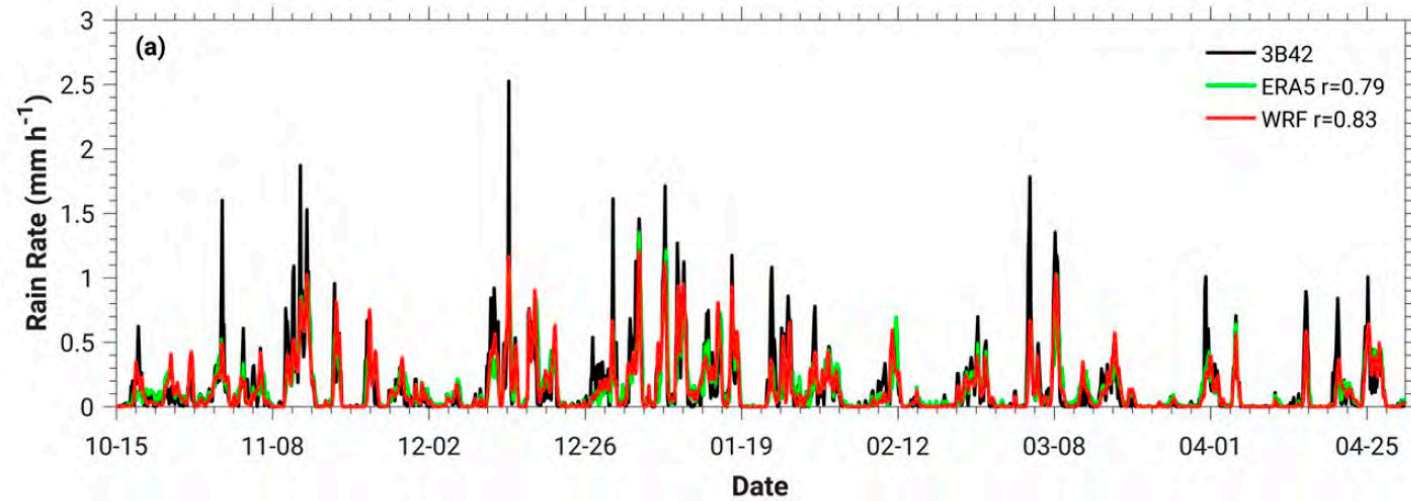


Increasing cell size east of the terrain is correlated with increasing radar echo top heights, and these increases occur immediately east of the highest terrain.

Feng, Z, et al., 2022, *MWR*, doi:10.1175/MWR-D-21-0237.1.

Campaign-long 3-km WRF Performance

Zhang, Z., et al., 2021, *MWR*, doi:10.1175/MWR-D-20-0411.1.



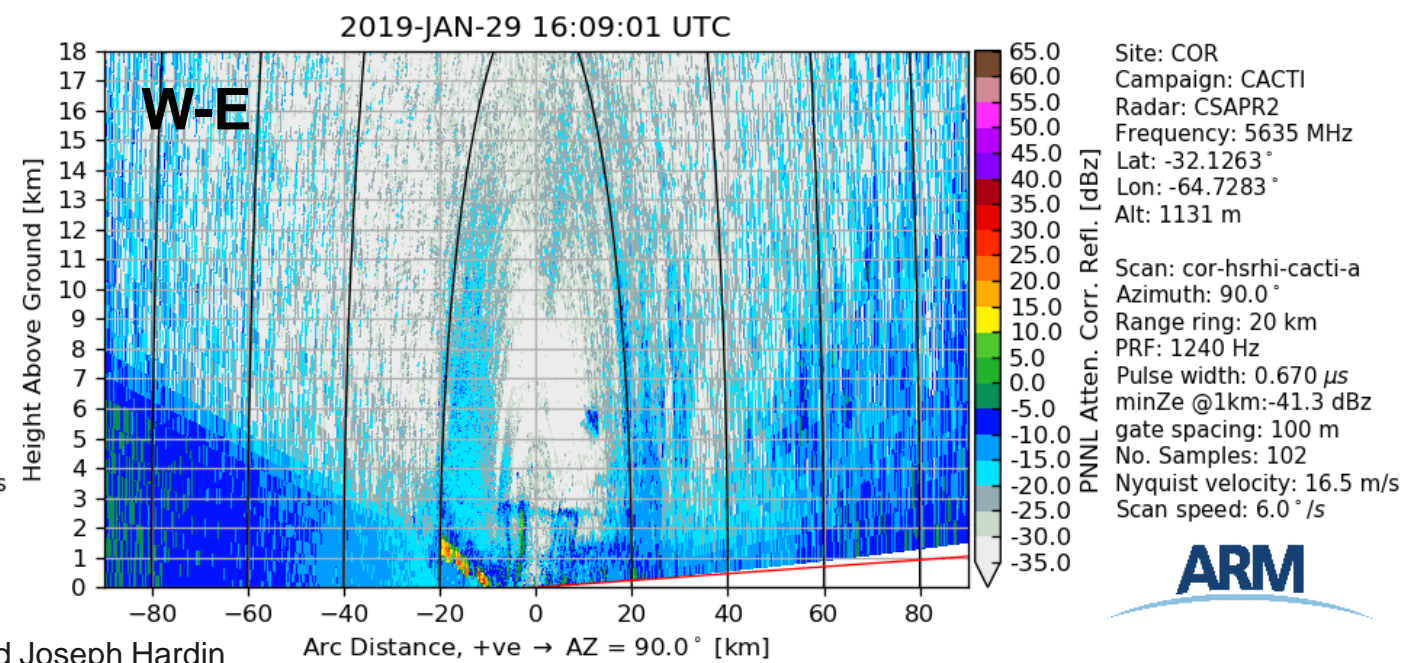
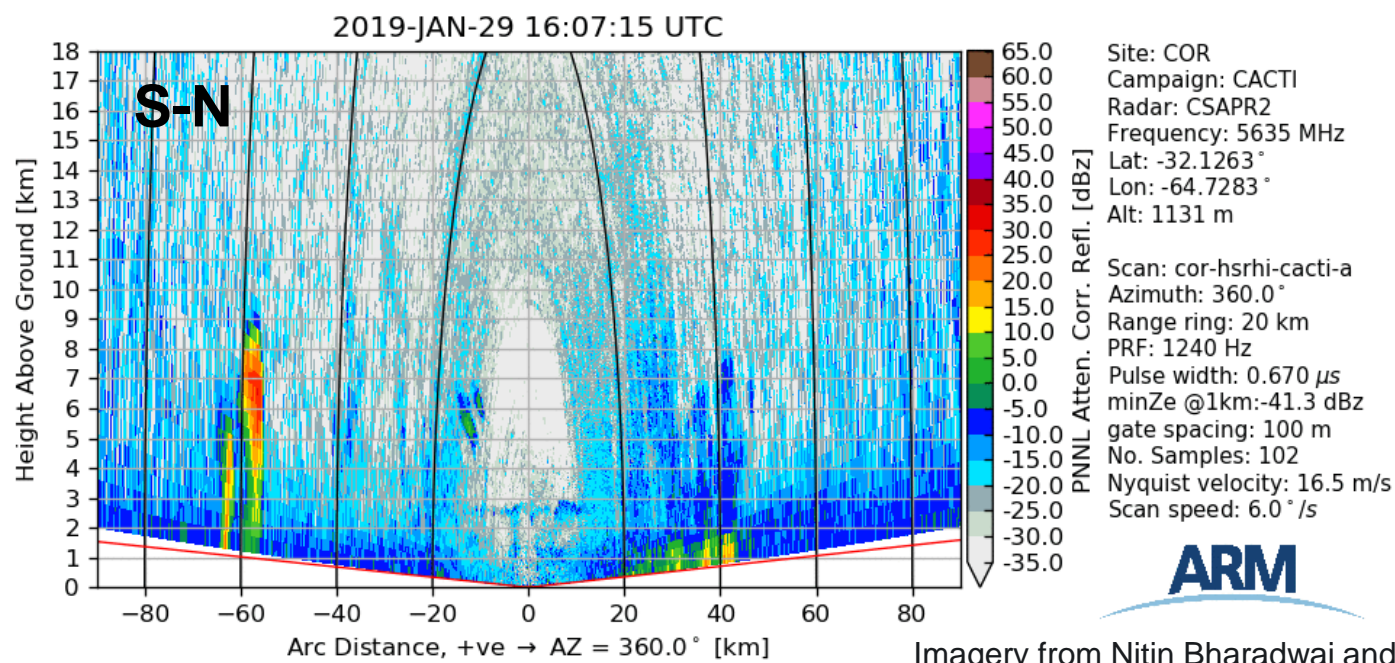
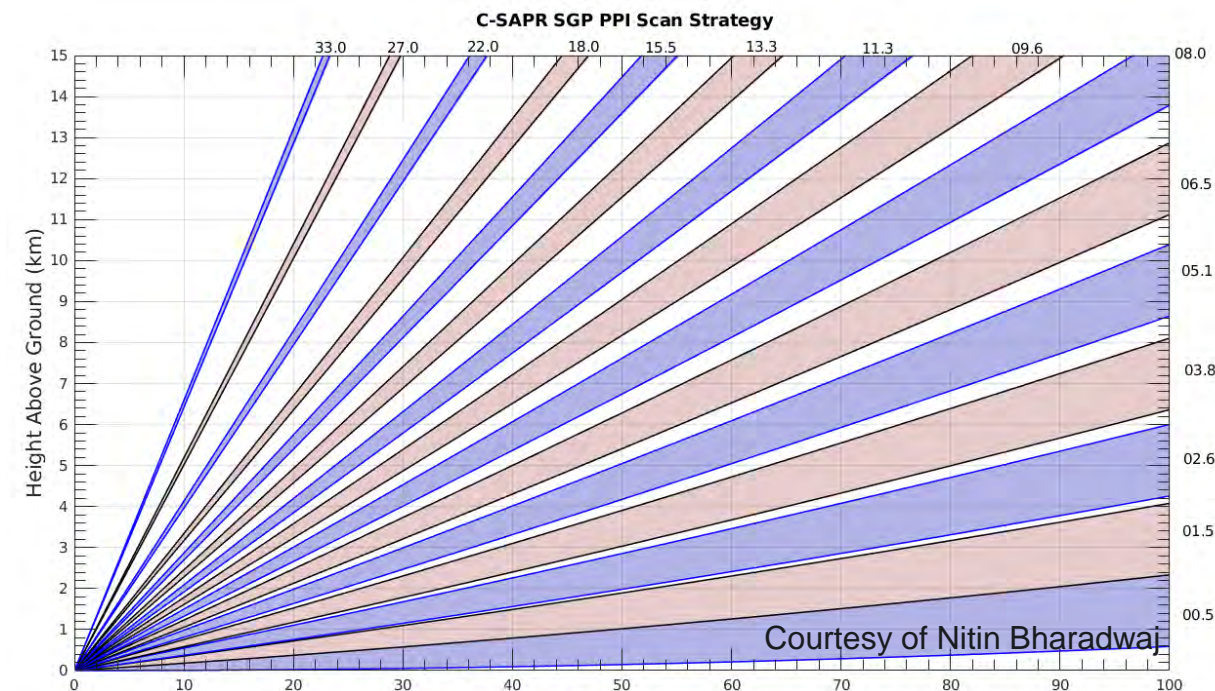
Radar Dataset Collection and Scan Sequences

Hardin, J. C., et al., 2020: CACTI Radar b1 Processing: Corrections, Calibrations, and Processes Report, DOE/SC-ARM-TR-244.



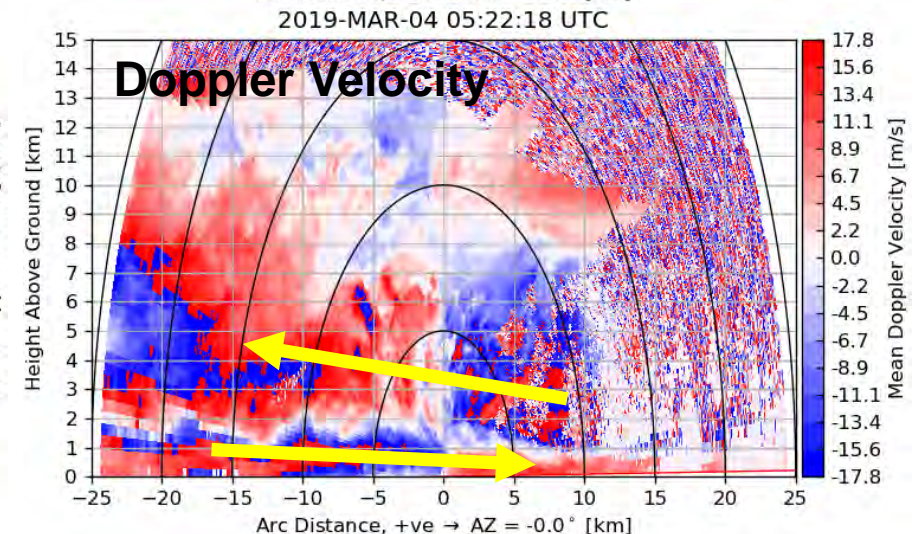
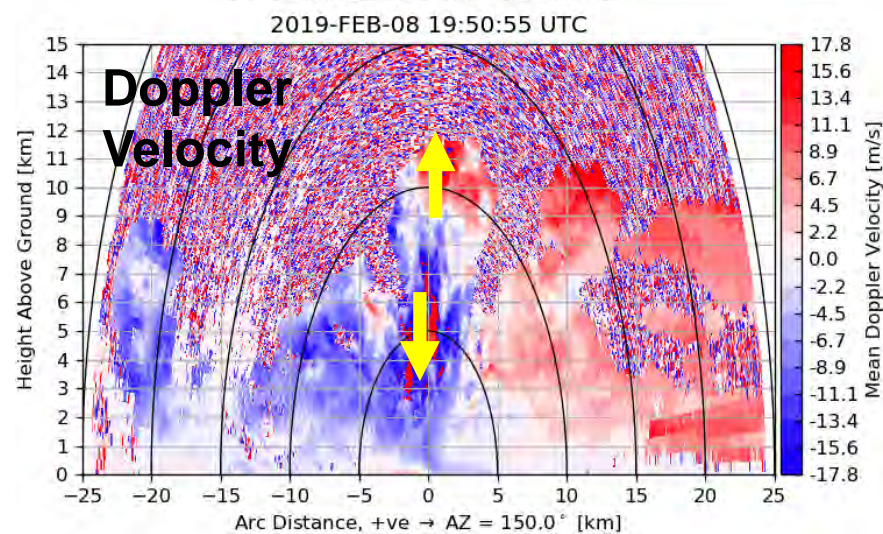
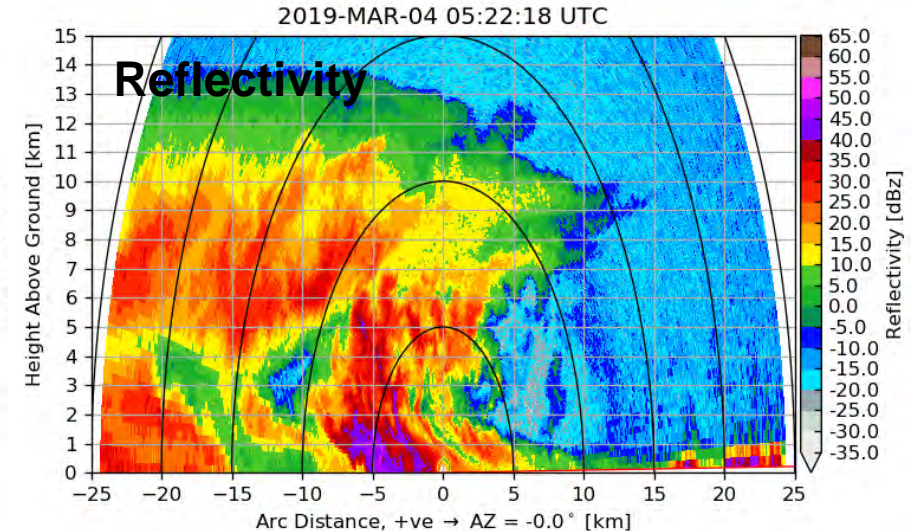
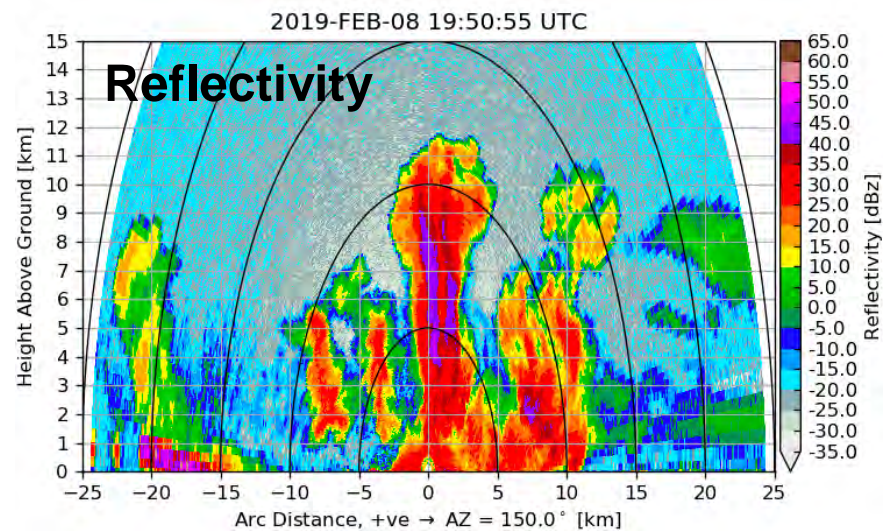
C-SAPR2 Scans

- 15-min update cycle (Oct 15-March 1)
 - 15-tilt PPI “volume”
 - ZPPI
 - 6-azimuth hemispheric RHI (HSRHI) pattern
 - Repeat 6-azimuth HSRHI pattern
- During the IOP, HSRHI patterns were occasionally replaced with sector RHIs targeting convective cells displaced from the AMF site
- Downtime: Dec 27-Jan 20, Feb 9-21, March 2-7
- Starting March 7th, only W-E HSRHIs were performed because of unfixable azimuthal rotation issue



X/Ka-SACR Scans

- 15-min update cycle (Oct 15-Mar 5)
 - 30-deg sector RHI (every 3 deg between 240 and 270 deg) within stereo camera FOV
 - 6-azimuth hemispheric RHI (HSRHI) pattern
 - Repeat 6-azimuth HSRHI pattern
 - Repeat 6-azimuth HSRHI pattern again
- Only limited outages
- Starting March 5th, a 15 tilt PPI “volume” was put in place to replace the sector RHI and 1 HSRHI pattern because of problems with C-SAPR2
 - Oversampling was decreased and range was increased to 62 km to “replace” missing C-SAPR2 scans

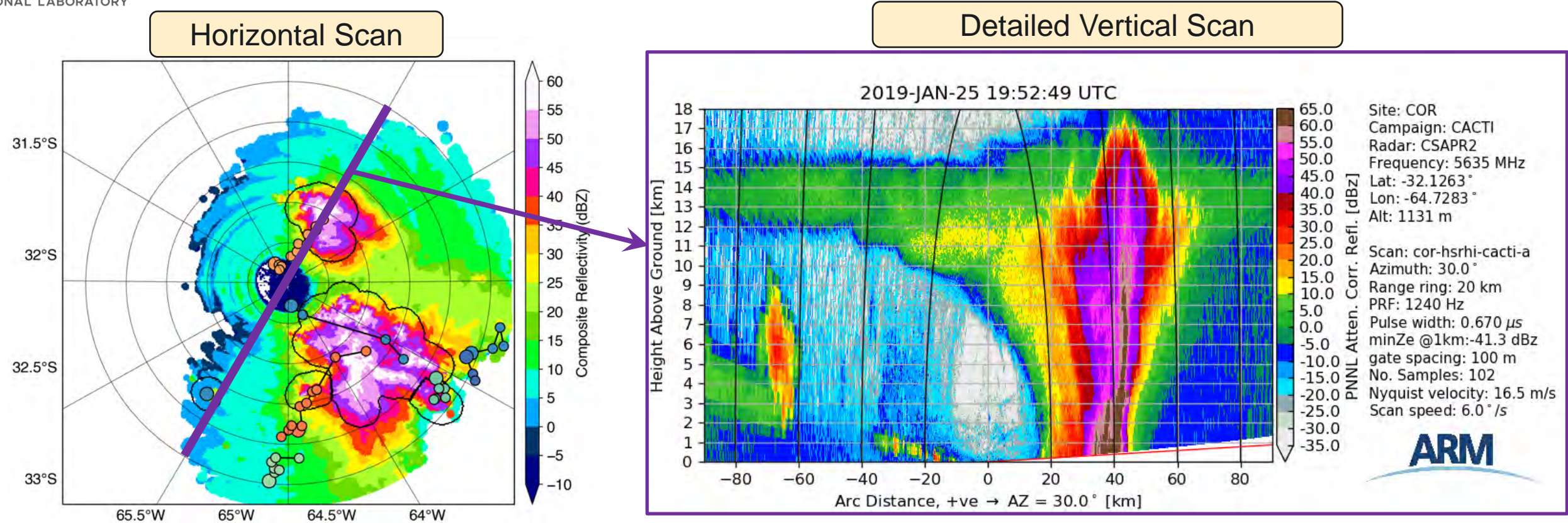


Imagery from Nitin Bharadwaj and Joseph Hardin

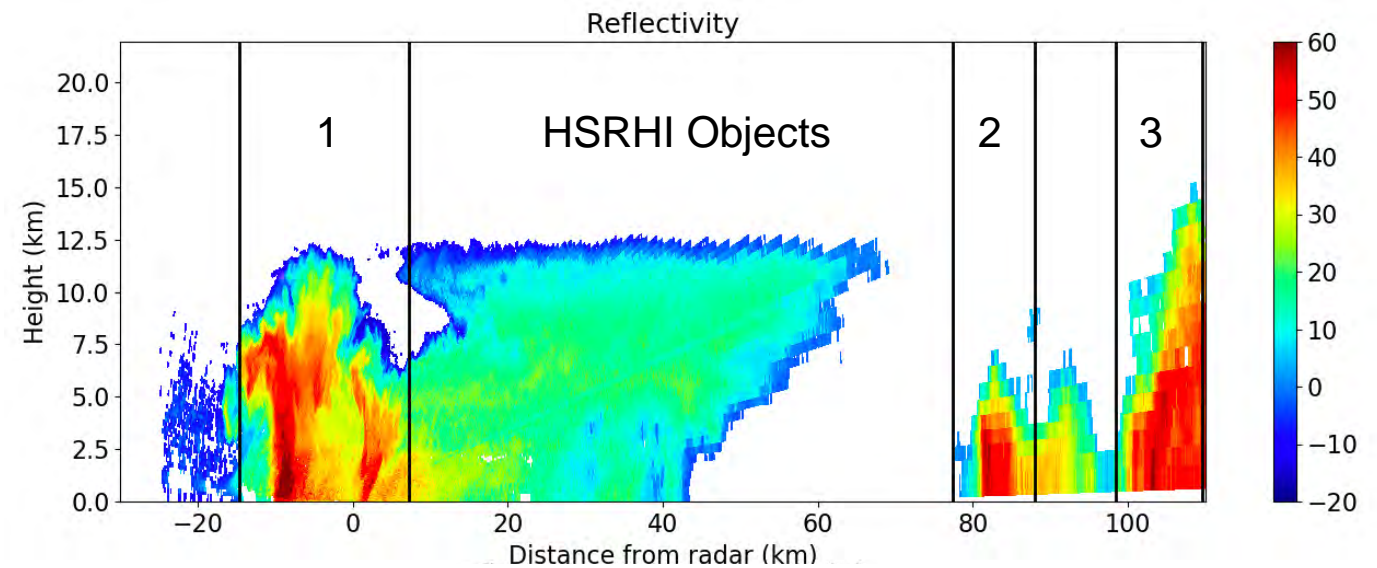
Images above from Joseph Hardin and Nitin Bharadwaj

HSRHI Objects Connected to Cell Tracks

Alexis Hunzinger, Joe Hardin



Our extensive database of HSRHI scans is being used to identify detailed HSRHI objects, which could be tied to the PPI-tracked objects.



Connecting microphysical, dynamical, and thermodynamical conditions in RHIs

Jim Marquis

South-North HSRHI

